

**“A comparative study of the boride layer morphology and diffusion kinetics on low alloy steels.”**

**M. Tech. Thesis**

By

**GARIMA DIXIT**

M. TECH (2016-2018)



**DISCIPLINE OF METALLURGY ENGINEERING &  
MATERIAL SCIENCE**

**INDIAN INSTITUTE OF TECHNOLOGY INDORE**

**July-2018**



**“A comparative study of the boride layer morphology and diffusion kinetics on low alloy steels.”**

**A THESIS**

*Submitted in partial fulfilment of the requirements for the award of the degree of*  
**Master of Technology**

*By*  
**Garima Dixit**



**DISCIPLINE OF METALLURGY ENGINEERING &  
MATERIAL SCIENCE**

**INDIAN INSTITUTE OF TECHNOLOGY  
INDORE**

**July-2018**





# INDIAN INSTITUTE OF TECHNOLOGY INDORE

## CANDIDATE'S DECLARATION

I hereby certify that the work which is being presented in the thesis entitled “**A comparative study of the boride layer morphology and diffusion kinetics on low alloy steels.**” in the partial fulfilment of the requirements for the award of the degree of *MASTER OF TECHNOLOGY* and submitted in the *DISCIPLINE OF METALLURGY ENGINEERING & MATERIAL SCIENCE* , Indian Institute of Technology Indore, is an authentic record of my own work carried out during the time period from July 2016 to July 2018 under the supervision of Dr. Santosh S. Hosmani, Assistant professor, IIT Indore .

The matter presented in this thesis has not been submitted by me for the award of any other degree of this or any other institute.

(GARIMA DIXIT)

-----  
This is to certify that the above statement made by the candidate is correct to the best of my knowledge.

Signature of the Supervisor  
Date  
(Dr. Santosh S. Hosmani)

-----  
**Garima Dixit** has successfully given her M. Tech. Oral Examination held on **5 July 2018**.

Signature of Supervisor of M.Tech. Thesis  
Date:

Convener, DPGC  
Date:

Signature of PSPC Member 1  
Date:

Signature of PSPC member 2  
Date:



## ACKNOWLEDGEMENTS

I express my deep sense of gratitude to the Almighty for guiding me and giving patience throughout this duration. Inspiration and guidance are valuable in all aspects of life. This venture has received the heartily support of my Guide **Dr. Sanotsh S. Hosmani**. Constant encouragement, motivation, and enthusiasm from my guide helped me to move forward with investigation in depth. I take this opportunity to express my profound gratitude to **Prof. Pradeep Mathur, Director, IIT Indore** for providing the essential facilities, valuable guidance and cooperation.

I am extremely happy to express my gratitude towards my PSPC members **Dr. Vinod Kumar** and **Dr. Rupesh S. Devan** for their guidance and support. I am thankful to **Dr. I.A. Palani, HOD, and Dept. of MEMS** for his support and cooperation. I am thankful to all the **faculty members** of the Department of **Metallurgy and Material Science** for their guidance and support.

I acknowledge and thankful to **the SIC facility** in IIT Indore, **Solid of Mechanics and Tribology** lab for allowing me to conduct my experiments and study I am thankful to **MHRD, Govt of India** for providing fellowship during my Master studies.

Last but not the least, I cannot forget the support and encouragement received from my Family, My husband **Mr. Abhishek Saini** and my friends **Mr. Digvijay Singh** and **Mr. Aditya Litoria** (research scholars, IIT Indore) without which this journey would not have been possible.

**Garima Dixit**



## **Abstract**

This work focuses on the low alloy steels (EN19, EN24, and EN41B). These steels have wide applications in the automotive sectors. They contain carbon (between 0.35-0.45 wt.%) and other minor alloying elements like Mn, Si, Mo, Ni and Al. Boronizing treatment provides the high load-bearing capacity, hardness, corrosion resistance, and wear resistance to the surface of steels. Metallurgical aspects of the boronizing of the steels were studied in this work. The boronizing treatment was carried out using the *pack* method. Pre-conditioned stainless-steel container with the powders of Boropak<sup>TM</sup>, SiC, and Al<sub>2</sub>O<sub>3</sub> was used for the boronizing treatment. The steels were boronized at 850, 950 and 1050°C for 2, 4 and 6 h. Boronized layer was analysed using optical microscopy, scanning electron microscopy (SEM), electron probe microanalyser (EPMA), Vickers micro-hardness tester, and X-ray diffraction (XRD). The columnar Fe<sub>2</sub>B was formed in the boronized layer. Nature of the boronized layer was dependent on the chemistry of the steels. The extent of zig-zag appearance of the interface between the boronized layer and core was more for the EN19 than the EN24 and EN41B steels. Unlike the EN19, small islands of borides were observed between the columnar morphology of Fe<sub>2</sub>B for the EN24 and EN41B steels. The effect of temperature and time on the kinetics of the boronizing was studied for these steels. The kinetics of boronizing was strongly dependent on the temperature, time and chemistry of the steels. The parabolic growth of the boronized layer with time was observed. Equations for the thickness of the boronized layer were determined for the steels using the obtained results. This study also focused on the corrosion behaviour of the boronized EN41B steel. Boronizing improved the corrosion resistance of the steel. Further, the boronizing-capability of the used pack-mixture was determined *with* and *without* the addition of activators. The appreciable thickness of the boronized layer was observed due to the addition of activators in the used pack-mixture.



# TABLE OF CONTENTS

<i>List of Figures</i> .....	xiv
<i>List of Tables</i> .....	xix
1. Introduction.....	1
1.1. General Introduction.....	1
1.1.1. Surface Modification Without Changing The Surface Chemically .....	3
1.1.1.1. Localized Surface Hardening.....	3
1.1.1.2. Laser Melting .....	3
1.1.1.3. Shot Peening .....	3
1.1.2. Surface Modification by changing the surface chemically. ....	3
1.1.2.1. Chemical or electrochemical treatment .....	3
1.1.2.2. Thermo-chemical Diffusion.....	4
1.1.2.3. Ion Implantation.....	4
1.1.3. Surface modification by adding a new material onto the surface .....	4
1.2. Why Boronizing .....	4
2. Literature Review.....	7
2.1. Boronizing (Boriding) .....	7
2.1.1. Introduction .....	7
2.1.2. Characteristics of FeB and Fe <sub>2</sub> B Layers.....	9
2.1.3. General advantages and disadvantages of boronizing.....	13
2.1.3.1. Advantages.....	13
2.1.3.2. Disadvantages .....	13
2.1.4. Influence of Alloying Elements .....	14
2.1.5. Influence of Process Parameters (Time &Temperatures) .....	16
2.1.6. Study of Transition Zone.....	17
2.1.7. Kinetics of Boronizing .....	19
2.1.8. Types of Boronizing Process.....	24
2.1.8.1. Pack boronizing .....	24
2.1.8.2. Paste Boronizing .....	26
2.1.8.3. Liquid Boronizing .....	27
2.1.8.4. Gas Boronizing .....	28
2.1.8.5. Plasma Boronizing .....	28

2.1.9.	Application of Boronized Steels .....	30
2.1.10.	Characterization of Boronized Specimen.....	31
2.1.11.	Effect of boronizing on Hardness.....	32
2.1.12.	Effect of boronizing on corrosion. ....	34
3.	Scope of the Study .....	38
3.1.	Gap Analysis.....	38
3.2.	Objectives .....	39
3.3.	Timeline for the study.....	40
4.	Experimental .....	45
4.1.	Substrate Study .....	45
4.1.1.	Substrate Material .....	45
4.1.1.1.	EN19/AISI4140 .....	45
4.1.1.2.	EN24/AISI4340 .....	45
4.1.1.3.	EN41B/905M31 .....	45
4.2.	Boronizing .....	46
4.2.1.	Process Selection.....	46
4.2.2.	Temperature & Time Selection .....	46
4.2.3.	Substrate for Boronizing .....	47
4.2.4.	Boronizing Container Design.....	47
4.2.5.	Specimen Preparation.....	48
4.2.6.	Packing of Components .....	48
4.2.7.	Boronizing Process.....	49
4.2.8.	Design of Experiment for Boronizing of Specimens .....	51
4.2.9.	Boronizing.....	53
4.3.	Post Boronizing Operations.....	54
4.4.	Heat Treatment with used Boropak Powder.....	55
4.4.1.	Packing of Components .....	55
4.5.	Characterization.....	57
4.5.1.	Chemical Composition.....	57
4.5.2.	Microstructure Study.....	57
4.5.2.1.	Optical Microstructure .....	57
4.5.2.2.	Coating Thickness Measurement Methods.....	58
4.5.2.3.	Scanning Electron Microscopy (SEM) Study.....	58

4.5.3.	X-ray Diffraction (XRD) Study .....	59
4.5.4.	Electron Probe Micro-Analyzer (EPMA) .....	59
4.6.	Kinetics Study.....	59
4.7.	Hardness Test .....	60
4.7.1.	Rockwell Hardness Tester.....	60
4.7.2.	Vickers Hardness Tester.....	60
4.8.	Corrosion Test .....	60
5.	Results and Discussions .....	63
5.1.	Base Material.....	63
5.1.1.	Chemical Composition.....	63
5.1.2.	Microstructure and Hardness .....	64
5.1.2.1.	Microstructure and Hardness of EN19 .....	64
5.1.2.2.	Microstructure and Hardness of EN24 .....	65
5.1.2.3.	Microstructure and Hardness of EN41B.....	66
5.2.	Boronizing .....	67
5.2.1.	Boronizing at 850°C .....	67
5.2.1.1.	Microstructure.....	68
5.2.1.2.	Coating Thickness.....	70
5.2.2.	Boronizing at 950°C .....	72
5.2.2.1.	Microstructure.....	73
5.2.2.2.	Coating Thickness.....	77
5.2.3.	Boronizing at 1050°C .....	79
5.2.3.1.	Microstructure.....	80
5.2.3.2.	Coating Thickness.....	87
5.3.	XRD Studies .....	89
5.4.	EPMA Analysis .....	92
5.5.	General Review on Boronizing .....	99
5.5.1.	Proposed Mechanism of Boronizing .....	101
5.6.	Growth Kinetics.....	102
5.7.	Effect of Boronizing on Surface Hardness .....	111
5.8.	Corrosion Test .....	114
5.9.	Heat Treatment with used Boronizing Mixture.....	116
5.9.1.	Heat Treatment with used Boronizing Mixture without activator .....	116

5.9.1.1.	Microstructure .....	116
5.9.1.2.	Microhardness .....	118
5.9.1.3.	XRD Study .....	118
5.9.2.	Heat Treatment with used Boronizing Mixture with activator .....	119
5.9.2.1.	Microstructure .....	119
5.9.2.2.	XRD Studies .....	122
5.9.2.3.	Microhardness .....	124
6.	Conclusion .....	125
7.	Future Scope of the Study .....	127
8.	References .....	129

## LIST OF FIGURES

Figure 1.1: Scientific and technical activity, adding up to create surface engineering [1] .....	2
Figure 2.1: The cross-section of boronized steel GS18 at 950°C for 6 h. [13] .....	9
Figure 2.2: SEM cross sectional view of AISI P20 steel boronized at 950°C for 4h showing the morphology of FeB and Fe <sub>2</sub> B. [14] .....	9
Figure 2.3: Fe-B Phase Diagram [15] .....	12
Figure 2.4: Effect of alloying elements in steel on boride layer thickness .....	14
Figure 2.5: Maximum thickness of boride coatings grown in 15h at 850°C on Fe-C-Me alloys using a 20 wt% B <sub>4</sub> C-10KBF <sub>4</sub> -SiC powder mixture: (a)Me=Cr (b) Me=Ni [20] .....	16
Figure 2.6: Variation of layer thickness as a function of boronizing time for AISI 1040. [25] .....	17
Figure 2.7: Optical micrograph of the cross section of AISI 4140 steel specimen boronized at 950°C for 3 h showing the presence of transition zone below the boride layer. [28].....	18
Figure 2.8 : Boride layer thickness versus boronizing time at various temperatures for: (a) AISI H13 steel and (b) AISI 304 steel. [18] .....	23
Figure 2.9: Growth rate constant versus temperature of boronized .....	23
Figure 2.10: Contour diagram of boride layer thickness of boronized: (a) AISI H13 steel and (b) AISI 304 Steel [18] .....	24
Figure 2.11: Schematic Diagram of Pack boronizing of single component [8].....	26
Figure 2.12: Layout of plasma boronizing facility. [11] .....	29
Figure 2.13: Optical microscope and SEM cross-sectional views of the borided AISI 4140 steel (a) at 850°C and (b) 950 °C for 4 h showing morphology of borides [45]. .....	31
Figure 2.14: X-ray diffraction (XRD) pattern of borided AISI 4140 steel at (a) 850 °C and (b) 950 °C for 6h. [45].....	32
Figure 2.15: Variation of hardness depth profile in plasma nitrided and borided AISI M2 steel [48].....	34
Figure 2.16: Weight loss of immersion tests of the plasma nitrided and borided AISI M2 steel in 4% M HCl solution [48] .....	35
Figure 2.17: Tafel curves of un-boride and boride steels at 900 °C [51].....	36
Figure 2.18 : Complex impedance curves (b) simulated spectrums and theirs experimentally generated for samples C, D and E in NaCl 3.5 % wt. Solution [51].....	36
Figure 3.1: Flow Chart Showing the Sequence of Tasks Performed .....	43
Figure 4.1: Photographs of container used for Pack Boronizing .....	48

Figure 4.2: Packing of the specimens for pack boronizing [28] .....	49
Figure 4.3: Heat treatment cycle of boronizing done at 850°C for 4h .....	50
Figure 4.4: Heat treatment cycle for specimens boronized at 850°C .....	53
Figure 4.5: Heat treatment cycle for specimens boronized at 950°C .....	54
Figure 4.6: Heat treatment cycle for specimens boronized at 1050°C .....	54
Figure 4.7: Packing of components with used boronizing mixture.....	55
Figure 4.8: Heat treatment cycle for the boronizing process with used boronizing mixture ..	56
Figure 4.9: Procedure to measure the FeB/Fe <sub>2</sub> B and diffusion zone thicknesses [52] .....	58
Figure 5.1: Optical micrograph of Cross section of as received EN19 specimen.....	65
Figure 5.2: Optical micrograph of Cross section of as received EN24 specimen.....	66
Figure 5.3: Optical micrograph of Cross section of as received EN41B specimen .....	67
Figure 5.4: Morphology of boride layer in specimens (a) EN19 (b) EN24(c) EN41B carried out at 850°C for 2h.....	68
Figure 5.5: Morphology of boride layer in specimens (a) EN19 (b) EN24 .....	69
Figure 5.6: Boronizing coating thickness, μm vs. time, h.....	72
Figure 5.7: Morphology of boride layer in specimens (a) EN19 (b) EN24 .....	74
Figure 5.8: Morphology of boride layer in specimens (a) EN19 (b) EN24 .....	74
Figure 5.9: SEM image showing the morphology of boride layer EN19 carried out at 950°C for 4h.....	75
Figure 5.10: SEM image showing the morphology of boride layer EN41B carried out at 950°C for 4h.....	75
Figure 5.11: Morphology of boride layer in specimens (a) EN19 (b) EN24 .....	76
Figure 5.12: Variation of boride layer thickness vs. Time for different specimens.....	79
Figure 5.13: Morphology of boride layer in specimens (a) EN19 (b) EN24 .....	80
Figure 5.14: Morphology of boride layer in specimens (a) EN19 (b) EN24 .....	81
Figure 5.15: SEM image showing the Morphology of boride layer in EN19 boronized at 1050°C for 4h.....	82
Figure 5.16: SEM image showing the Morphology of boride layer in EN19 boronized at 1050°C for 4h.....	82
Figure 5.17: SEM image showing the Morphology of boride layer in EN24 boronized at 1050°C for 4h.....	83
Figure 5.18: Optical images showing the Morphology of boride layer in (a)EN19 (b)EN24 (c)EN41B boronized at 1050°C for 6h.....	84

Figure 5.19: SEM images showing the Morphology of boride layer in EN19 boronized at 1050°C for 6h.....	84
Figure 5.20: SEM images showing the Morphology of boride layer in EN24 boronized at 1050°C for 6h.....	85
Figure 5.21: SEM images showing the Morphology of boride layer in EN41B boronized at 1050°C for 6h.....	85
Figure 5.22: Variation of Boride layer thickness vs. Time for different specimens.....	88
Figure 5.23: XRD patterns of boronized EN19 Steel at 1050°C for 6h.....	89
Figure 5.24: XRD patterns of boronized EN24 Steel at 1050°C for 6h.....	90
Figure 5.25: XRD patterns of boronized EN24 Steel at 1050°C for 6h.....	90
Figure 5.26: XRD patterns of boronized EN41B Steel at 950°C for 4h. ....	91
Figure 5.27: SEM image showing the presence of FeB phase.....	92
Figure 5.28: WDS line scan performed on boronized EN19 steel.....	94
Figure 5.29: Wavelength dispersive spectra analysis showing the alloying elements distribution across the boride layers in EN19 steel.....	94
Figure 5.30: Schematic boron concentration profile from experimental data for two phase boride layers.....	95
Figure 5.31: Wavelength dispersive spectra analysis showing the silicon distribution across the boride layers.....	97
Figure 5.32: Elemental Mapping (wt %) of EN41B Steel.....	98
Figure 5.33: Elemental Mapping (atomic %) of EN41B Steel.....	99
Figure 5.34: Schematic presentation of the mechanism of boronized layer formation on the steel surface.....	102
Figure 5.35: Variation of Boriding layer thickness with time at different temperatures: (a) EN19 (b) EN24 (c) EN41B.....	103
Figure 5.36: Square of boride layer thickness versus boronizing time at various temperatures for EN19 steel.....	104
Figure 5.37: Square of boride layer thickness versus boronizing time at various temperatures for EN24 steel.....	105
Figure 5.38: Figure 5.38: Square of boride layer thickness versus boronizing time at various temperatures for EN41B steel.....	105
Figure 5.39: Natural logarithm of growth rate as a function of reciprocal of boronizing temperature for (a) EN19, (b) EN24 (c) EN41B steel.....	107

Figure 5.40: Micro hardness depth profile for EN19 Steel boronized at (a) 850°C (b) 950°C (c) 1050°C .....	111
Figure 5.41: Micro hardness depth profile for EN24 Steel boronized at (a) 850°C (b) 950°C (c) 1050°C .....	112
Figure 5.42: Micro hardness depth profile for EN41B Steel boronized at (a) 850°C (b) 950°C (c) 1050°C .....	113
Figure 5.43: Weight loss of immersion tests of the untreated and boronized EN41B steel in HCl 5M solutions .....	114
Figure 5.44: Optical micrograph of EN19 specimen boronized at 1050°C for 4h at (a) 100X (b) 200X magnifications .....	116
Figure 5.45: Optical micrograph of EN24 specimen boronized at 1050°C for 4h at (a) 100X (b) 200X magnifications .....	117
Figure 5.46: Optical micrograph of EN41B specimen boronized at 1050°C for 4h at (a) 100X (b) 200X magnifications .....	117
Figure 5.47: Optical micrograph of EN19 specimen boronized at 1050°C for 4h at (a) 100X (b) 200X magnifications .....	120
Figure 5.48: Optical micrograph of EN24 specimen boronized at 1050°C for 4h at (a) 100X (b) 200X magnifications .....	120
Figure 5.49: Optical micrograph of EN41B specimen boronized at 1050°C for 4h at (a) 100X (b) 200X magnifications .....	121
Figure 5.50: XRD patterns of boronized with used boronizing mixture specimens(a)EN19, (b)EN24, (c)EN41B .....	123

## LIST OF TABLES

Table 2.1: Showing the comparison between Fe <sub>2</sub> B and FeB .....	11
Table 2.2: Values of the Activation Energies of the Borided Steels from the Literature .....	20
Table 2.3: Typical combinations of borided steels and their applications .....	30
Table 2.4: Typical surface hardness of borided steels compared with other treatments and hard materials .....	33
Table 2.5: Summary of results obtained from corrosion tests performed in 3.5 % wt. NaCl solution [48] .....	36
Table 4.1: Table showing different parameters for heat treatment .....	47
Table 4.2 .....	50
Table 4.3: Design of experiment for optimization of boronizing process .....	51
Table 4.4: Design of experiment for optimization of boronizing process for EN24 .....	52
Table 4.5: Design of experiment for optimization of boronizing process for EN41B .....	52
Table 4.6: Design of experiment for optimization of boronizing process with used boronizing mixture .....	56
Table 5.1: Chemical composition of standard and test material EN19 steel .....	63
Table 5.2: Chemical composition of standard and test material EN24 steel .....	64
Table 5.3: Chemical composition of standard and test material EN41B steel .....	64
Table 5.4: Showing the layer thickness for different samples boronized at 850° c for 2h .....	71
Table 5.5: Showing the layer thickness for different samples boronized at 850° c for 6h .....	71
Table 5.6: Showing the layer thickness for different samples boronized at 950° c for 2h .....	78
Table 5.7: Showing the layer thickness for different samples boronized at 950° c for 4h .....	78
Table 5.8: Showing the layer thickness for different samples boronized at 950° c for 6h .....	78
Table 5.9: Showing the layer thickness for different samples boronized at 1050° c for 2h .....	87
Table 5.10: Showing the layer thickness for different samples boronized at 1050° c for 4h .....	87
Table 5.11: Showing the layer thickness for different samples boronized at 1050° c for 6h .....	88
Table 5.12: The element contents (at. %) of the corresponding spots A, B and C .....	93
Table 5.13: The element contents (at. %) of the corresponding spots A, B and C .....	96
Table 5.14: Growth rate (R) as a function of Boriding temperature for EN19, EN24 and EN41B specimens .....	106
Table 5.15: Shows the growth rate(R) and activation energies (Q) with a function of boronizing temperature for EN19, EN24 and EN41B specimens .....	108

Table 5.16: Values of the Activation Energies of the Borided Steels from the Literature and current study..... 109

# *Chapter 1*

---

## **1. Introduction**

### **1.1. General Introduction**

Low-alloy steels are generally considered to comprise plain carbon steels and steels with a total alloying content of up to 12%. They are much cheaper than the more highly alloyed materials and are used in large quantities in heavy engineering industries. The surfaces of engineering components manufactured from steels are subjected to extreme working conditions, i.e., higher stresses, greater abrasion, fatigue damage as well as more direct corrosive attack by the environment. As a result of these working conditions, failures occur and start on the surface by brittle fracture, fatigue, wear, corrosion or combinations of these.

It is therefore important to modify the surface properties of these steels. There is a constant need to improve the surface properties of these steels due to the need for improved performance, efficiency and life of machine tools. Now a day's a new technique has been utilized by industries and researchers to improve or alter the properties of the surface of the material. The technique is known as Surface Engineering.

Surface Engineering refers to a wide range of technologies designed to modify the surface properties of metallic and non-metallic components.

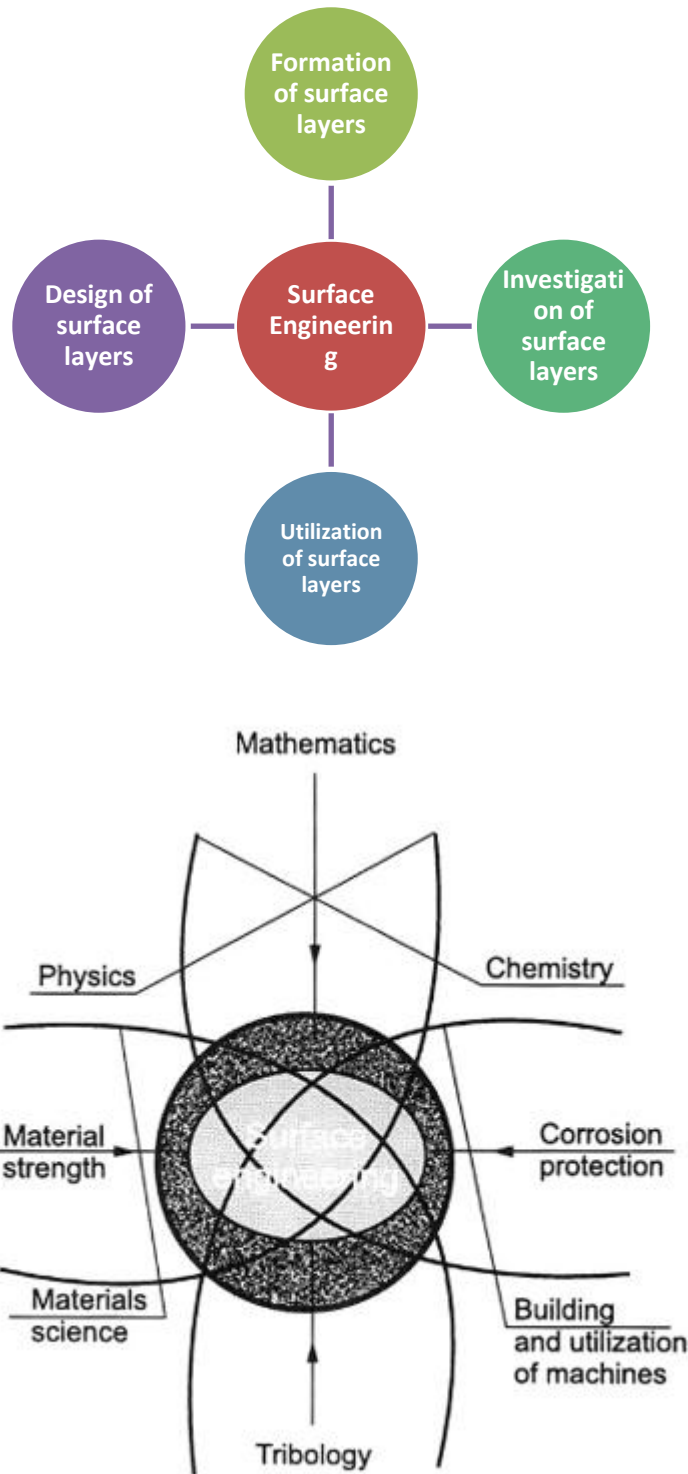


**Figure 1.1: Scientific and technical activity, adding up to create surface engineering [1]**

The surface properties can be modified in three ways:

- a. Surface modification without changing the material chemically.

- b. Surface modification by changing surface chemically.
- c. Surface modification by adding new material onto the surface (Coating).

### **1.1.1. Surface Modifications Without Changing The Surface Chemically**

In this technique, the surface is modified without changing the chemistry of the surface. The properties like wear behavior, corrosion resistance and fatigue properties are changed by changing surface metrology. Some of the examples are:

#### ***1.1.1.1. Localized Surface Hardening***

In this the surface properties are improved by the development of a hard martensitic.[\[1\]](#) Examples: Flame, Induction, Laser and Electron Beam Hardening

#### ***1.1.1.2. Laser Melting***

The surface properties are improved by grain refinement with the help of a laser.[\[1\]](#)

#### ***1.1.1.3. Shot Peening***

Surface properties are improved by developing the beneficial compressive residual stress on the metallic surfaces.[\[2\]](#)

### **1.1.2. Surface Modification by changing the surface chemically.**

In this technique, the surface is modified by changing the chemistry of the surface. A new product is formed on the surface. This type of modification has certain advantages over coating because they impart compressive stresses near the surface and usually they will not delaminate from the surface as they have good adhesion.

#### ***1.1.2.1. Chemical or electrochemical treatment***

Surface properties are improved by producing complex phosphate, chromates and oxides on the metallic surfaces.

### ***1.1.2.2. Thermo-Chemical Diffusion***

Thermo-chemical diffusions are the heat treatment processes where the diffusion of some interstitial elements like C, N, and B takes place in the metal surface and form new compounds by combining with the surface atoms. Some examples are carburizing, boronizing and nitriding.

### ***1.1.2.3. Ion Implantation***

Surfaces are modified by introducing the ionized species into the surface by some ion beam of high-velocity electrons.

### **1.1.3. Surface modification by adding new material onto the surface**

Surfaces are modified by applying an external coating to the metal surface. There are two basic types of coatings widely used that are soft coatings and hard coatings.

Hard coatings include oxides, carbides, nitrides, borides and carbon-based compositions (diamond, low hydrogenated diamond-like carbon [DLC]).

Soft coatings include polymers, soft metals, halides and sulfates of alkaline earth metals. Soft coatings also include highly hydrogenated DLC as well as lamellar solids like MoS<sub>2</sub>, WS<sub>2</sub>, etc.

## **1.2. Why Boronizing**

Among all the surface modification processes boronizing is gaining much attention due to the advantages it offers:

- ✓ High hardness 1400-2600 HV, even on non-alloyed steel.
- ✓ The hardness of the boride layer retained at higher temperatures than Nitriding.
- ✓ A wide variety of metals are compatible with the process.
- ✓ High abrasion resistance.
- ✓ Excellent thermal stability.
- ✓ The self-lubricating effect at high temp.
- ✓ Superior bonding strength.
- ✓ Good resistance against molten metal's.

- ✓ Provides good corrosion-erosion resistance of ferrous materials in dilute acids



## *Chapter 2*

---

### **2. Literature Review**

#### **2.1. Boronizing (Boriding)**

##### **2.1.1. Introduction**

The surface of the industrial component and machine elements require treatment to enhance the Surface characteristic. Now a day's many different surface hardening process have been commonly applied to metals to increase their surface performances. In general, two methods for that are known:

- i. Diffusing of small atoms on the metal surface leading to the formation of an interstitial solid solution.
- ii. A chemical reaction between the diffused atoms and those of basic metal forming of new compounds in the superficial layer. [4] [5]

Various surface coatings like carburizing, nitriding and boronizing have been applied. Amongst all these coatings boronizing is gaining much attention due to several advantages it offers.

Boronizing, is a thermo-chemical treatment in which boron atoms diffuse through the surface of metallic substrates. As boron is an element of the relatively small size, it diffuses into a variety of metals; including ferrous, nickel and cobalt alloys, metal-bonded carbides and most refractory alloys. [6]

The diffused boron atoms chemically react with the atoms of the base material and result in the formation of Borides. According to the Iron–Boron equilibrium diagram, diffusing boron into the iron crystalline lattice results in the formation of two kinds of iron borides (FeB and Fe<sub>2</sub>B). [7]

Boronizing of ferrous materials is generally performed at different temperatures ranging from 800 to 1100°C for 1h to 12h. Boronizing can be carried out in solid, liquid or gaseous medium. [8]

Borides produced by boronizing have relatively high hardness values ranging from 1600 to 2100HV which improves the resistance to abrasive wear. Boride layers have good tribological characteristics at high temperatures. [9]

Boronizing can be successfully applied to the variety of materials, ferrous materials like metals, carbon steels, low alloy steels, tool steels, etc. Boronizing is found to be very effective, on low alloy steels with chromium content. [10]

<b>Ferrous Metals</b>	<ul style="list-style-type: none"> <li>• Low alloy steels, Carbon steels, Tool steels</li> <li>• Stainless steel, Grey &amp; Ductile Cast Iron</li> </ul>
<b>Non-Ferrous Metals</b>	<ul style="list-style-type: none"> <li>• Tantalum, Titanium, Tungsten</li> <li>• Niobium, Molybdenum</li> </ul>
<b>Ti &amp; Ni based Alloys</b>	<ul style="list-style-type: none"> <li>• Inconel, Inconel 718, Inconel 625</li> <li>• Hastelloy, Nimonic 80A</li> </ul>

Boronizing produces a thin, compact compound layer which includes either a single-phase layer of Fe<sub>2</sub>B or a double phase layer consisting of Fe<sub>2</sub>B with FeB. FeB phase appears dark while Fe<sub>2</sub>B appears white. Available boron potential affects the formation of Fe<sub>2</sub>B and FeB. Boride phases have a column or sawtooth morphology along the diffusion axis. Boron-rich FeB phase is formed with 16.23 wt. % boron and has an orthorhombic crystal structure while, whereas Fe<sub>2</sub>B has body central tetragonal structure with 8.83 wt. % boron. Cracking occurs at the interface of these phases due to different thermal expansion coefficient ( $\alpha_{Fe_2B} = 5.1 \times 10^{-6}/^{\circ}C$ ,  $\alpha_{FeB} = 23 \times 10^{-6}/^{\circ}C$ ) [11]. Also, FeB forms under tensile residual stress while Fe<sub>2</sub>B forms under compressive residual stress. Due to these problems, two phases FeB/Fe<sub>2</sub>B layer is generally not preferred over single phase Fe<sub>2</sub>B, but these two phases are not inferior to single phase FeB layer is removed by grinding. The preferred methods to prevent FeB growth are

- i. Diluting the boron concentration by pack boronizing of powder mixtures.
- ii. Applying a much thinner boronizing agent.
- iii. Working at high boronizing temperatures for long enough to transform FeB into Fe<sub>2</sub>B phase.
- iv. Another approach for reducing the amount of highly brittle FeB phase is post-laser heat treatment after the boronizing process. [12]

### 2.1.2. Characteristics of FeB and Fe<sub>2</sub>B Layers

Boronizing produces a thin, compact compound layer which includes either a single-phase layer of Fe<sub>2</sub>B or double phase layer of Fe<sub>2</sub>B along with FeB.

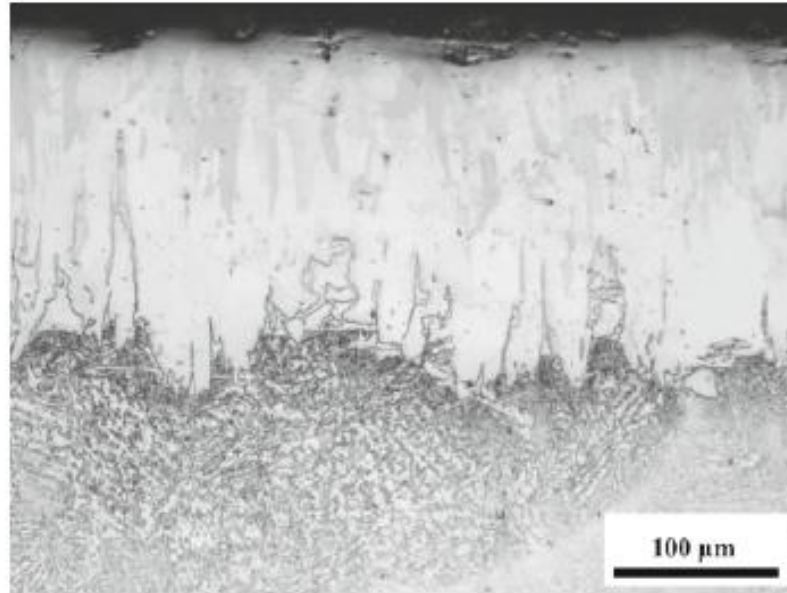


**Figure 2.1: The cross-section of boronized steel GS18 at 950°C for 6 h. [13]**

FeB phase appears dark while Fe<sub>2</sub>B appears white. Figure 2.2 shows an optical micrograph of a cross-section of GS18 steel boronized at 950°C for 6h [13]. FeB and Fe<sub>2</sub>B phases are clearly seen.

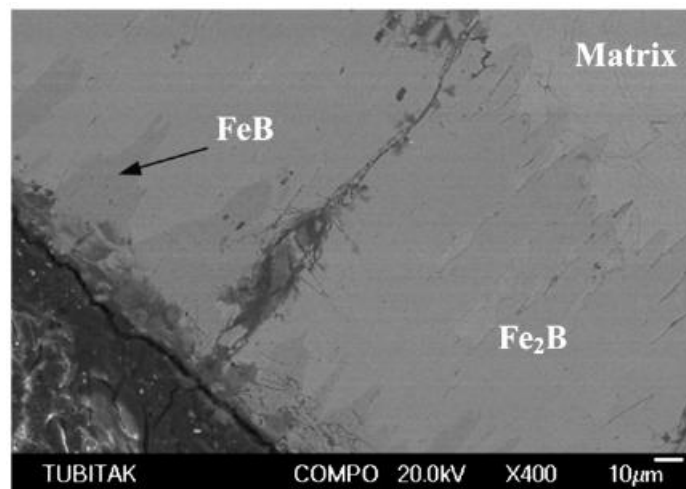


**Figure 2.2: SEM cross-sectional view of AISI P20 steel boronized at 950°C for 4h showing the morphology of FeB and Fe<sub>2</sub>B. [14]**

➤ ***Fe<sub>2</sub>B Phase***

- ✚ Micro hardness of about 18 to 20 GPa.
- ✚ Modulus of elasticity of 285 to 295 GPa.
- ✚ Thermal expansion coefficient of 7.65 ppm/°C and 9.2 ppm/°C in the range of 200 to 600 °C and 100 to 800 °C, respectively.
- ✚ Density of 7.43 g/cm<sup>3</sup>.
- ✚ Composition with 8.83 wt% boron.
- ✚ Body-centered tetragonal structure with 12 atoms per unit cell
- ✚ Lattice parameters:  $a = 5.078 \text{ \AA}$  and  $c = 4.249 \text{ \AA}$

➤ ***FeB Phase***

- ✚ Micro hardness of about 19 to 21 GPa.
- ✚ Modulus of elasticity of 590 GPa.
- ✚ Density of 6.75 g/cm<sup>3</sup>.
- ✚ The thermal expansion coefficient of 23 ppm/°C between 200 and 600°C.
- ✚ Composition with 16.23 wt% boron
- ✚ Orthorhombic crystal structure with 4 iron and 4 boron atoms per unit cell.
- ✚ Lattice parameters:  $a = 4.053 \text{ \AA}$  ,  $b = 5.495 \text{ \AA}$  and  $c = 2.946 \text{ \AA}$

**Table 2.1: Showing the comparison between Fe<sub>2</sub>B and FeB**

<b>Properties</b>	<b>Fe<sub>2</sub>B</b>	<b>FeB</b>
<b>Micro hardness</b>	<b>1650-2000 HV</b>	<b>1900-2100 HV</b>
<b>Modulus Of Elasticity (GPa)</b>	<b>285-295</b>	<b>590</b>
<b>Thermal Expansion Coefficient</b>	<b>5.1 x 10<sup>-6</sup> / °C</b>	<b>23 x 10<sup>-6</sup> / °C</b>
<b>Density</b>	<b>7.43 g/cm<sup>3</sup></b>	<b>6.75 g/cm<sup>3</sup></b>
<b>% Boron</b>	<b>8.83%</b>	<b>16.23%</b>
<b>Lattice Structure</b>	<b>Body-Centered Tetragonal</b>	<b>Orthorhombic</b>
<b>Lattice Parameters</b>	<b>a = 5.078 Å c = 402499 Å</b>	<b>a = 4.053 Å b = 5.495 Å c = 2.946 Å</b>

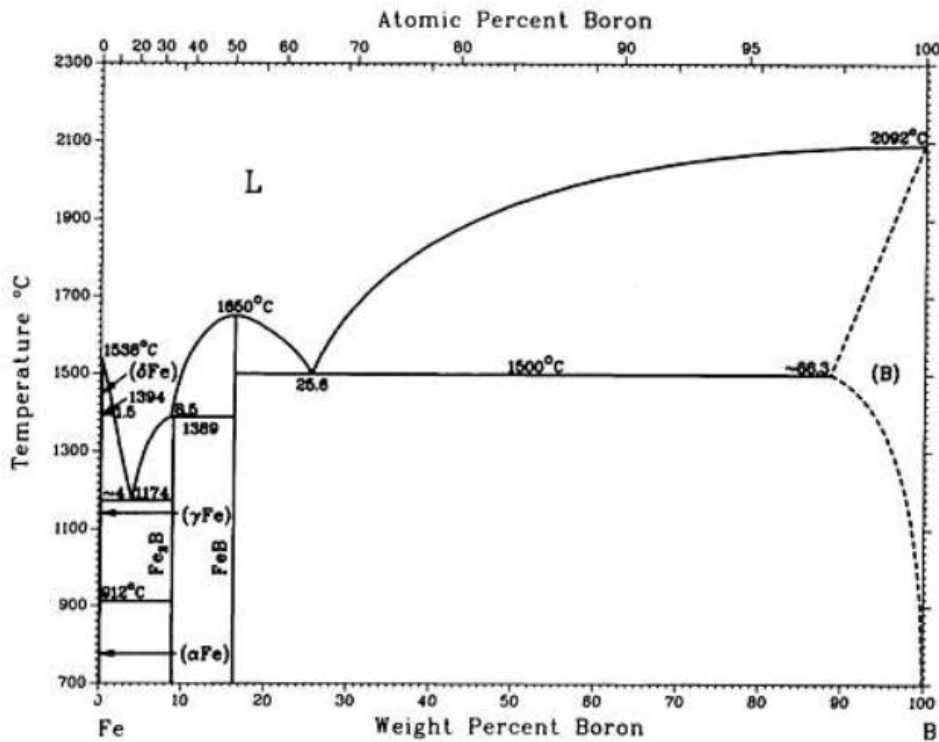


**Figure 2.3: Fe-B Phase Diagram [15]**

Figure 2.4 shows the iron-boron phase diagram; the Y-axis indicates temperature (°C) and X-axis wt. % Boron. In the case of unalloyed low carbon steels and low alloy steels saw tooth, morphology is dominant, whereas, as the percentage of alloying elements in the substrate increases ex. High alloy steels, smooth interface developed.

First, the concentration of boron (B) in iron (Fe) increases up to a small fraction of a percent (Figure 2.3). Since there is a very small solubility of B in Fe; the solid-state solution will be formed until the maximum solubility of B in Fe is reached. a  $\alpha$ Fe based solution of boron in iron will be there (one-phase system). If the boron concentration keeps on increasing, the amount of B in Fe will exceed the solubility limit, and no more B will enter the iron lattice. At this point (8.83 wt %) Fe<sub>2</sub>B will start forming, and a two-phase system with bcc-Fe (B) and Fe<sub>2</sub>B will be there. This will not be a eutectic-type microstructure, because eutectic mixture forms from the melt, not from the solid state. At this point, there are 2 atoms of Fe per 1 atom of B and a single-phase Fe<sub>2</sub>B will be formed. If the boron concentration continues to increase up to 16.23wt%, FeB will start forming. Fe<sub>2</sub>B will combine with the "next" boron atoms and forms the next phase Fe<sub>3</sub>B, and the system will be two-phase. The

process of conversion of Fe<sub>2</sub>B to FeB (forced by an excessive amount of B) will continue until there is 1 atom of B per 1 atom of Fe. Then, there will be a single-phase system consisting of FeB. Continuation of boron supply will result in precipitation of (almost pure) beta-boron in the system. [16]



### 2.1.3. General advantages and disadvantages of boronizing

#### 2.1.3.1. Advantages

- i. Boride layers have extremely high hardness values (between 1450 and 5000 HV) with high melting points of the constituent phases.
- ii. The hardness of the boride layer retained at higher temperatures than, nitriding.
- iii. A wide variety of steels, including through-hardenable steels, are compatible with the processes.
- iv. Boronizing enhances the corrosion-erosion resistance of ferrous materials in non-oxidizing dilute acids and alkali media.
- v. Boronized surfaces have moderate oxidation resistance (up to 850 °C, or 1550 °F) and they are a molten metal attack.
- vi. Boronized parts have an increased fatigue life and service performance under oxidizing and corrosive environments.

#### 2.1.3.2. Disadvantages

- i. The techniques are inflexible and rather labor intensive, making the process less cost-effective than other thermochemical surface hardening treatments such as gas carburizing and plasma nitriding.
- ii. The growth (that is, the increase in volume) resulting from boronizing is 5 to 25% of the layer thickness.

- iii. Partial removal of the boride layer for closer tolerance requirements is made possible only by a subsequent diamond lapping because conventional grinding causes fracture of the layer.
- iv. In general, the rolling contact fatigue properties of borided alloy steel parts are very poor compared to carburized and nitrided steels at high contact loads (2000 N). Therefore, boronizing treatments of gears are limited to those screw designs where transverse loading of gear teeth is minimized.
- v. There has frequently been a need to harden and temper the tool after boriding, which requires a vacuum or inert atmosphere to preserve the integrity of the boride layer.

#### 2.1.4. Influence of Alloying Elements

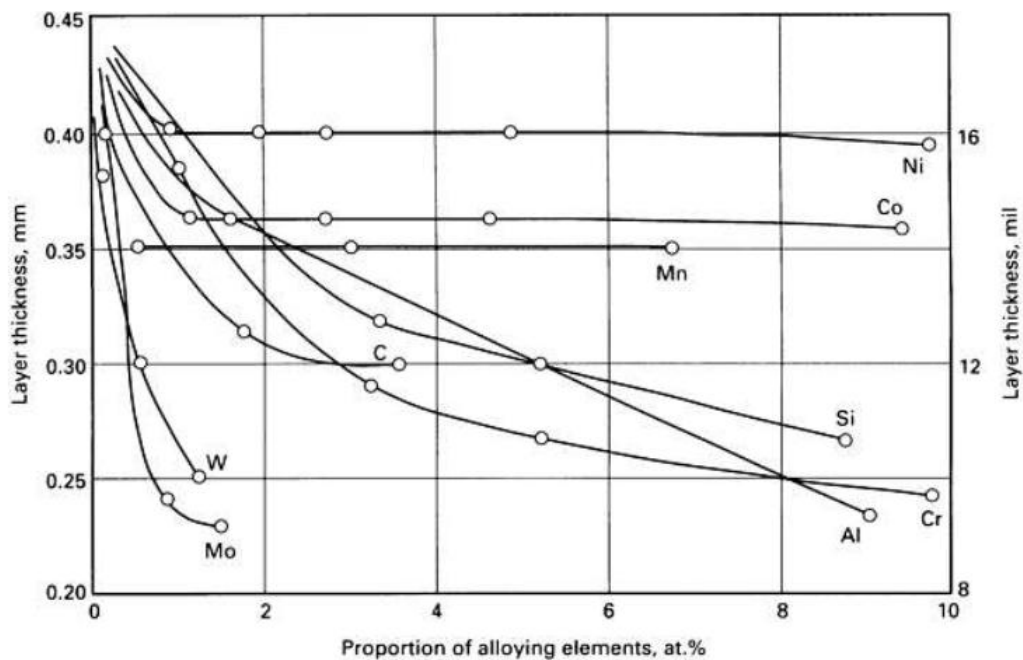


Figure 2.4: Effect of alloying elements in steel on boride layer thickness

Pure iron, unalloyed low-carbon steels, and low-alloy steels show saw tooth morphology predominantly. As the alloying element and carbon increases saw tooth morphology decreases at the substrate interface and a smooth layer is formed at the interface [14] [16] [18]. Boronized layer thickness growth suppressed by alloying

elements. This is due to the restricted diffusion of boron into the steel because of the formation of a diffusion barrier. Carbon does not dissolve significantly in the boride layer and does not diffuse through the boride layer.

During boriding carbon is driven (or diffused away) from the boride layer to the matrix and forms, together with boron, borocementite  $\text{Fe}_3(\text{B}, \text{C})$  [or more appropriately,  $\text{Fe}_3(\text{B}_{0.67}\text{C}_{0.33})$  in the case of Fe-0.08% C steel] as a separate layer between  $\text{Fe}_2\text{B}$  and the matrix. Steels containing high contents of these ferrite-forming elements should not be used for boriding because they reduce the wear resistance of the normal boride layer; they produce a softer ferrite zone beneath the boride layer than that of the core. At higher surface pressure, this type of layer build-up results in the eggshell effect, that is, at greater thicknesses extremely hard and brittle boride layer penetrates the softer intermediate layer and is consequently destroyed.

From the figure 2.5, it can be observed that as the concentration of some alloying elements like Mo, W, Cr, Al, Si, C increase in the base material, boride layer thickness decreases whereas some elements like Mn, Co, Ni do not affect the layer thickness considerably. Chromium considerably modifies the structure and properties of iron borides. As the chromium content in the base material increases, progressive improvements in the following effects are observed: formation of boron-rich reaction products, decrease in boride depth, and flattening or smoothening of the coating/substrate interface. The solubility of chromium in the  $\text{Fe}_2\text{B}$  phase causes the replacement from iron to chromium and forms  $(\text{Fe}, \text{Cr})\text{B}$  and  $(\text{Fe}, \text{Cr})_2\text{B}$  on the surface. The diffusion leads to the decreasing of the thickness of the boride layer and the increasing of the smooth boride

Layer/substrate interface.<sup>24</sup> Chromium also promotes the formation of boron-rich phases, such as  $\text{FeB}$  phase, onto the boride layer [18][19].

The composition of the base alloys greatly affects the diffusion of boron, the thickness of the boride layer, the crystallographic order of boride coating and morphology at the interfaces. They all can be controlled by selecting the composition of the base alloy [19][20][21]. The crystallographic order is important for mechanical compactness, and the interface morphology at the interfaces is the determining factor for the adherence between adjacent phases, i.e., between iron borides as well as between coating and substrate.

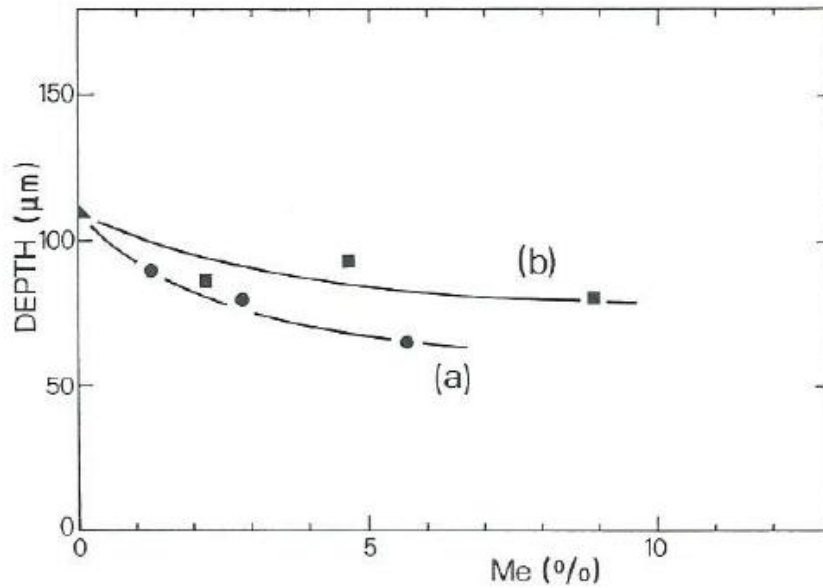


**Figure 2.5: Maximum thickness of boride coatings grown in 15h at 850°C on Fe-C-Me alloys using a 20 wt% B<sub>4</sub>C-10KBF<sub>4</sub>-SiC powder mixture: (a)Me=Cr (b) Me=Ni [20]**

### 2.1.5. Influence of Process Parameters (Time & Temperatures)

Boronizing results in the formation of boride layer. With the diffusion of boron into the steel, iron borides (FeB, Fe<sub>2</sub>B) are formed. It has been examined by many researchers that the thickness of the boride layer is determined by the process temperature and time. [22][23]

*M. Tabur et al.* reported the same by conducting boronizing on AISI 8620 steel using the solid-state boronizing method. Processes were carried out at the different temperatures of 850, 900 and 950°C for 2, 4 and 6 h of treatment. He observed that increasing the boronizing temperature and treatment duration increases the boride layer thickness. Boride layer thickness was observed to increase more than twice depending on boronizing time. [24]

O. Kayacan, S. Sahin, and F. Tastan also observed the same effect of boronizing time on boride developed in AISI1040 steel. The highest boride layer thickness was observed for 6h (hours) followed by 4h and 2h respectively. The thickness of the borided layer of AISI 1040 steel ranged from 42 μm to 115 μm depending on the

boronizing time. According to the results, the longer the boronizing time, the thicker the boride layer was. [25]

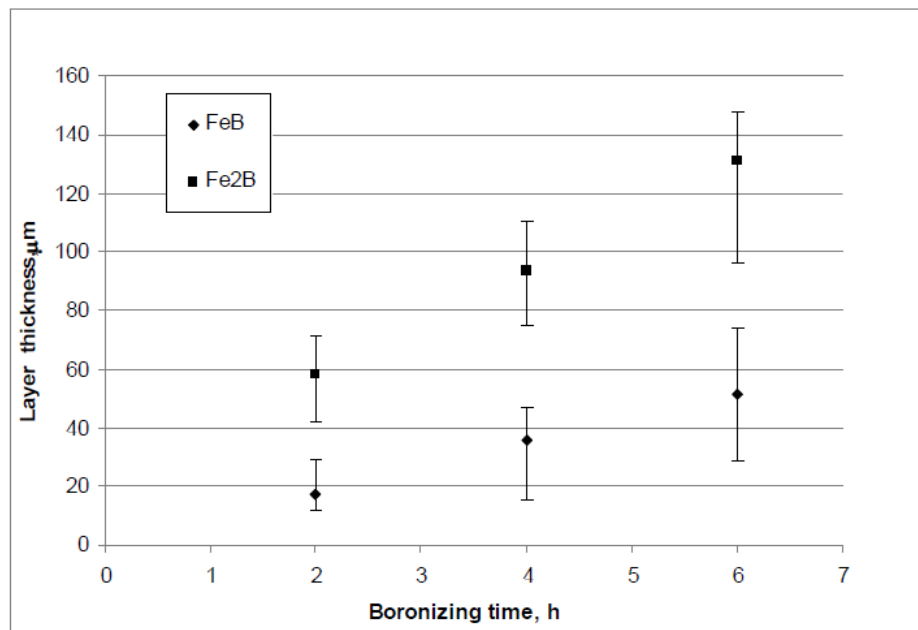


**Figure 2.6: Variation of layer thickness as a function of boronizing time for AISI 1040. [25]**

### 2.1.6. Study of Transition Zone

As discussed in section 2.3.4, the alloying elements and their solubility in borides have a greater impact on the boride layer morphology. The structure of the transition zone also depends on the composition of the steel. [26]

During boronizing, redistribution of the alloying elements takes place depending on the solubility of the elements and the ability of the elements to form stable compounds with boron. The alloying elements which have less solubility in borides are diffused away from the borides, and they accumulate in a zone below the boride layer. This zone is known as the transition zone or diffusion zone. The formation of such a zone was also reported [27].

Elements such as carbon, silicon, and aluminium are not soluble in iron borides. If steel contains these elements, they are diffused away from the substrate by boron atoms and displaced ahead between the boride layer and the substrate. This results in the formation of iron-silicon-borides (soft ferrite) beneath the boride layer. Steels

containing more than 0.5 wt-% silicon is stated to be unsuitable for boronizing because of the formation of a soft ferrite region and the difficulty in producing thicker boride layers [27].

A. A. JOSHI & S. S. HOSMANI also observed the same phenomenon in their study. They reported the formation of a softer zone beneath the boride layer [28].

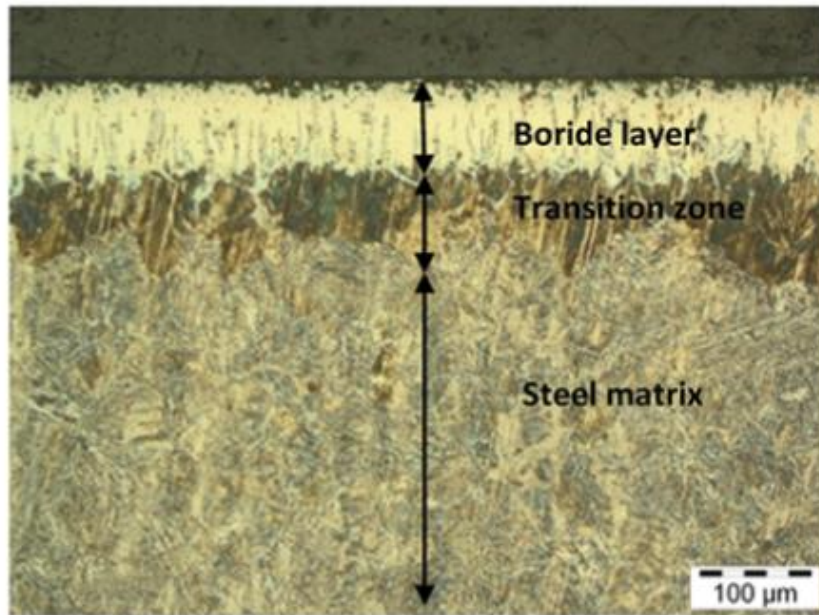


**Figure 2.7: Optical micrograph of the cross-section of AISI 4140 steel specimen boronized at 950°C for 3 h showing the presence of a transition zone below the boride layer. [28]**

Vera Cárdenas et al. has also reported that Cr dissolves in iron borides thus it is not diffused away from the iron borides whereas The solubility of chromium in the  $Fe_2B$  phase causes the replacement from iron to chromium and forms  $(Fe, Cr) B$  and  $(Fe, Cr)_2B$  on the surface. He also observed the low amount of manganese in the boride layer as compared to iron because of lower solubility. Figures 2.8 shows the high amount of C and Si at the interface as compared to the boride layer due to their less solubility and being displaced to the diffusion zone, and there they form some complex compounds of Si, C, B like Silicoborides ( $FeSi_{0.4}B_{0.6}$  and  $Fe_5SiB_2$ ) and boron cementite ( $Fe_3B_{0.67}C_{0.33}$ ). [29]

Tsipas and J Rus have reported that When Cr is in excess, more than what iron borides could absorb, it segregates along the boride-metal interface in the form of a layer consisting of chromium borides. [30]

Campos Silva et al. has confirmed in their study of boronized AISI 4140 steel (by using glow discharge optical emission spectroscopy (GDOES) technique that carbon is pushed towards diffusion zone and tended to form boron cementite in the substrate.[31]

Sukru Taktak has observed a diffusion zone beneath the boride layer, the region below boride layers, where boron makes a solid solution, which has a hardness less than that of borides but greater than that of steel matrix. He also observed that at the interface, the concentration of Ni is higher than that of both the boride layer and base metal. This case can be due to the displacement of Ni from borides. Silicon also concentrated strongly at the interface as it is insoluble in iron borides. [18]

### **2.1.7. Kinetics of Boronizing**

The modeling of the boronizing kinetics is considered as a suitable tool in the optimization of process parameters for obtaining adequate boride layers thickness with their practical applications. So, the modeling of the growth kinetics of boride layers has been gaining much attention to simulate the boronizing kinetics during these last decades.

The kinetics of the growth layer is controlled by the diffusion of boron in the borides ( $\text{Fe}_2\text{B}$ ) and layer growth occurs because of the boron diffusion perpendicular to the substrate surface.

The Fick's laws establish the concentrations of boron in the FeB and  $\text{Fe}_2\text{B}$ . The  $\text{Fe}_2\text{B}$  growing obeys the parabolic law

$$x^2 = Rt \quad (\text{Equation 1})$$

Where x is the depth of the boride layer, R is the growth rate constant depending on boriding temperature and is calculated from the slopes of the  $x^2$  vs. treatment time graphs. [11][18]

Growth rate constant depends on diffusion temperature. The relationship between rate constant R and temperature can be expressed by an Arrhenius-type equation as follows: [11][18]

$$R = A \exp (-Q/R_0T) \text{ (Equation 2)}$$

Where A is a constant, Q is the activation energy (J/mol), T is the absolute temperature in Kelvin and R<sub>0</sub> is the gas constant (J/mol K).

Taking the logarithm of equation (2)

$$\ln R = \ln A - (-Q/R_0)T^{-1} \text{ (Equation 3)}$$

Eq. (3) reveals a linear relationship between the natural logarithm of growth rate constant and reciprocal diffusion temperature.

The activation energy Q can be easily calculated from the slope of the curve between lnR and inverse of temperature.

Many investigations have been done to calculate the value of the diffusion coefficient and the activation energy for different boronizing medium or for different types of steel. [32][33][34][35][36][37][38][39][40]

The reported values of the activation energies of the borided steels from the literature are listed in Table 2.2

**Table 2.2: Values for Activation Energies of the Borided Steels from the Literature**

Steel	Temperature Range (K)	Boronizing Medium	Activation Energy (kJ/mol)	References
AISI316	1073-1223	Pack Boronizing	199	[11]
AISI304 H13	1073-1223	Salt Boronizing	244.37-253.35	[18]

AISI4140	1023-1223	Paste	168.5	[32]
AISI 316	973-1073	Plasma Paste	250.8	[33]
AISI 1040 AISI P20	1073-1223	Pack Boronizing	168-200	[34]
AISI 51100	1173-1273	Plasma	106	[35]
X200CrMoV1 2 P	1173-1273	Powder	199.37	[36]
AISI420, AISI304 AISI304L	1123-1223	Pack Boronizing	206.161,234.641 222.818	[37]
31CrMoV9 34CrAlNi7	1123-1223	Pack boronizing	230-270	[38]
AISI 52100, AISI 440C	1123-1223	Pack Boronizing	269.638,340.426	[39]
AISI P20	1123-1223	Pack Boronizing	Conventional furnace: 256.485, Micro-wave furnace: 213.935	[40]
AISI 304	1023-1223	Plasma paste Boronizing	123	[42]
AISI5140 AISI4340/EN 24 AISID2	1123-1223	Salt Bath	223 234 170	[46]

As seen in Table 2.2, it can be observed that the activation energy of borided steel is affected by the medium of Boriding process [18][32][37]. While the minimum activation energy was obtained by plasma-paste boronizing for stainless steels of type AISI 304 with different mediums. The maximum activation energy was obtained by the salt boronizing process.

The other factor that is important for the activation energy is the composition of the steel being boronized. Presence of additional alloying elements is the controlling factor in the boronizing process. Alloying elements are responsible for hindering the diffusion process during boronizing. Steels are having a higher concentration of alloying elements needed a higher amount of activation energy.[18][34][37][38][39][46]

It can also be seen that the activation energy of boronized steel is affected by the heating medium. The minimum activation energy was obtained for AISI P20 steel boronized in microwave furnace as compared to the specimen boronized in the conventional furnace [40].

The activation energy for boronized steels is also affected by the boron potential of the boronizing mixture. Higher the availability of boron potential in the boronizing mixture lower will be the activation energy required.

Figure 2.9, showing the plot between layer thicknesses versus squared treatment time graphs from where the value of growth rate constant was calculated [18].

Figure 2.10, showing the plot between  $\ln R$  and inverse of time from where activation energy was calculated for different steels [18].

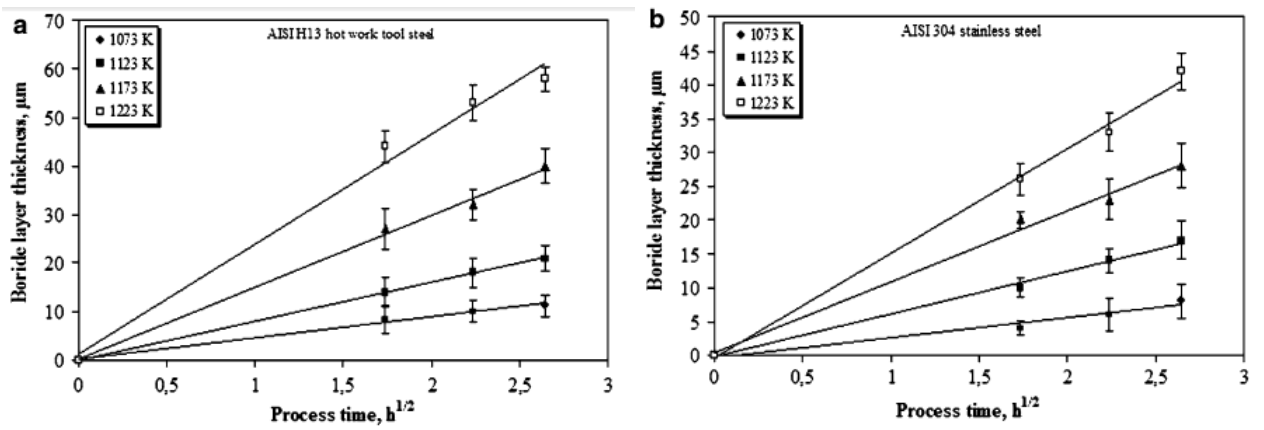


Figure 2.8: Boride layer thickness versus boronizing time at various temperatures for (a) AISI H13 steel and (b) AISI 304 steel. [18]

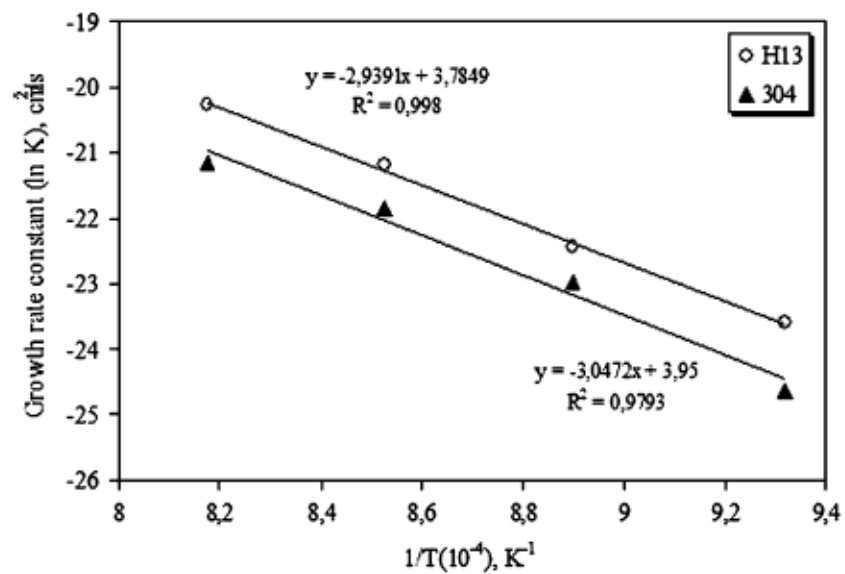
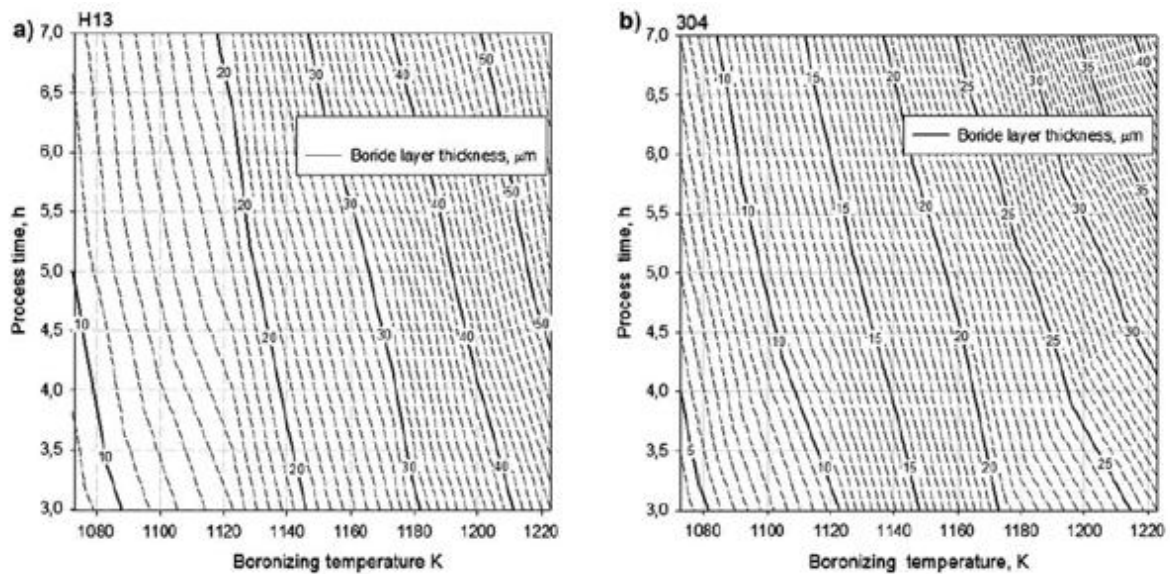


Figure 2.9: Growth rate constant versus temperature of boronized AISI H13 tool steel and AISI 304 stainless steel [18]



**Figure 2.10: Contour diagram of boride layer thickness of boronized: (a) AISI H13 steel and (b) AISI 304 Steel [18]**

### 2.1.8. Types of Boronizing Process

There are various types of boronizing processes are available but main types of boronizing process are [11]

- i. Pack boronizing
- ii. Paste boronizing
- iii. Liquid boronizing
- iv. Plasma boronizing

#### 2.1.8.1. Pack boronizing

Pack boronizing is the widely used method because of safety and easy handling and low cost. In the process cleaned and smooth components are packed in boronizing powder mixture having powder thickness 10 to 20 mm in a heat resistant steel box, then it is heated until determined temperature (800 ~ 1100° C) and time. The boron is diffused to the metal forming the boride layer. Powder mixture generally consists of:

- I. Boron yielding substances,
  - i. Diluents
  - ii. Activators

Boron yielding substances are  $B_4C$ , amorphous carbon and ferroboron. Generally,  $B_4C$  is suitable, having low boron potential compared to amorphous carbon and ferroboron and less expensive. Diluents do not take part in the reaction, but controls the percentage of boron and prevents caking of boronizing powder.  $SiC$  and  $Al_2O_3$  are widely used diluents. Activators are used to start and accelerate the reactions. Figure 2.12 shows schematic of Pack boronizing of single component. Various compositions are given below

- 5%  $B_4C$ , 90%  $SiC$ , 5%  $KBF_4$
- 50%  $B_4C$ , 45%  $SiC$ , 5%  $KBF_4$
- 85%  $B_4C$ , 15%  $Na_2CO_3$
- 95%  $B_4C$ , 5%  $Na_2B_4O_7$
- 84%  $B_4C$ , 16%  $Na_2B_4O_7$
- Amorphous boron (containing 95 to 97% B)
- 95% amorphous boron, 5%  $KBF_4$

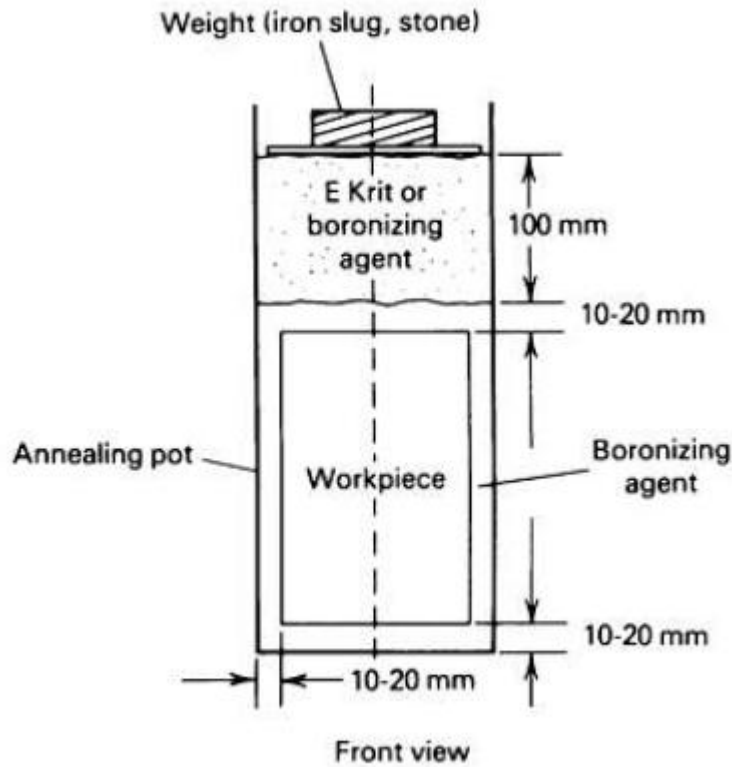


**Figure 2.11: Schematic Diagram of Pack boronizing of single component [8]**

### **2.1.8.2. Paste Boronizing**

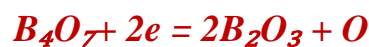
Paste boronizing is used commercially when pack boronizing is difficult, more expensive, or time-consuming. In this process, a paste of 45%  $B_4C$  (grain size 200 to 240  $\mu m$ ) and 55% cryolite ( $Na_3AlF_6$ , flux additive), or conventional boronizing powder mixture ( $B_4C-SiC-KBF_4$ ) in a good binding agent (such as nitrocellulose dissolved in butyl acetate, aqueous solution of methyl cellulose, or hydrolyzed ethyl silicate) is repeatedly applied (that is, brushed or sprayed) at intervals over the entire or selected portion of parts until, after drying, a layer about 1 to 2 mm thick is obtained. Subsequently, the ferrous materials are heated to 900°C, for 4 h) inductively, resistively, or in a conventional furnace to 800 to 1000°C for 5 h. In this process, a protective atmosphere (for example, argon, cracked  $NH_3$ , or  $N_2$ ) is necessary. A layer more than 50  $\mu m$  thicknesses may be obtained after inductively or resistively heating to 1000°C for 20 min. Paste boronizing is suitable for large size components.

### 2.1.8.3. *Liquid Boronizing*

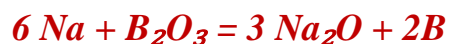
Liquid boronizing is grouped into two type's-electro less salt bath boronizing and electrolytic salt bath boronizing

- ***Electro less salt bath boriding*** of ferrous materials is carried out in a borax-based melt at about 900 to 950 °C to which about 30 wt% B<sub>4</sub>C is added. The boronizing action can be further improved by replacing up to 20 wt% B<sub>4</sub>C with ferro-aluminum because it is a more effective reductant. However, superior results have been found by using a salt bath mixture containing 55% borax, 40 to 50% ferroboration, and 4 to 5% ferro-aluminum. It has also been shown that 75:25 KBF<sub>4</sub>-KF salt bath can be used at temperature below 670°C for boronizing nickel alloys, and at higher temperatures for ferrous alloys, to develop the desired boride layer thickness.
- ***Electrolytic Salt Bath Boriding.*** In this process, the ferrous part acting as the cathode and a graphite anode are immersed in the electrolytic molten borax at 940 °C for 4 h using a current density of about 0.15 A/cm<sup>2</sup>. The parts are then air cooled. In general, the parts are rotated during the treatment to obtain a uniform layer. A high current density produces a thin coating on low- alloy steels in a short time. For high-alloy steels of greater thickness, lower current densities are required for a longer time.

In the fused state tetra-borate decomposes into boric acid and nascent oxygen.



Simultaneously, sodium ions, after being neutralized near cathode, react with boric acid to liberate boron.



In this manner, a high boriding potential is established near the cathode region. Other satisfactory electrolytic salt bath compositions include:

***KBF<sub>4</sub>-LiF-NaF-KF*** Mixture for parts to be treated at 600 to 900 °C.

#### ***2.1.8.4. Gas Boronizing***

Gas boriding may be accomplished with:

- i. Diborane ( $B_2H_6$ )- $H_2$  mixture
- ii. Boron halide- $H_2$ /or (75:25  $N_2$ - $H_2$ ) gas mixture
- iii. Organic boron compounds such as  $(CH_3)_3B$  and  $(C_2H_5)_3B$

Boronizing with  $B_2H_6$ - $H_2$  mixture is not commercially viable due to the high toxic and explosive nature of diborane. When organic boron compounds are used, carbide and boride layers form simultaneously. Because  $BBr_3$  is expensive and is difficult to handle (with violent reactions with water), and because  $BF_3$  requires high reduction temperature (due to its greater stability) and produces HF fumes,  $BCl_3$  remains the attractive choice for gas boriding.

When parts are gas borided in a dilute (1:15)  $BCl_3$ - $H_2$  gas mixture at a temperature of 700 to 950°C and a pressure up to 67 kPa, a boride layer 120 to 150  $\mu m$  thick is reported to be produced at 920 °C in 2 h. Recent work has suggested the use of 75:25  $N_2$ - $H_2$  gas mixtures instead of  $H_2$  gas for its better performance because of the production of boride layers with minimum FeB content. The latter phase can be easily eliminated during the subsequent diffusion treatment before hardening.

#### ***2.1.8.5. Plasma Boronizing***

Both mixtures of  $B_2H_6$ - $H_2$  and  $BCl_3$ - $H_2$ -Ar may be used successfully in plasma boronizing. However, the former gas mixture can be applied to produce boride layer on various steels at relatively low temperatures such as 600°C, which is impossible with a pack or liquid boronizing process. It has been claimed that plasma boriding in a mixture of  $BCl_3$ - $H_2$ -Ar gases shows good features such as better control of  $BCl_3$  concentration, reduction of the discharge voltage, and higher micro hardness of the boride films. Figure 2.12 shows a schematic layout of a plasma boriding facility the dual-phase layer is characterized by visible porosity, occasionally associated with a black boron deposit. This porosity, however, can be minimized by increasing the  $BCl_3$  concentration. Boride layers up to 200  $\mu m$  in thickness can be produced in steels after 6h treatment at a temperature of 700 to 850°C and a pressure of 270 to 800 Pa (2 to 6 torr).

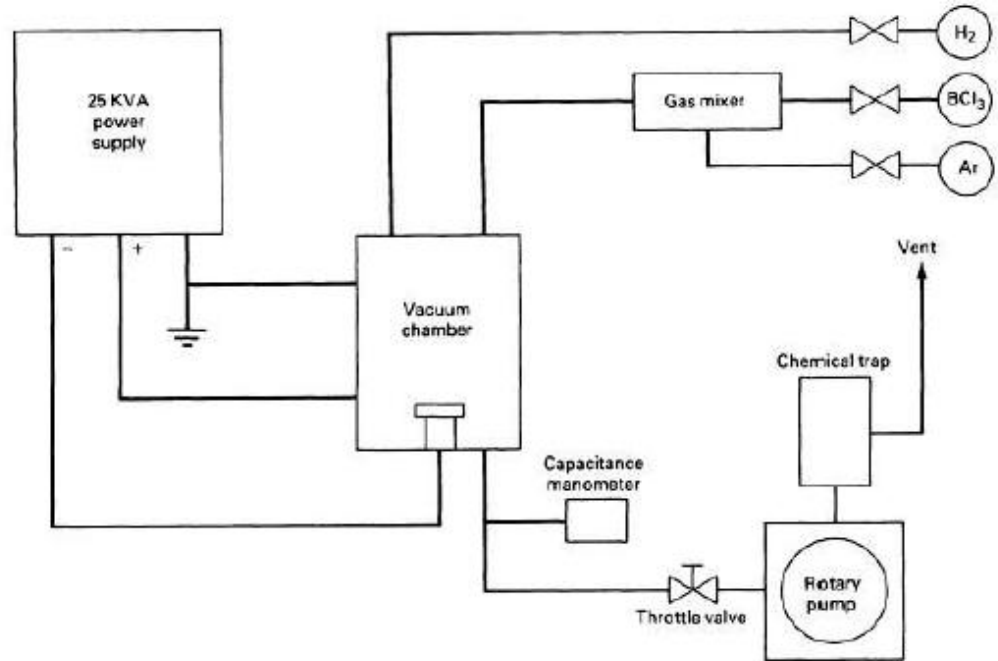


**Figure 2.12: Layout of plasma boronizing facility. [11]**

All these above boronizing processes have their advantages and disadvantages, but gas based processes are having major disadvantage. The gas based boronizing treatments use very toxic gas for boronizing, making their use limited for industrial applications. Liquid based systems use cyanides and other salts these are also toxic and hazardous sources imposing limitation on its use. Solid (pack) boronizing and to some extent paste boronizing is widely used process for boronizing of industrial parts.

It is also observed that boron diffusion, layer thickness and morphology of boride layer can also be affected by boronizing process [41].

Yoon et al. [42] reported that by using the plasma paste boronizing method for stainless steel, a thick boride layer with a flat structure could be obtained in a shorter time and at a lower temperature than that obtained using conventional thermal diffusion boronizing. [Kinetics]

Texture and size of powder particles, composition of boronizing medium being used also has effect on the boride layers. S. Sahin investigated the effect of particle size of powder used in the boronizing process with solid boron-yielding substances on the boride layer by using EKABOR powder as the boronizing agent which was classified into four groups according to particle size [43]. Layer thickness and

morphology can also be controlled by changing the composition of boronizing medium [44].

### 2.1.9. Application of Boronized Steels

The type of steels (borided) and corresponding applications are summarised in the following Table.

**Table 2.3: Typical combinations of borided steels and their applications**

<b>Steel (AISI)</b>	<b>Applications</b>
C1020	bushes, pipe bends, conveyor tubes, baffle plates, runner, base plates, helical gear drive for oil pumps, pump shafts
C1043	Pins, guide rings, grinding disks, bolts
C1138	shaft protection sleeves, mandrels
C1042	swirl elements, nozzles (for oil burners), rollers, bolts
D3	press tools, punches, dies
L2	drawing punches
H11	plungers, injection cylinders, sprue orifices, ingot moulds
H13	
H10	forging dies
D6	straightening rollers
S1	dies, necking rings, punches, drawing dies
D2	drawing tools, rolls for cold mills
L6	bolts, casting inserts, drop forges, forging dies
O2	bending dies, moulds, engraving rollers, drawing dies, press tools, piercing punches
E52100	balls and rollers for rolling bearings
410	valve components
420	parts for chemical plants
302	screw cases, box screws
316	perforated screens, valve plugs
321	rings, conveyor jets, injectors
316 Ti	parts for the chemical industry
4317	bevel gears
EN41B	Valve stems, connecting rods, Clutch plates, Shackle pins, Die casting dies
4140/EN19	press tool dies, extruder screws, extruder barrels, non-return valves
EN24/4340	gears, shafts, studs and bolts

### 2.1.10. Characterization of Boronized Specimen

Characterization of boronized specimen can be done by various methods such as optical microscope, SEM, X-ray diffraction, EPMA. Boronized layer morphology and types of borides formed can be confirmed by optical microscopy, scanning electron microscopy (SEM) and X-ray diffraction analysis. The characterization of boronized steels by using these methods has been done by many investigators.

S. Sen et.al. Followed same methods for characterization of borides formed on AISI 4140 steel and borides formed after short duration oxidizing treatment to obtain low friction. Figure 2.13 shows optical as well as SEM cross-sectional view of boronized samples at 850 and 950°C for 4h. Fig. reveals a needle shaped compact and porosity free structure to a depth of 202  $\mu\text{m}$  and good bonding to substrate [45].

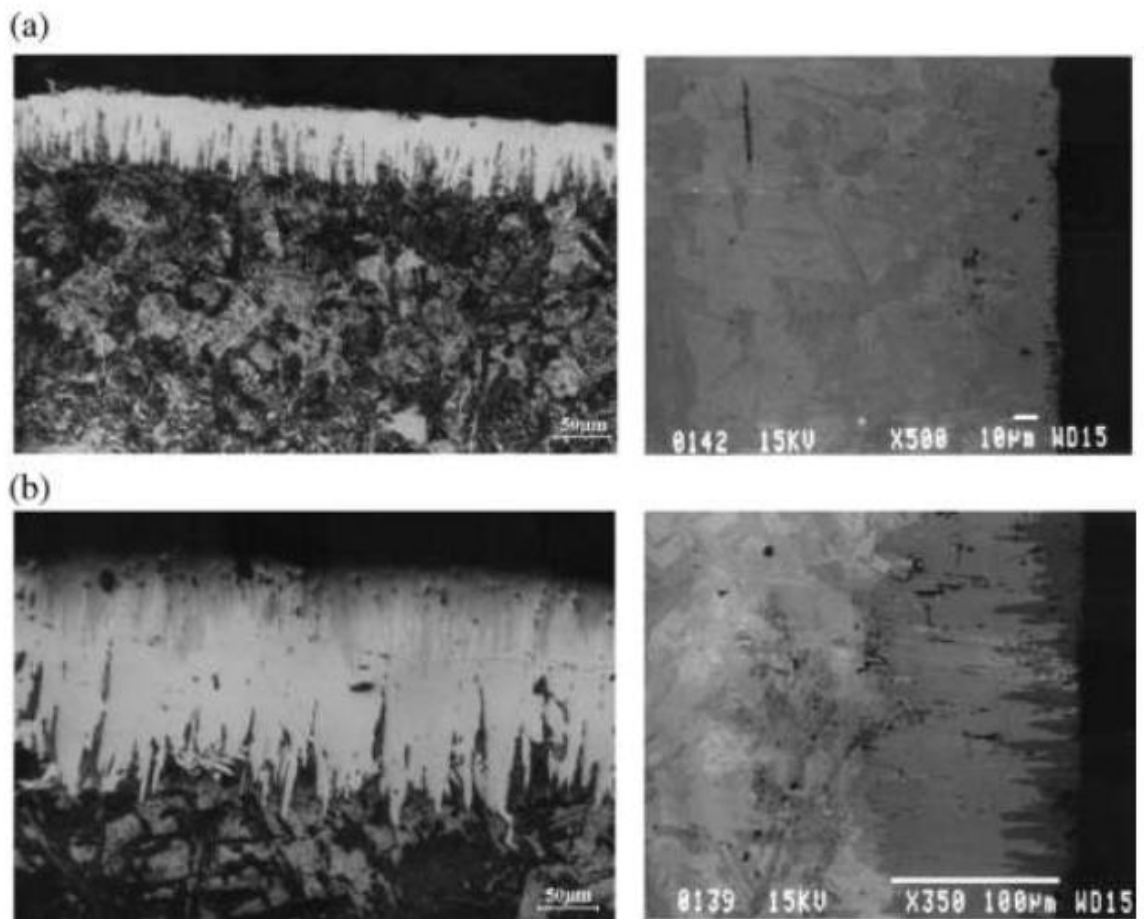


**Figure 2.13: Optical microscope and SEM cross-sectional views of the borided AISI 4140 steel (a) at 850°C and (b) 950 °C for 4 h showing morphology of borides [45].**

X-ray diffraction analysis by using high resolution diffractometer with  $\text{CoK}\alpha$  radiation of 0.17902nm shows various borides formed on AISI 4140 steels (Figure 2.14).

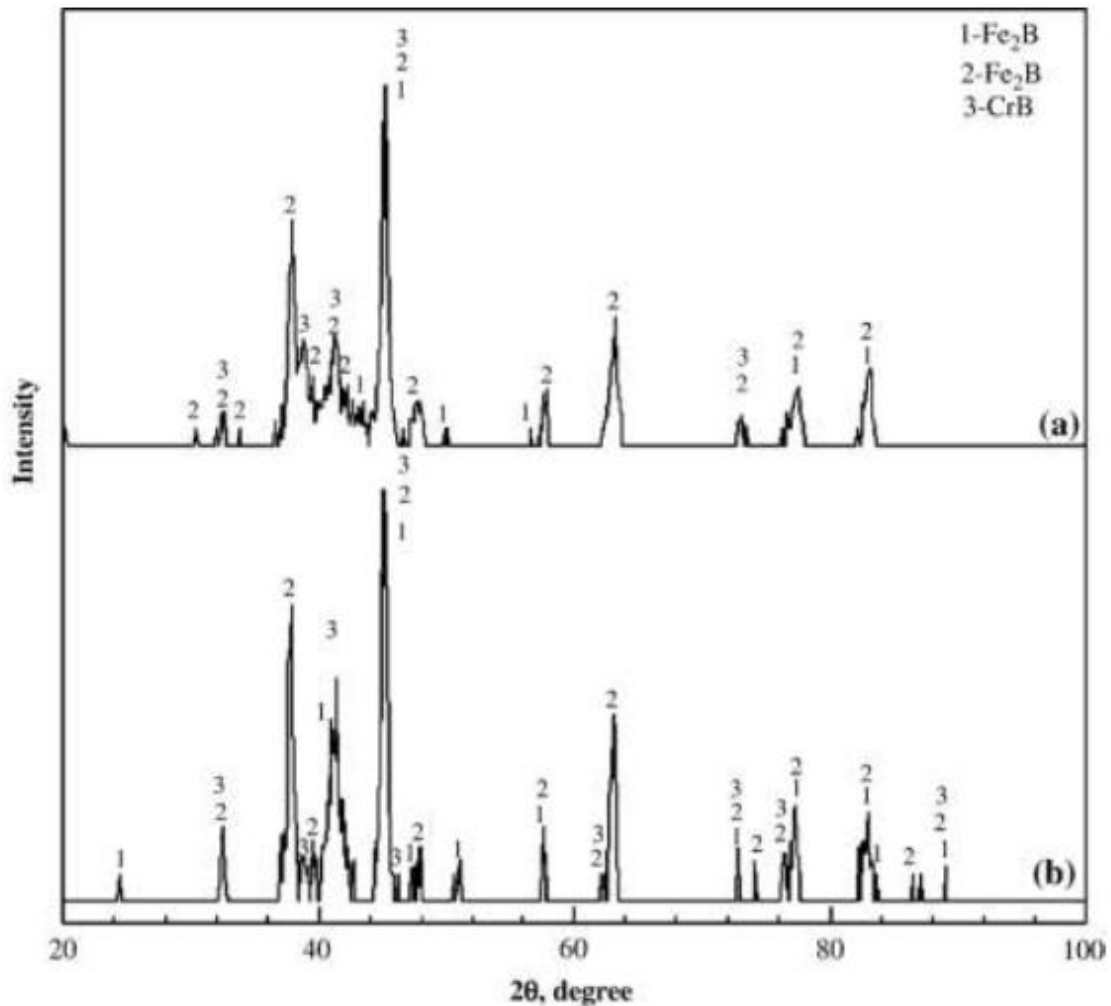


**Figure 2.14: X-ray diffraction (XRD) pattern of borided AISI 4140 steel at (a) 850 °C and (b) 950 °C for 6h. [45]**

### 2.1.11. Effect of boronizing on Hardness

Boronizing is one of the promising surface modification methods to produce extremely hard surfaces on steels under industrial conditions [17].

Boride layer can develop a layer having hardness in the range of 1400 -2100 HV on steel. Hardness of the boride layer can be retained at higher temperatures also. Many researchers have reported that the hardness achieved with boronizing is much higher

than the hardness achieved with carburising [47], nitriding [48], carbonitriding [49] and chromium plating [50].

The typical surface hardness of borided steels compared with other treatments and hard materials are given in the Table 2.4[17].

**Table 2.4: Typical surface hardness of borided steels compared with other treatments and hard materials**

Material	Micro Hardness (HV)
Borided steels	1400 – 2100
Quenched steel 900	900
Hardened and tempered H13 die steel	540-600
Hardened and tempered A2 die steel	630-700
High speed steel (BM-42)	900-910
Nitrided steels	650-1100
Carburised low-alloy steel	650-950
Hard chromium plating	800-1100
Cemented carbides, WC+Co	1160-1820
TiN	2000
TiC	3500
SiC	4000
B4C	5000
Diamond	>10000

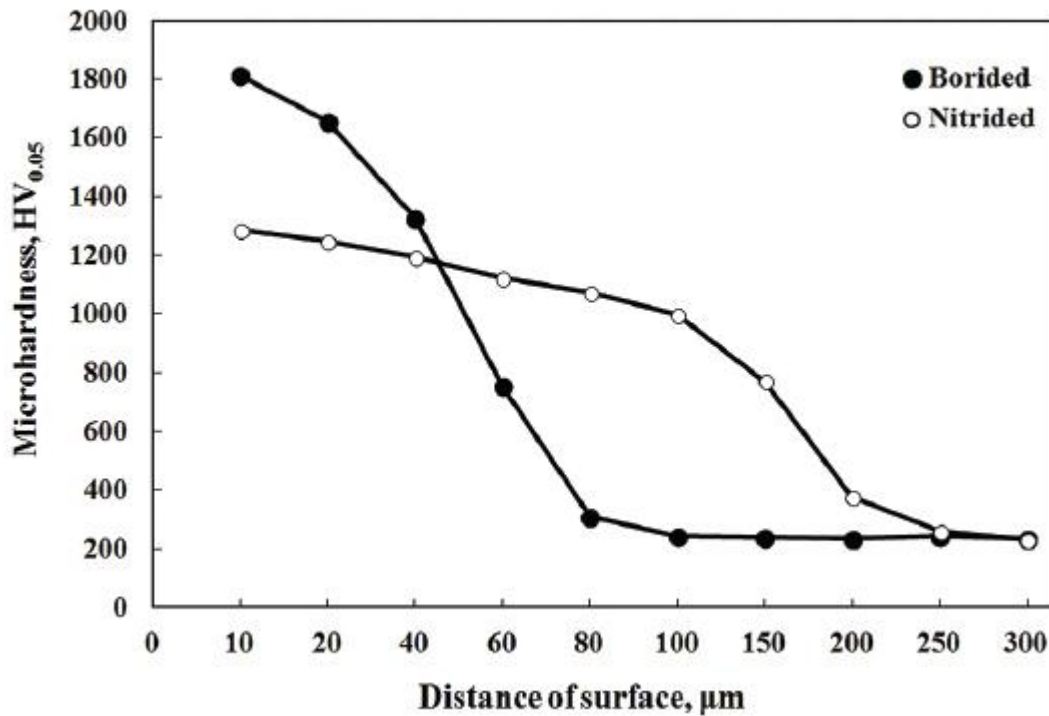


Figure 2.15: Variation of hardness depth profile in plasma nitrided and borided AISI M2 steel [48].

### 2.1.12. Effect of boronizing on corrosion.

Borided steel parts have an increased service performance under oxidizing and corrosive environment [17]. It has been seen that the chemical stability of plain carbon steels against acids, to HCl, increased significantly by boriding.

Boride layer on steels show good corrosion resistance against different acids HCl, H<sub>2</sub>SO<sub>4</sub>, HNO<sub>3</sub>.

Gunes et al. reported that steel AISI M2 boronized at 950°C for 6h had shown better corrosion resistance as compared to nitrided and untreated AISI M2[48].

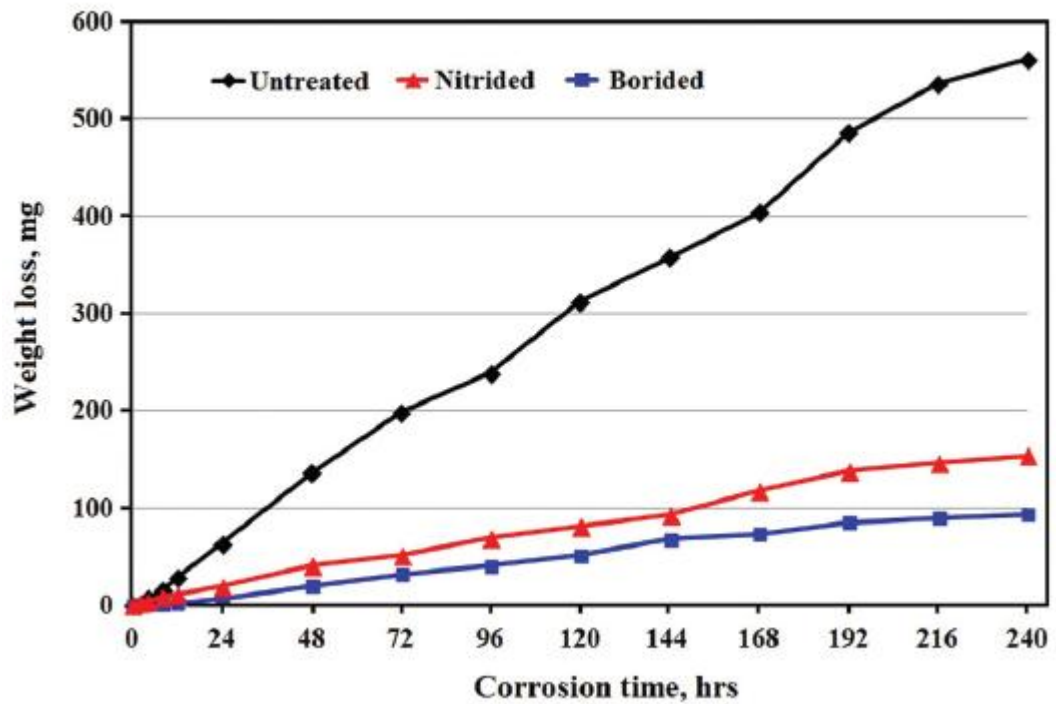


**Figure 2.16: Weight loss of immersion tests of the plasma nitrided and borided AISI M2 steel in 4% M HCl solution [48]**

A. Márquez-Herrera et al. also investigated the corrosion behaviour of ASTM A-36 Steel boronized at 900°C for 2h, 4h and 6h and untreated specimen. Corrosion was analyzed by using TAFEL and electro-chemical impedance spectroscopy (EIS) curves. It was observed that corrosion current,  $I_{corr}$  for specimen's C and D was lower than that of the untreated specimen. Sample E showed the highest corrosion current despite being boronized for 6h due to the surface degradation and increased surface roughness [51].

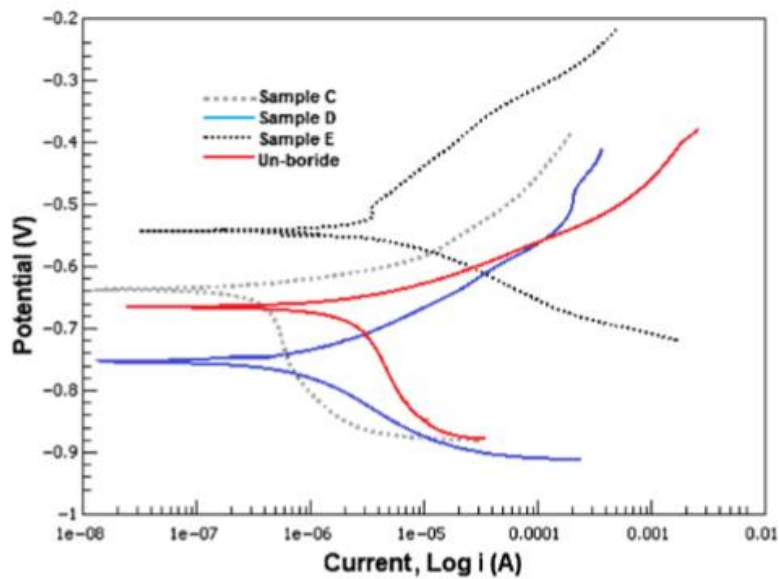


Figure 2.17: Tafel curves of un-boride and boride steels at 900 °C [51].

Table 2.5: Summary of results obtained from corrosion tests performed in 3.5 %wt. NaCl solution [48]

Sample	$E_{corr}$ (mV)	$I_{corr}$ ( $\mu$ A)
Un-boride	$-665 \pm 7$	$2.3 \pm 0.2$
C	$-636.68 \pm 6.31$	$0.32 \pm 0.03$
D	$-750.08 \pm 9.32$	$1.51 \pm 0.03$
E	$-542.02 \pm 11.01$	$2.72 \pm 0.23$

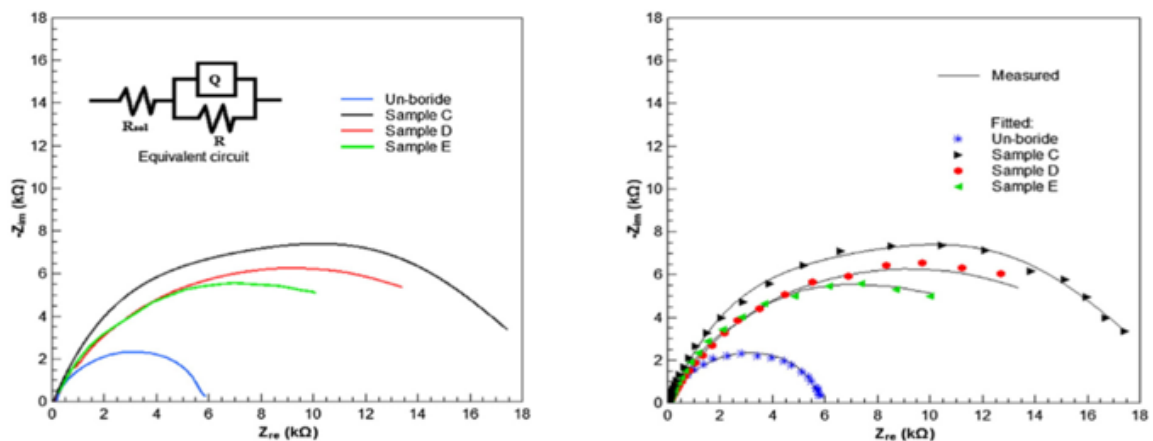


Figure 2.18 : Complex impedance curves (b) simulated spectrums and theirs experimentally generated for samples C, D and E in NaCl 3.5 %wt. Solution [51].



## *Chapter 3*

---

### **3. The scope of the Study**

Now a day's one of the major issues is developing innovative and economical surface modification processes using easily available and low-cost material that can impart better qualities to the surface of the material without altering its bulk properties.

In these processes optimization of process, parameters need to be done for low cost and time-saving methods for the surface modification. Kinetic studies can also be carried out, and activation energies and diffusion coefficients can be calculated for different low alloy steels. Based on which empirical relations can be drawn which can be convenient for technological and industrial application, and can be used for estimation of boride layer thickness independence on boronizing parameters (temperature and time)?

During literature review, it was found that no work has been done to know about the remaining boron potential in the boronizing mixture. Weather the mixture can be used further for boronizing process, or it would not have any boron potential left. It can be an important aspect because if the used mixture can be utilized for further boronizing treatment, it would be cost-effective. A comparison can be done between the boride layer obtained in boronized specimens with the fresh boronizing mixture and the boride layer obtained in boronized specimens with the used boronizing mixture. This comparison can give an idea about the left boronizing potential in the powder.

#### **3.1. Gap Analysis**

Better surface properties provided by the boronized layer have been attracting the attention of researchers and manufacturers. But there is insufficient knowledge related to the various aspects of the Boronizing method. Although many investigators have been working on boronizing, there is a lack of reproducibility and uniformity in the reported data. During the literature review some gaps were found in the available data which are as follows:

- i. Not much work has been done to see the *effect of process parameters on KINETICS and MICROSTRUCTURE*.
- ii. No data are available which investigated Kinetics of diffusion of boron into EN19, EN24, and EN41B (low alloy) steels.
- iii. Not much work has been done to study the *TRANSITION ZONE*.
- iv. No study has been done to measure the boron potential of the already used boronizing mixture.

### **3.2. Objectives**

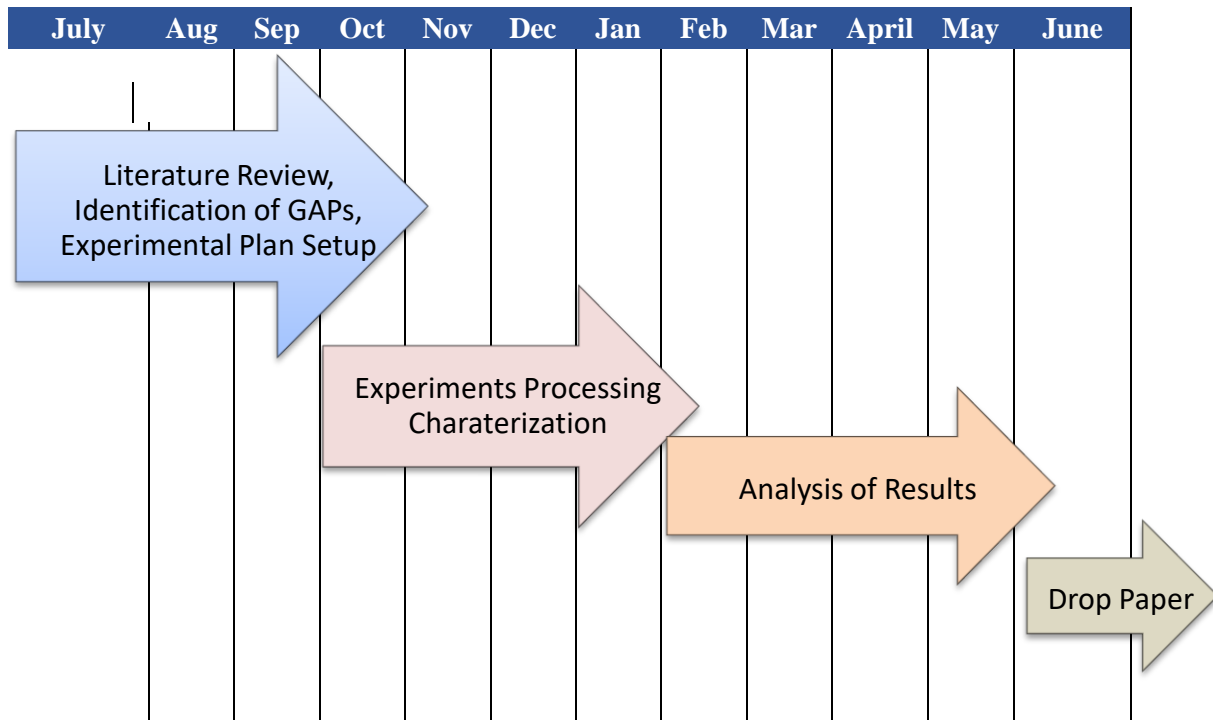
Based on the gaps found during the literature survey the objectives of this study are:

- i. To study the effect of process parameters on the morphology of borides, Microstructure and Kinetics.
- ii. Kinetic study of diffusion of boron in EN19, EN24, and EN41B steels.
- iii. To conduct the Boronizing process with the used Boronizing mixture and study its effects on boride layer morphology.
- iv. To study the effect of post boronizing heat treatment process like chromizing, aluminizing, etc on Boronized samples.

### 3.3. Timeline for the Study

Project Duration: **12 Months**

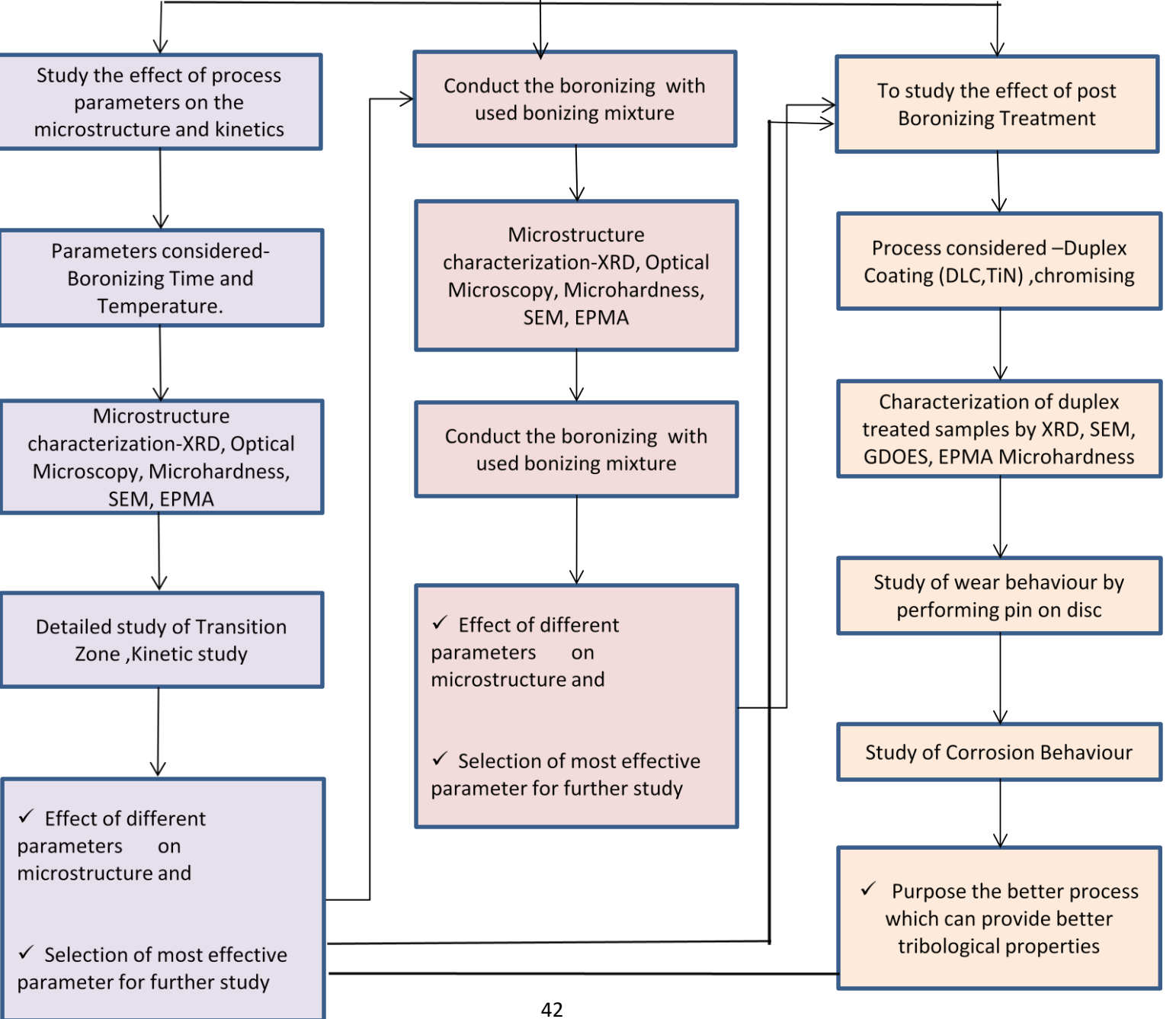
**JULY 2017-JUNE 2018**





Experimental Plan

Selection Process & Set-Up Design



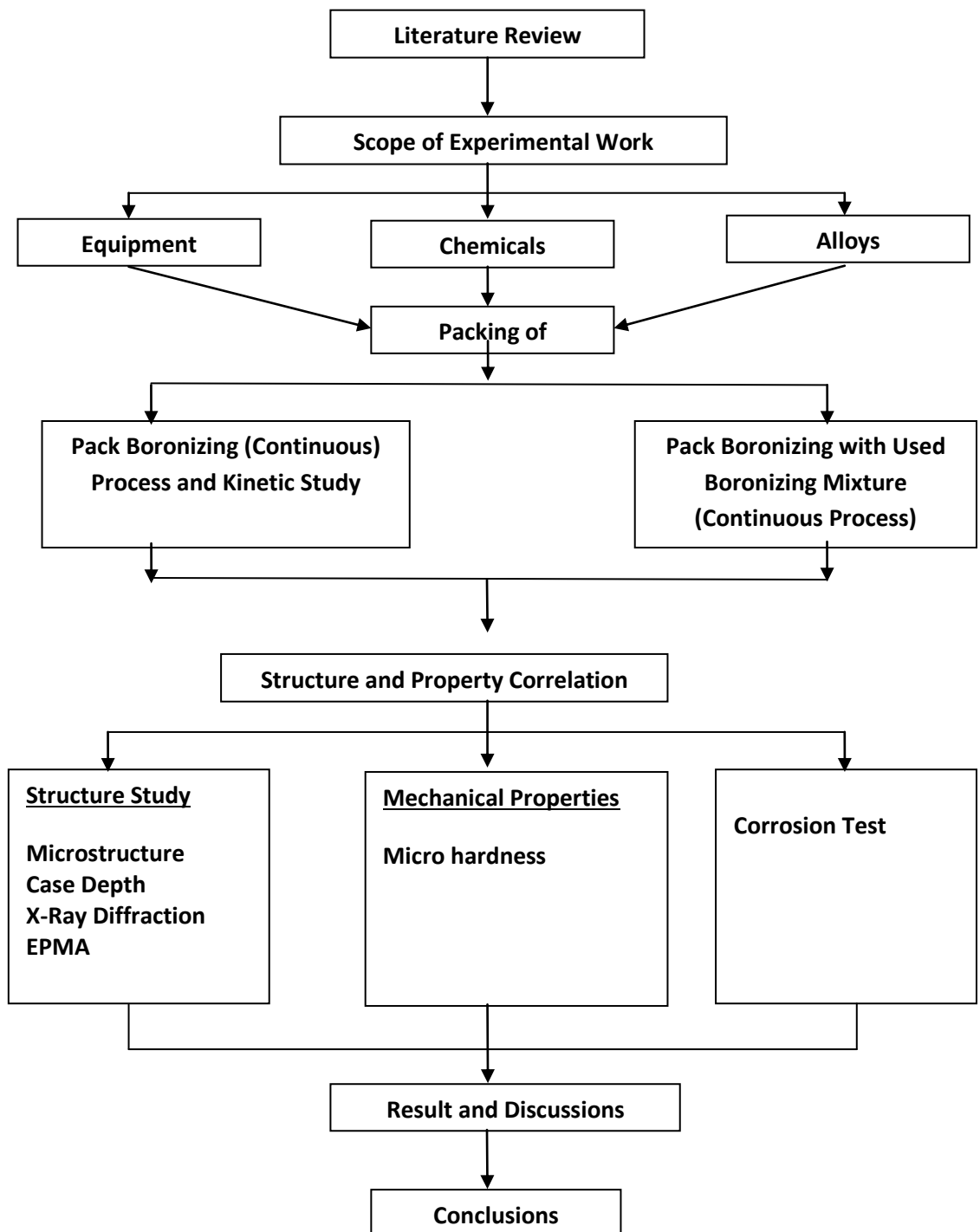


**Figure 3.1: Flow Chart Showing the Sequence of Tasks Performed.**



## *Chapter 4*

---

### **4. Experimental**

#### **4.1. Substrate Study**

This section deals with the study of substrate steel properties before boronizing.

##### **4.1.1. Substrate Material**

Substrate material used for heat treatment was EN19, EN24, EN41B. All steels were received in extruded bar condition having the diameter as respectively. EN19, EN24, EN41B are critical materials in industrial applications such as automotive, aerospace and in manufacturing industries.

###### ***4.1.1.1. EN19/AISI4140***

EN19 contains Cr and Mo as main alloying elements, which provide the high harden ability along with toughness. EN19 is high-quality alloy steel with tensile strength. With a combination of good ductility and shock resistance, EN19 is suitable for applications with very high loading such as engine gearboxes. Popular in the automotive sector, it is possible to machine the material extremely accurately, in recent years EN19 has become an established material in the Oil & Gas sector. The material lends itself well to any application where strength is a primary consideration. Its hardness is in the range 220/330HB

###### ***4.1.1.2. EN24/AISI4340***

EN24 is a very high strength steel alloy which is supplied hardened and tempered. The grade is a nickel-chromium, molybdenum combination - this offers high tensile steel strength, with good ductility and wear resistance characteristics with relatively good impact properties at low temperatures. EN24 is also suitable for a variety of elevated temperature applications. EN24T is used in components. Its hardness is in the range 248/302 HB.

###### ***4.1.1.3. EN41B/905M31***

EN41 is a chromium aluminium molybdenum nitriding steel. The material offers high wear resistance together with toughness and ductility. EN41 is defined by its

suitability for nitriding which gives the material a hard, wears resistant case. Its hardness is in the range 200/300HB.

The steel is widely used in Valve stems, connecting rods, Clutch plates, Shackle pins, Die casting dies.

As received bars of En19, EN24, EN41B steel was cut. Transverse and longitudinal sections were used for microstructure observations. The hardness of the steels was measured. Chemical composition of EN19, EN24, and EN41B steel was measured on optical emission spectrometer of the spark analyzer maker.

## **4.2. Boronizing**

**Boronizing** is the process by which boron was introduced to EN19, EN24, and EN41B steel to form a hard surface. In this process, boron atoms could diffuse into the surface of a metal component. Various parameters like container, temperature, time and heating rate were utilized to optimize the heat treatment process.

### **4.2.1. Process Selection**

Pack boronizing was selected as the boronizing process for this study due to the several advantages it offers. During literature survey, it was found that it's a widely used technique for boronizing because it requires little easily available equipment. However, the relative ease of handling and safety makes it the most popular process for boronizing. Some drawbacks are associated with the pack boronizing process. High process temperatures (850°C-1050°C), long duration (4-16h) are required to get an effective boride layer thickness.

### **4.2.2. Temperature & Time Selection**

As per the literature Boronizing can be carried out from temperature 800 to 1000 °C for process duration of 1h to 12h. It is clear from the phase diagram that Fe<sub>2</sub>B phase starts forming at a temperature above 800°C.

For this study three different working temperatures were selected, i.e., 850°C, 950°C and 1050°C for boronizing. Many investigators have reported a good parabolic relationship between layer thickness and process time in this temperature range. [\[37\]](#)[\[38\]](#)[\[39\]](#)[\[40\]](#).

**Table 4.1: showing different parameters for heat treatment**

<b>Sr. No.</b>	<b>Temp. (°C)</b>	<b>Time (h)</b>
1	850	2,4, 6
2	950	2, 4, 6
3	1050	2,4, 6

### **4.2.3. Substrate for Boronizing**

The substrates used for boronizing were EN19, EN24, EN41B steel having the dimensions of  $\phi 10*5\text{mm}$ ,  $\phi 15*5\text{mm}$ , and  $\phi 40*5\text{mm}$  respectively. For pack boronizing small specimens were used so EN41B was cut into four parts, and one part had been put in the pack boronizing container. After pack boronizing, those substrates were used to check coating morphology, coating thickness and other properties of boronized layer.

### **4.2.4. Boronizing Container Design**

Stainless steel containers were designed for boronizing treatment. One side was kept open for uniform heating of the component packed in the containers while one side of the container was kept closed. The container dimensions were selected as  $\text{Ø } 100 \times 120 \text{ mm}$  and thickness 5 mm as reported by A. A. JOSHI AND S. S. HOSMANI. In this study three mild-steel containers of different size, namely, small-size

container(SC), medium-size container (MC), and big-size container (BC) having the dimensions of (diameter\*height\*thickness) of 50mm\*120mm\*1 mm, 100mm\*120mm\*5.5 mm, and 200mm\*120mm\*2 mm, respectively, were utilized for pack boronizing and they reported that medium-size container was suitable for the formation of the single phase  $\text{Fe}_2\text{B}$  layer while double phase layer consisting of FeB and  $\text{Fe}_2\text{B}$  was produced with big size container[28].



**Figure 4.1: Photographs of container used for Pack Boronizing**

#### **4.2.5. Specimen Preparation**

The specimens were of dimension  $\phi 10*5$  mm,  $\phi 15*5$ mm and  $\phi 40*5$ mm having a disc shape. 100, 200, 400, 600 and 800-grade polishing paper were used to polish the samples on the polishing machine (Make: Struers; model: LaboPol-5) to obtain a good surface finish. The samples were cleaned with soap water solution and rinsed in tap water. After that, the samples were cleaned with acetone solution for 5 minutes.

#### **4.2.6. Packing of Components**

Specimens to be boronized were packed in the stainless-steel container prepared for the boronizing. The bottom of the container was filled with 20mm layer of the SiC powder which worked as an inert filler. Above the SiC layer, the container was filled

with 20mm layer of boronizing powder mixture (Boropak™). Polished and Cleaned specimens were carefully placed on top of the boronizing powder mixture. After specimens were placed container was again filled with 20mm thick layer of boronizing powder mixture followed by a 20mm thick layer of SiC on the top. After that to avoid oxidation or contact of air with the component, the container was filled with 20 to 25 mm thick layer of glass powder or alumina. This packed container was kept in the electrically heated muffle furnace for boronizing.

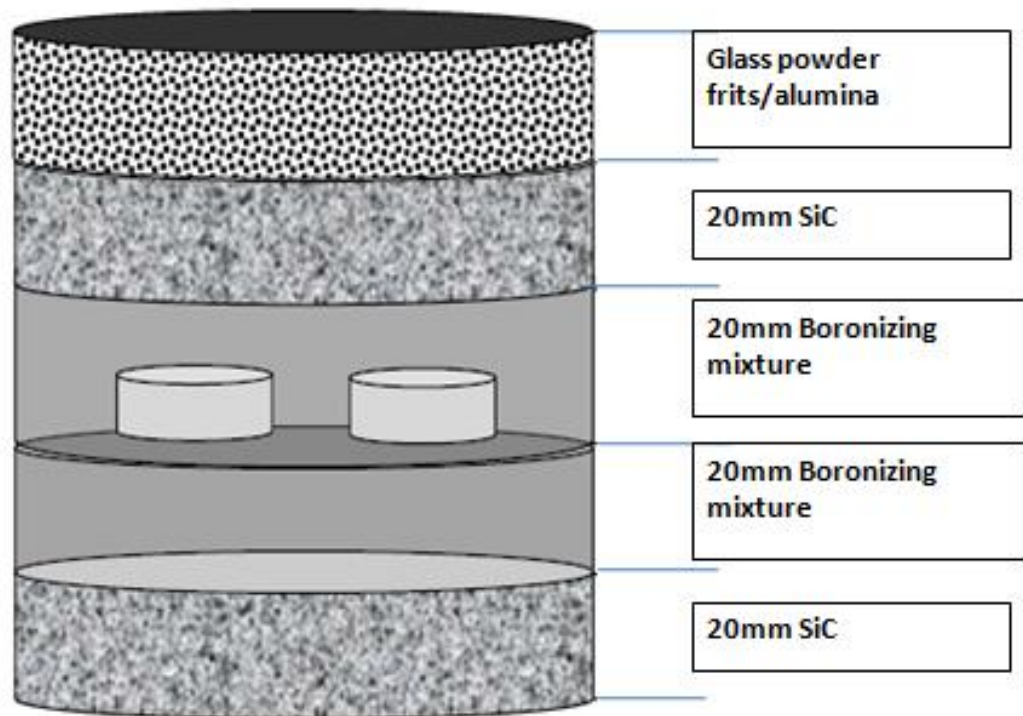


**Figure 4.2: Packing of the specimens for pack boronizing [28]**

#### **4.2.7. Boronizing Process**

The packed container with the samples was kept inside the heated muffle furnace for boronizing. Boronizing was done on the steel specimens of a small disc shape.

The specimens were packed boronized at 950° C for 4h in the electrically heated muffle furnace. After boronizing, the container was kept in open air for cooling. Details of the trial are given below in table 4.2.

**Table 4.2 Details of first Heat Treatment performed.**

<b>ID*</b>	<b>Temperature °C</b>	<b>Time h</b>	<b>Cooling</b>	<b>Heating rate</b>
<b>B1T2E1</b>	<b>950</b>	<b>4</b>	<b>air</b>	<b>4.5°C/min 650°C 15min,5°C/min 950°C</b>

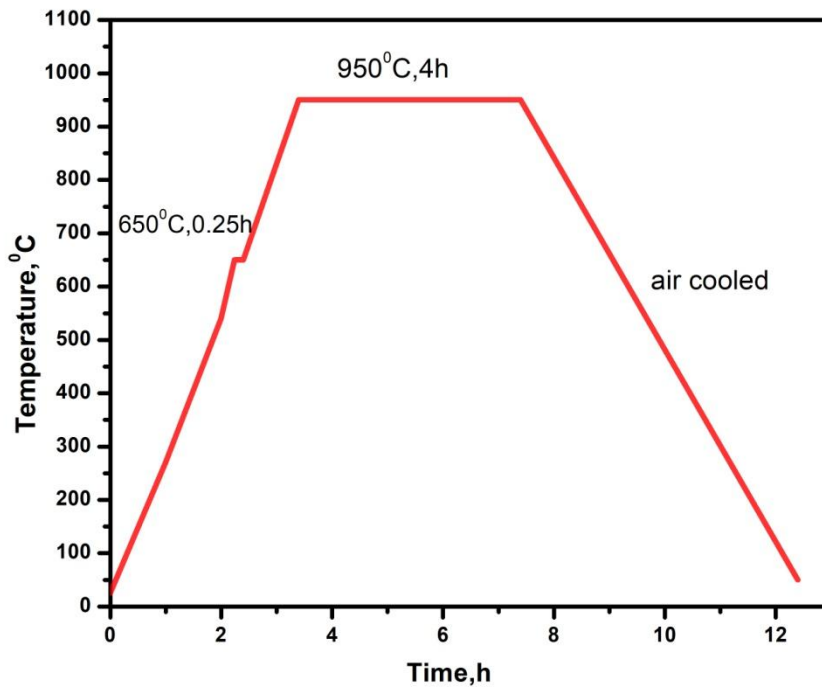


**Figure 4.3: Heat treatment cycle of boronizing done at 950°C for 4h**

#### 4.2.8. Design of Experiment for Boronizing of Specimens

After the successful trail experiment, design of experiment (DOE) was prepared for the study with the final parameters (temperature and time). Table 4.3-Table 4.5 shows the design of experiments that were planned for this study.

**Table 4.3: Design of experiment for optimization of boronizing process**

<b>Sr.No.</b>	<b>Material</b>	<b>Heat Treatment</b>	<b>Temperature °C</b>	<b>Time h</b>	<b>Cooling</b>
<b>1</b>	<b>EN19</b>	<b>Boronizing</b>	<b>850</b>	<b>2,4,6</b>	<b>Air</b>
<b>2</b>	<b>EN19</b>	<b>Boronizing</b>	<b>950</b>	<b>2,4,6</b>	<b>Air</b>
<b>3</b>	<b>EN19</b>	<b>Boronizing</b>	<b>1050</b>	<b>2,4,6</b>	<b>Air</b>

**Table 4.4: Design of experiment for optimization of boronizing process for EN24**

<b>Sr.No.</b>	<b>Material</b>	<b>Heat Treatment</b>	<b>Temperature °C</b>	<b>Time h</b>	<b>Cooling</b>
<b>1</b>	<b>EN24</b>	<b>Boronizing</b>	<b>850</b>	<b>2,4,6</b>	<b>Air</b>
<b>2</b>	<b>EN24</b>	<b>Boronizing</b>	<b>950</b>	<b>2,4,6</b>	<b>Air</b>
<b>3</b>	<b>EN24</b>	<b>Boronizing</b>	<b>1050</b>	<b>2,4,6</b>	<b>Air</b>

**Table 4.5: Design of experiment for optimization of the boronizing process for EN41B**

<b>Sr.No.</b>	<b>Material</b>	<b>Heat Treatment</b>	<b>Temperature °C</b>	<b>Time h</b>	<b>Cooling</b>
<b>1</b>	<b>EN41B</b>	<b>Boronizing</b>	<b>850</b>	<b>2,4,6</b>	<b>Air</b>
<b>2</b>	<b>EN41B</b>	<b>Boronizing</b>	<b>950</b>	<b>2,4,6</b>	<b>Air</b>
<b>3</b>	<b>EN41B</b>	<b>Boronizing</b>	<b>1050</b>	<b>2,4,6</b>	<b>Air</b>

The specimens used to be of different dimensions having a disc shape. Total twenty-seven samples were used to study the effect of boronizing on the specimen. The specimens were ground up to 800-grade emery paper and polished on polishing machine (Make: Struers; model: LaboPol-5) to obtain a good surface finish. The samples were cleaned with soap water, rinsed in tap water and then cleaned with acetone solution for 5 minutes.

#### 4.2.9. Boronizing

The three specimens were packed in a stainless steel container. The container was 100 mm diameter and 120 mm height. The pack mixture contained “Boropak” which acted as boronizing mixture and SiC, acted as diluents or inert filler. The thickness of the boronizing powder layer and the SiC layer was kept to 20mm. As already discussed in section 3.2.6 that the top of the container was covered with glass powder or alumina to prevent oxidation of pack powders and specimens. The container used for packing shown in the photograph. After the packing of all the components, the container was boronized at 850°C 950 °C and 1050°C for 2, 4 and 6 hours in an electrically heated muffle furnace with heat treatment cycle. After the cycle was completed container was kept in air for air cooling.

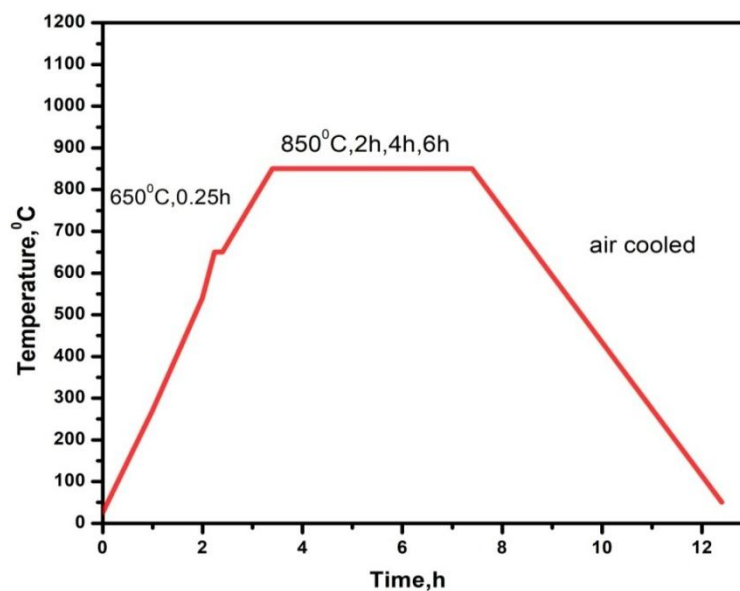
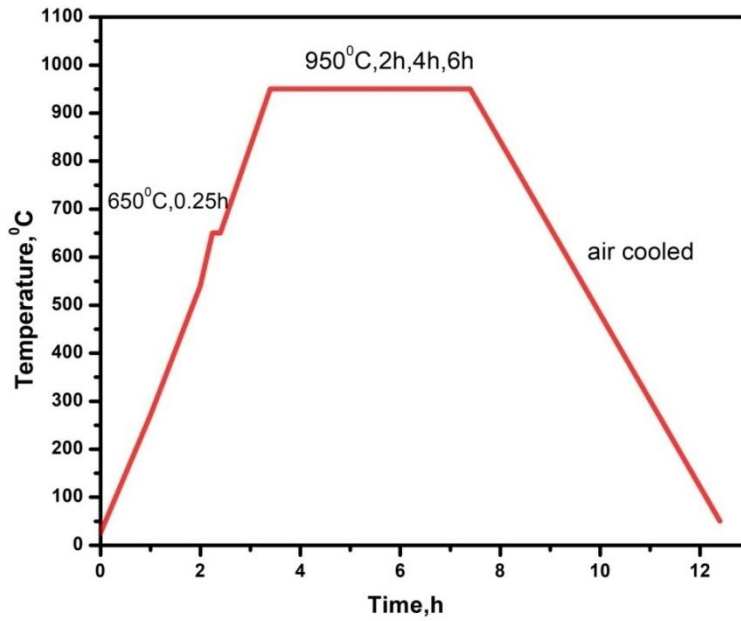
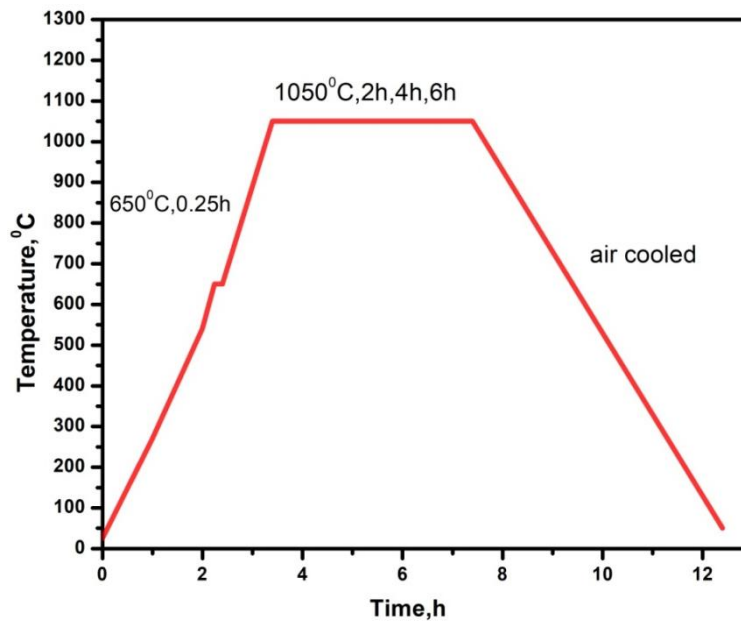


Figure 4.4: Heat treatment cycle for specimens boronized at 850°C



**Figure 4.5: Heat treatment cycle for specimens boronized at 950°C**



**Figure 4.6: Heat treatment cycle for specimens boronized at 1050°C**

### **4.3. Post-Boronizing Operations**

After boronizing all the specimens were removed from the container. They were cleaned with soap solution and rinsed with tap water followed by cleaning with acetone for 5 minutes. After cleaning the specimens were prepared for further investigations.

#### 4.4. Heat Treatment with used Boropak Powder

In this heat treatment, the boronized layers were formed on the surfaces of specimens using a pack boronizing method. The processes were performed at the temperature of 1050°C at a holding time of 4 hours with a used boronizing mixture (Boropak powder). The experiment aimed to know about the remaining boron potential in the boronizing mixture.

##### 4.4.1. Packing of Components

Packing of specimens was done with the same method discussed in section 3.2.6. The specimens were placed on the top of the layer of boronizing mixture which was already used in the heat treatment cycle discussed in section 3.2.8.

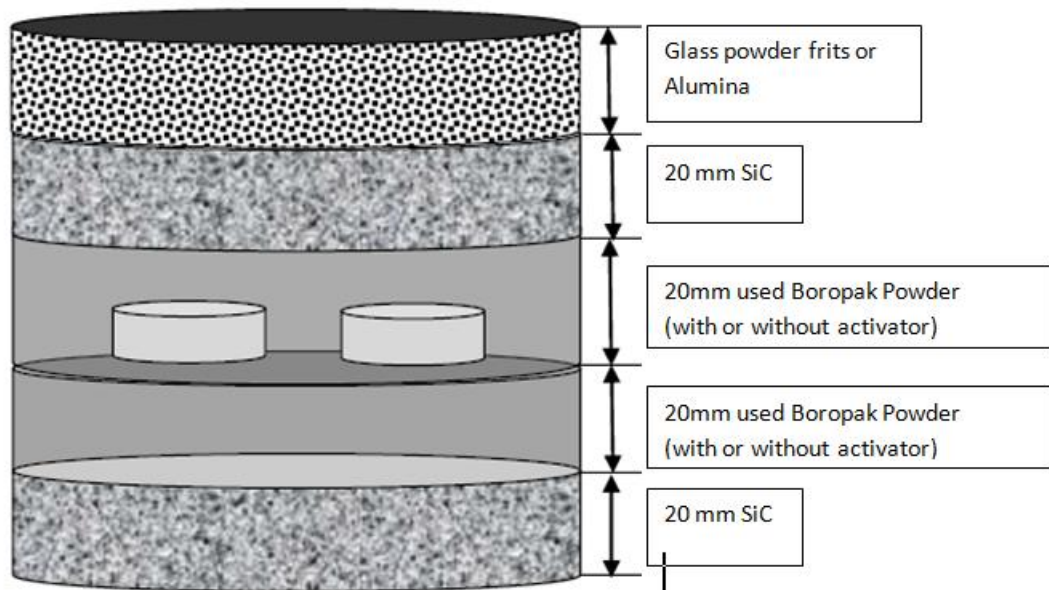


**Figure 4.7: Packing of components with used boronizing mixture.**

**Table 4.6: Design of experiment for optimization of the boronizing process with used boronizing mixture**

Sr.No	Material	Heat Treatment	Boronizing Mixture	Temp. °C	Time h	Cooling
1	EN19, EN24, EN41B	Boronizing	Without activator	1050	4	Air
2	EN19, EN24, EN41B	Boronizing	With activator (NH <sub>4</sub> Cl)	1050	4	Air

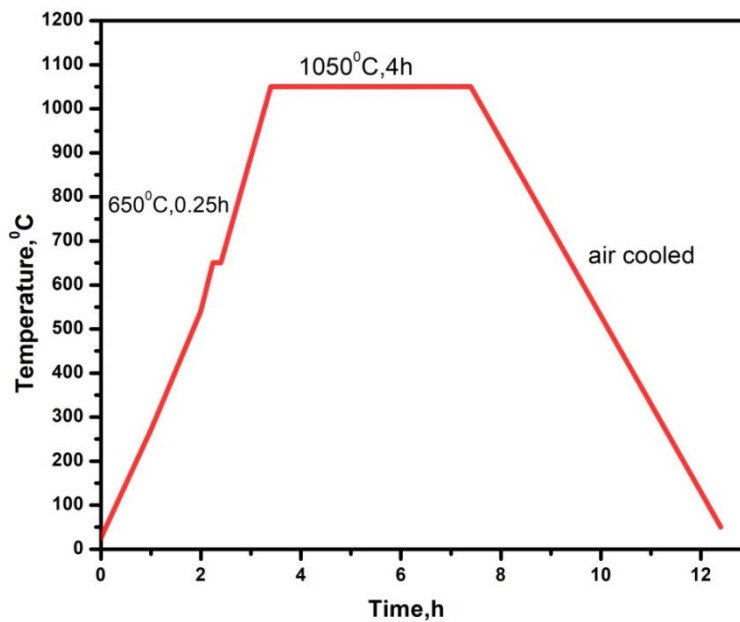


**Figure 4.8: Heat treatment cycle for the boronizing process with the used boronizing mixture.**

## **4.5. Characterization**

### **4.5.1. Chemical Composition**

Chemical composition of substrate steels was measured using optical emission spectrometer (Model: Spectro lab M).

### **4.5.2. Microstructure Study**

Specimens were prepared for the metallographic study by taking cross sections of all specimens. Specimens were cut on the slow speed diamond cutter. The cutting speed was kept low to make sure that there was no damage to the boride layer. These specimens were mounted using hot compression mounting machine using thermosetting powder (Bakelite) with temperature of 200°C and a force of 15 kN with cooling time of 3 min. After mounting, grinding of specimens was done using 220 to 2000 grade SiC paper by wet polishing method on polishing machine (make: Struers, model: LaboPol-5). Polishing of grinded specimens was also done with 3µm and 1µm diamond paste in order to obtain a mirror finish on the specimens. Polished specimens were cleaned ultrasonically with acetone and etched by using 2% Nital. After etching the samples were rinsed under the tap water and again were cleaned with acetone.

#### ***4.5.2.1. Optical Microstructure***

The etched specimens were observed under an optical microscope (make: Leica, model: DMI) for micro structural study. Magnifications from 100X to 500X were utilized to study the borided specimens. Coating thickness of boronized specimens was measured using a digital camera attached to the optical microscope and by using analysis software (*ZEISS software*). readings for Coating thickness of specimens were taken at different locations. 10 to 15 readings were taken at different locations and their arithmetic average was reported.

#### 4.5.2.2. Coating Thickness Measurement Methods

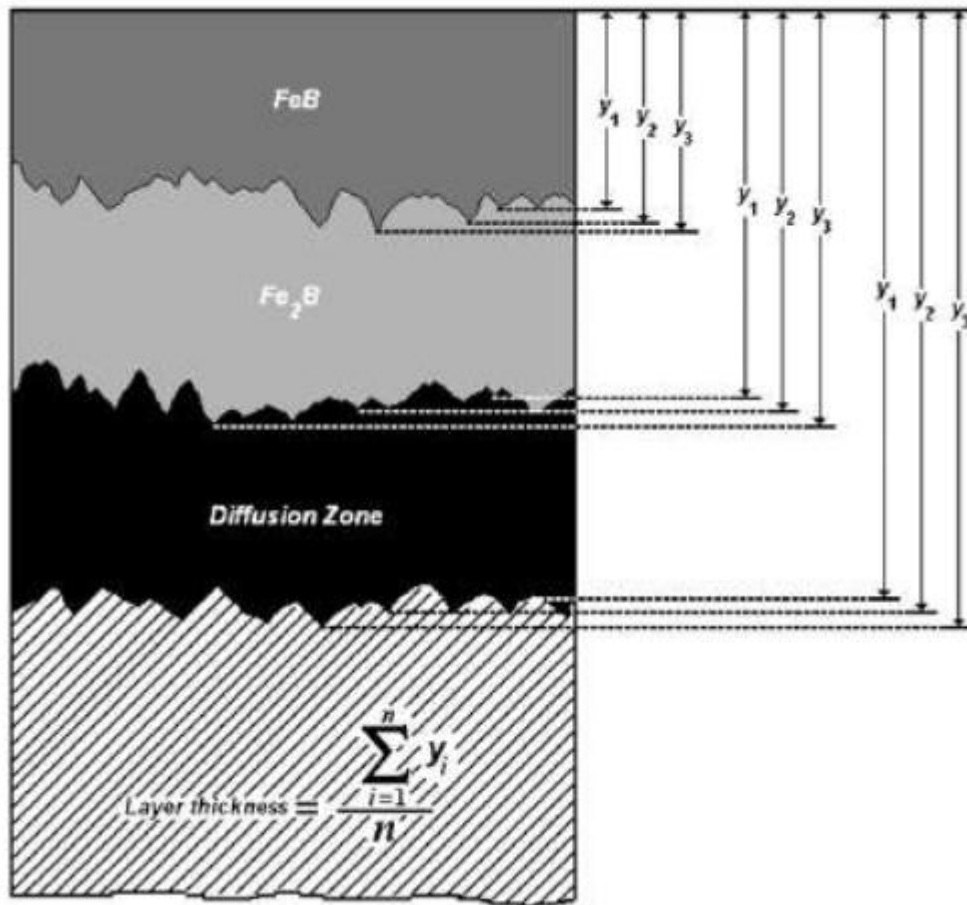


Figure 4.9: Procedure to measure the FeB/Fe<sub>2</sub>B and diffusion zone thicknesses [52]

#### 4.5.2.3. Scanning Electron Microscopy (SEM) Study

For SEM study, the mounted specimens used for the optical microstructure study were utilized. Boronized specimens were studied on SEM by secondary electron imaging and back scattered imaging. Surface and coating morphology of specimens, phases present were observed and studied. Energy dispersive spectroscopy (EDS) analysis with SEM was also done to know about the variation in the concentration of alloying elements through the boride layer.

### **4.5.3. X-ray Diffraction (XRD) Study**

X-ray diffraction technique was used to identify phases present in the coating as well as substrate steel. XRD patterns were also obtained and analyzed. XRD study was done on the x-ray diffractometer (make: Bruker D2 Phaser).  $2\theta$  angles were taken from  $20-80^\circ$ . The XRD pattern was compared with JCPDS files to identify various x-ray peaks obtained. Specimens were of semi-disc shape, having 1mm thickness for XRD test.

### **4.5.4. Electron Probe Micro-Analyzer (EPMA)**

An electron probe micro-analyzer is a micro beam instrument used primarily in the non-destructive chemical analysis of minute solid samples. It is fundamentally the same as an SEM, with the added capability of chemical analysis. The primary importance of an EPMA is the ability to acquire precise, quantitative elemental analyses at very small "spot" sizes (as little as 1-2 microns), primarily by wavelength-dispersive spectroscopy (WDS). The spatial scale of analysis, combined with the ability to create detailed images of the sample, makes it possible to analyze materials and to resolve the complex chemical variability within single phases. The electron optics of an SEM or EPMA allow much higher resolution images to be obtained than can be seen using visible-light optics, so features that are irresolvable under a light microscope can be readily imaged to study detailed micro textures or provide the fine-scale context of an individual spot analysis.

Elemental mapping and WDS analysis of boronized samples were done with the electron probe micro analyzer in order to analyze the variation in the chemical composition of alloying elements in the boride layer.

## **4.6. Kinetic Study**

Kinetic study was done in order to estimate the diffusion coefficient and activation energies for boron in the boride layer formed on low alloy steels. Equation (1) and (2) were used as governing equations for the kinetic study (section 2.1.7).

The plot between the square of layer thickness versus treatment time was obtained which was a straight line. It was clear from the plot that the growth of the layer had a parabolic dependence to time.

The activation energy for the diffusion of boron in the boride layer was determined by the slope obtained in the plot of  $\ln R$  vs.  $1/T$ , using Eq. (2). Kinetic equations and parameters were determined at a temperature range of 850°C-1050°C for time periods of 2h, 4h and 6

## **4.7. Hardness Test**

Rockwell hardness tester as well as Vickers micro hardness tester was used to measure the hardness of boronized and non boronized specimens.

### **4.7.1. Rockwell Hardness Tester**

Bulk hardness of non boronized measured on the Rockwell hardness tester. Diamond cone indenter was used to measure the hardness on C scale with load 150Kg. Five readings were taken at the surface of non boronized specimens and their average was reported as the surface hardness of non boronized samples. All the hardness readings were taken at room temperature. Specimens were having cylindrical shape and dimensions of  $\phi 10\text{mm}$ ,  $\phi 15\text{mm}$ ,  $\phi 40\text{mm}$  and thickness of 20mm. Hardness measurement carried out as per ASTM E18-05 standard.

### **4.7.2. Vickers Hardness Tester**

Hardness depth profiles of boride layer were taken on the Vickers hardness test. A load of 100 gm was used for thick layers and 50gm was used for the comparatively thin layer. Hardness readings were taken as per ASTM standards. Indentations were taken on the mirror polished cross sections of boronized specimens with the help of Vickers diamond micro indenter. Three readings were taken and their average was reported.

## **4.8. Corrosion Test**

The corrosion resistance of the boride layer formed on EN41B specimen was investigated by acid immersion tests. A non boronized specimen and boronized EN41B specimens were immersed in 4%M HCL acid solution. The specimens were

also weighted before immersion with the accuracy of 0.01mg on a digital weighing machine. At specific time intervals (24hrs) the specimens were withdrawn from the acid solution and weighted without any additional treatment. The weight loss was recorded for 10 days. Before and after each corrosion test, each specimen was cleaned with ethanol.



## Chapter 5

### 5. Results and Discussions

#### 5.1. Base Material

Base materials (steels) selected for this study were EN19, EN24, and EN41B steel. These steels are basically used in the industry for their good mechanical properties like strength and toughness. After boronizing the steel's properties were improved that are beneficial to the industry. Better surface properties were obtained without altering the bulk properties. Bulk properties of steels are important as load bearing capacity is being mainly provided by the base material. Diffusion coating also results in better tribological properties of the surface. In this section basically the study of the base material was carried out.

##### 5.1.1. Chemical Composition

The Chemical composition of EN19, EN24 and EN41B steels were measured on optical emission spectrometer of spark analyzer. The Chemical composition of standard EN19, EN24, EN41B samples and tested samples is shown in the tables. It was examined that the chemical composition of test material matches with the standard composition of EN19, EN24 and EN41B confirming the steel grades.

**Table 5.1: Chemical composition of standard and test material EN19 steel**

Element	C	Mn	Si	P	S	Cr	Mo	Fe
Std. EN19 wt. %	0.35- 0.45	0.5- 0.8	0.1- 0.35	0.05max	0.05max	0.9- 1.5	0.2- 0.4	Balance
Sample wt. %	0.42	0.60	0.31	0.05	0.049	1.20	0.20	96.80

**Table 5.2: Chemical composition of standard and test material EN24 steel**

Element	C	Mn	Si	P	S	Cr	Mo	Ni	Fe
Std. EN24 wt. %	0.35-0.45	0.45-0.70	0.10-0.35	0.05 max	0.05 max	0.90-1.40	0.20-0.35	1.30-1.80	Balance
Sample wt. %	0.391	0.587	0.23	0.032	0.025	1.088	0.292	1.357	

**Table 5.3: Chemical composition of standard and test material EN41B steel**

Element	C	Mn	Si	P	S	Cr	Mo	Ni	Al	Fe
Std. EN41B wt. %	0.35-0.45	0.65max	0.10-0.45	.05 max	.05max	1.40-1.80	0.10-0.25	.40 max	0.90-1.30	Balance
Sample wt. %	0.409	0.616	0.292	0.043	0.036	1.664	0.155	0.110	0.914	

## 5.1.2. Microstructure and Hardness

### 5.1.2.1. Microstructure and Hardness of EN19

Microstructure of EN19 sample was studied in transverse direction. Fig5.1 shows typical extruded and air-cooled structure in transverse section. White grains in image shows ferrite while light blackish areas show the presence of pearlite. Pearlite lamellas which are present can be seen at higher magnification. Bulk Hardness of as received specimens found to be 245 HB. Micro hardness of the same sample was also tested, which was obtained as 255HV at 100gm load.

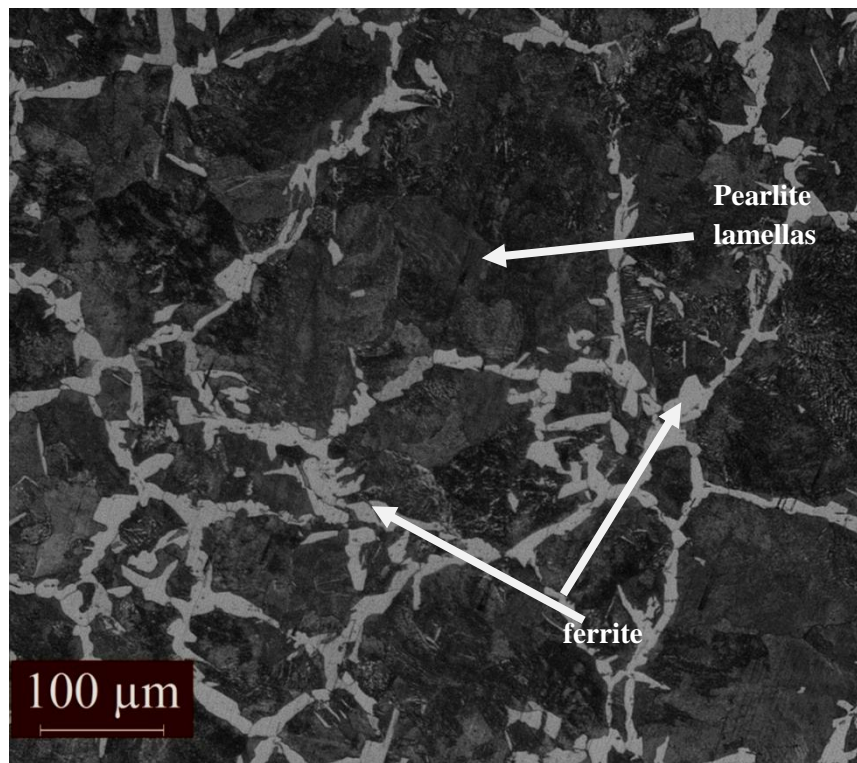


**Figure 5.1: Optical micrograph of Cross section of as received EN19 specimen**

#### ***5.1.2.2. Microstructure and Hardness of EN24***

Microstructure of EN24 sample was studied in transverse direction. The specimen was received in heavily tempered condition. Optical image was taken on a cross section of the specimen. Optical micrograph showed the presence of martensite steel. A bushy type martensite was observed with carbide precipitation. Bulk Hardness of as received specimen was found to be 248 HB. Micro hardness of the same sample was also tested, which was obtained as 365HV at 100gm load.

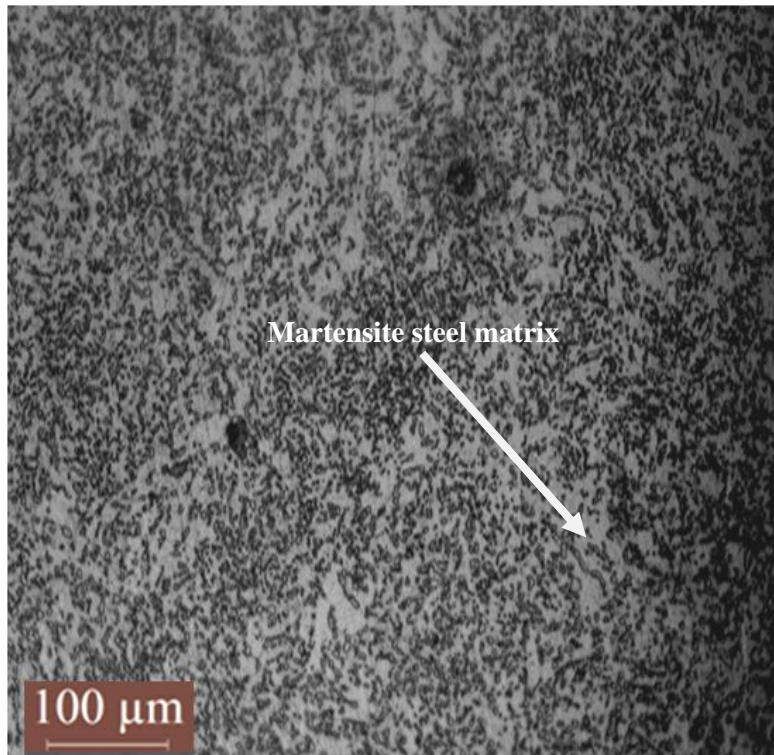


**Figure 5.2: Optical micrograph of Cross section of as received EN24 specimen**

### ***5.1.2.3. Microstructure and Hardness of EN41B***

Microstructure of EN41B sample was studied in transverse direction. The specimen was received in annealed condition. Optical image was taken on a cross section of the specimen. Optical micrograph showed the presence of ferrite with pearlite steel. Bulk Hardness of as received specimen was found to be 240HB. Microhardness of the same sample was also tested, which was obtained as 350HV at 100gm load.

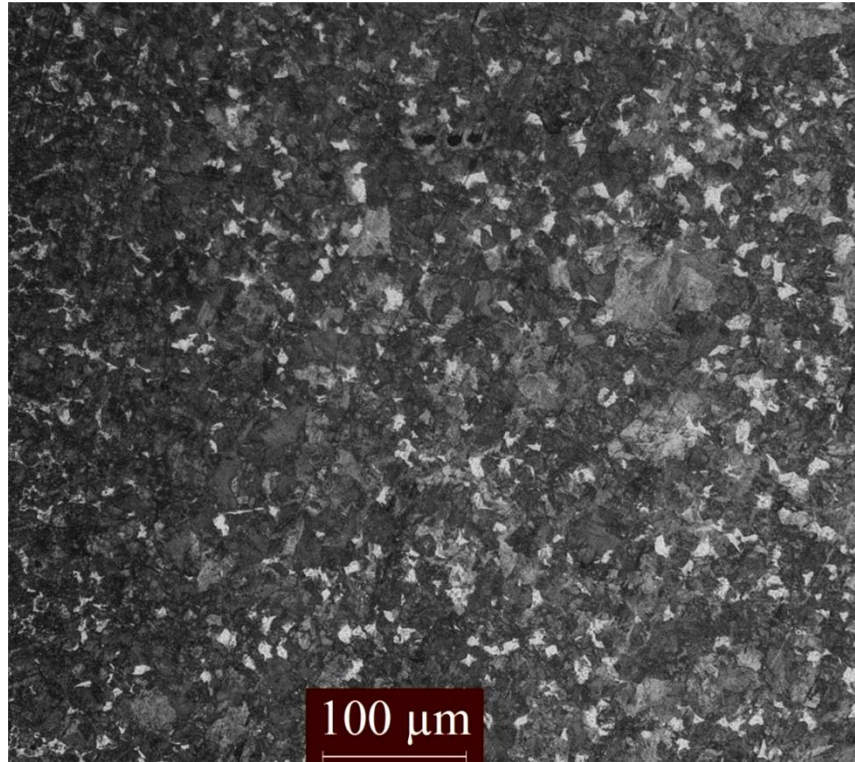


**Figure 5.3: Optical micrograph of a cross section of as received EN41B specimen**

## **5.2. Boronizing**

Pack boronizing was conducted at three different temperatures i.e. 850°C, 950°C and 1050°C for 2h, 4h and 6h holding time by using the commercial Boropak powder inside the muffle furnace. After boronizing was completed container was opened and the specimens were taken out from the container.

### **5.2.1. Boronizing at 850°C**

Pack boronizing was conducted at 850°C for 2h, 4h and 6h holding by using the commercial Boropak powder inside the muffle furnace.

After boronizing was completed container was opened and the specimens were taken out from the container and the following observations were made:

- i. A smooth surface was obtained as powder did not stick to the surface in case of EN19 and EN41B.

- ii. In case of EN24 powder was sticking around the specimen. The Powder was fused powder and did not loosen even after the washing and cleaning. Top and bottom surfaces were free from the fused salt.

### 5.2.1.1. *Microstructure*

The cross sectional optical micrographs of the boronized EN19, EN24 and EN41B steel at temperature 850°C for 2h, 4 h, and 6h are shown in figures below.

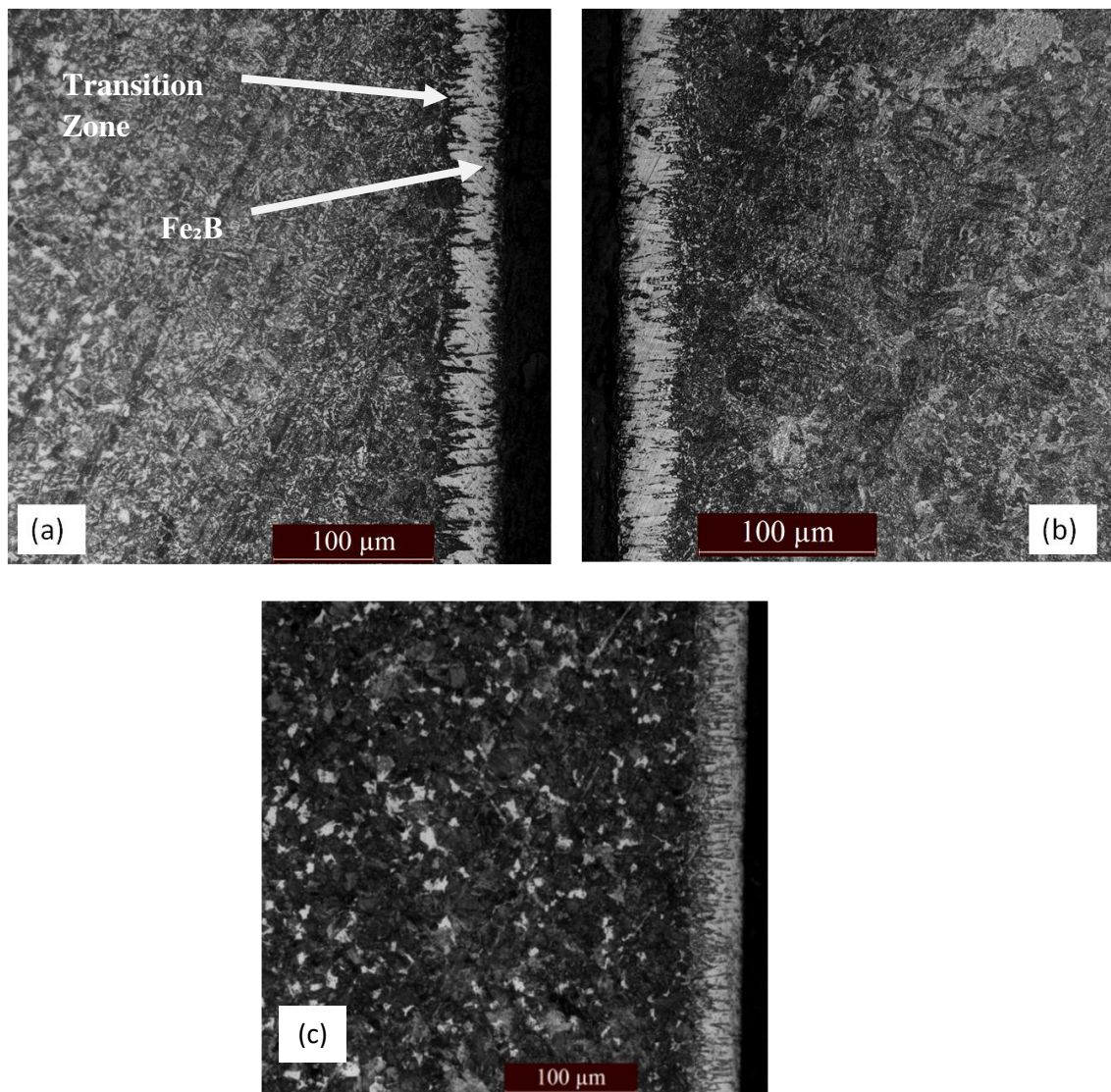


**Figure 5.4: Morphology of boride layer in specimens (a) EN19 (b) EN24 (c) EN41B carried out at 850°C for 2h**

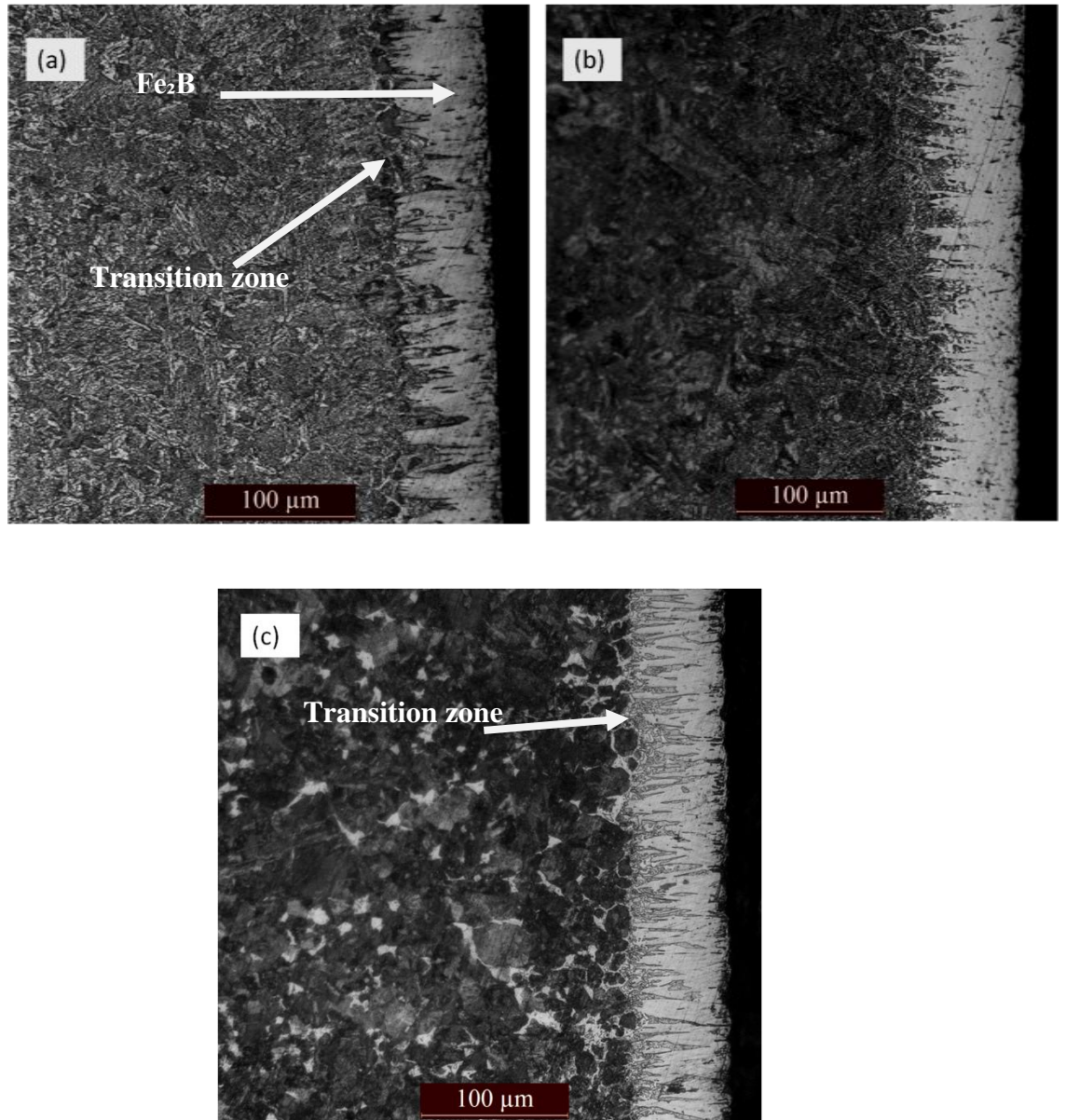


**Figure 5.5: Morphology of boride layer in specimens (a) EN19 (b) EN24 (c) EN41B carried out at 850°C for 6h**

During the process of Boronizing of steels, small atoms of boron were introduced into the metal work pieces to produce FeB and Fe<sub>2</sub>B phase on the steel. Generally, the boride layers are characterised by saw tooth morphology of needle shape structure [17].

Optical micrographs of the specimens boronized at 850°C for 2h, 6h showed the presence of boride layer. The following observations were made

- i. Boride layers were having the saw tooth/needle shaped morphology.

- ii. Boride layer only consisted of  $\text{Fe}_2\text{B}$ . Optical micrographs revealed the absence of FeB phase.
- iii. Optical micrographs showed two different zone, which were
  - a) Iron boride layer including  $\text{Fe}_2\text{B}$  only.
  - b) Diffusion zone beneath the boride layer.
  - c) Steel matrix.
- iv. Boride layer thickness was increasing with time and became more homogeneous and compact as the boronizing treatment time was increased. [\[14\]](#)
- v. As the %concentration of alloying elements was increased the boride layer became smoother [\[54\]](#) i.e. the layer was having sharp saw tooth morphology in EN19 specimen whereas saw tooth morphology was decreased in EN41B specimen as compared to EN19 and EN24 specimens.
- vi. In case of EN41B specimen some precipitation was observed at the interface of boride layer and steel. It could be due to the presence of Al and Ni. These elements have low solubility in borides as a result of which they might have been displaced away from the boride layer.

#### ***5.2.1.2. Coating Thickness***

Coating thickness measured on the optical microscope for each treatment is shown in the tables given below. From the table, it can also be observed that the boride layer thickness was increasing with time and boride layer thickness was decreasing with increased the % of alloying concentration.

**Table 5.4: Showing the layer thickness for different samples boronized at 850 °c for 2h.**

<b><i><u>Sr.NO.</u></i></b>	<b><i><u>Sample</u></i></b>	<b><i><u>Layer thickness(<math>\mu</math>m)</u></i></b>
1	EN19	37 $\pm$ 5
2	EN24	32 $\pm$ 4
3	EN41B	34 $\pm$ 4

**Table 5.5: Showing the layer thickness for different samples boronized at 850 °c for 6h.**

<b><i><u>Sr.NO.</u></i></b>	<b><i><u>Sample</u></i></b>	<b><i><u>Layer thickness(<math>\mu</math>m)</u></i></b>
1	EN19	71 $\pm$ 5
2	EN24	60 $\pm$ 10
3	EN41B	55 $\pm$ 10

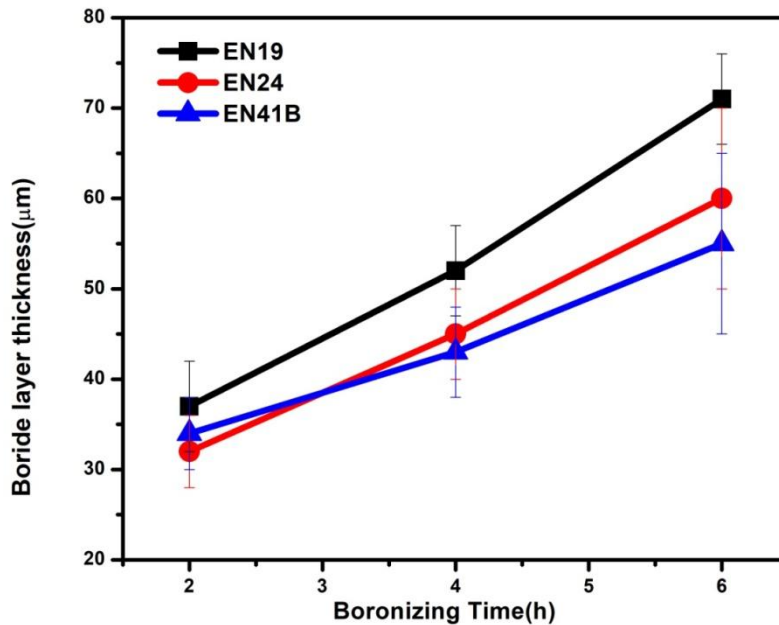


**Figure 5.6: Boronizing coating thickness ( $\mu\text{m}$ ) vs. time (h).**

Figure 5.6 shows the variation of layer thickness with time for different specimens. From the plot, it is observed that the thickness of boride layer is increasing with time for all the specimens. But as the concentration of alloying elements is increasing the layer thickness is decreasing, which is also supported by [54]. It can be observed that EN41B is having more layer thickness as compared to EN24 boronized for 2h. This difference could be the effect of different packing conditions and heating rate. Otherwise coating thickness decrease with the increased concentration of alloying elements.

### 5.2.2. Boronizing at 950°C

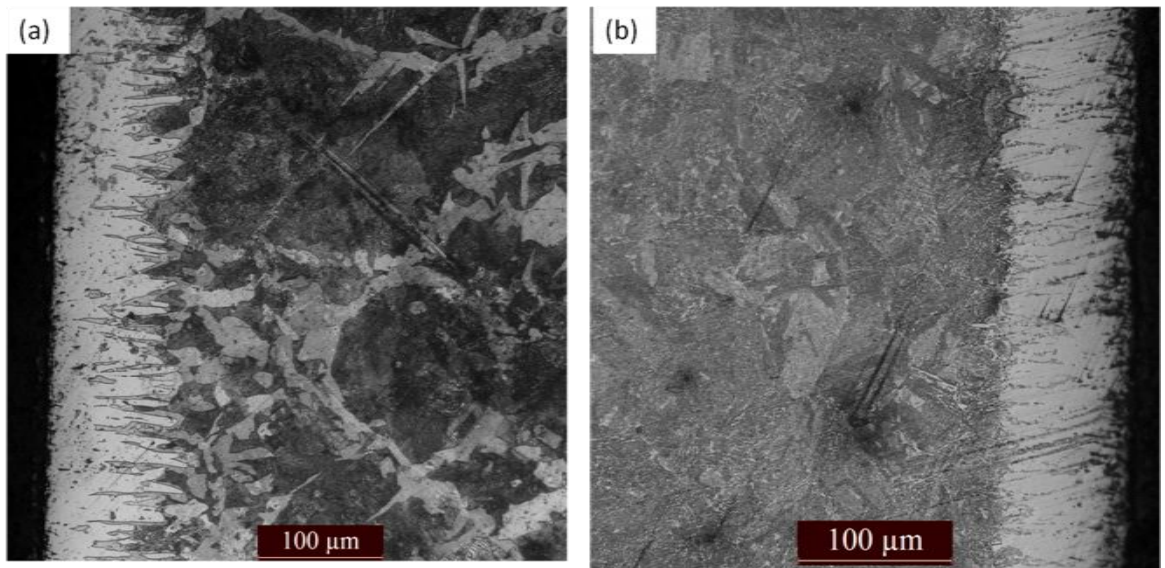
Pack boronizing was conducted at 950°C for 2h, 4h and 6h holding time. After boronizing was completed container was opened and the specimens were taken out from the container and the following observations were made:

- i. A homogeneous rough surface was obtained as the powder was stuck on all the samples. The powder was removed with soap water.

- ii. In case of EN24 powder was sticking around the specimen. The Powder was fused powder and did not loosen even after the washing and cleaning of the specimens.

### ***5.2.2.1. Microstructure***

The cross section optical micrographs of the boronized EN19, EN24 and EN41B steel at temperature 950°C for 2h, 4 h, and 6h are shown in figures below.



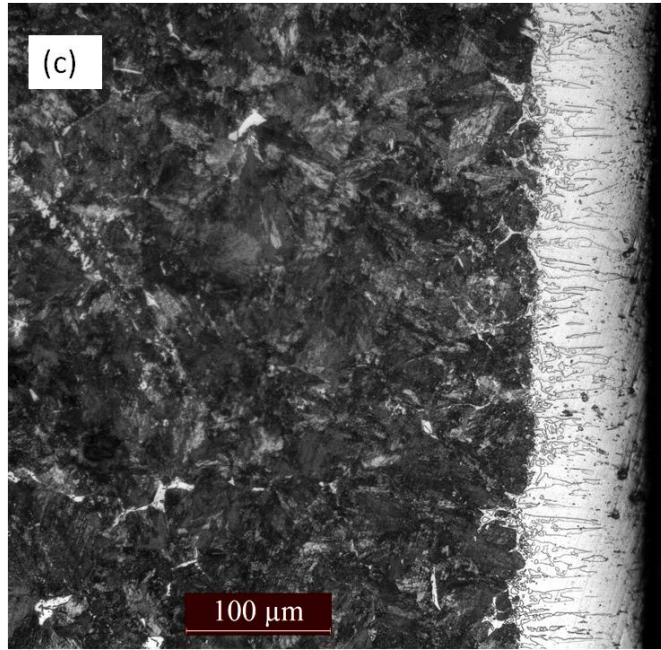


**Figure 5.7: Morphology of boride layer in specimens (a) EN19 (b) EN24 (c) EN41B carried out at 950°C for 2h.**

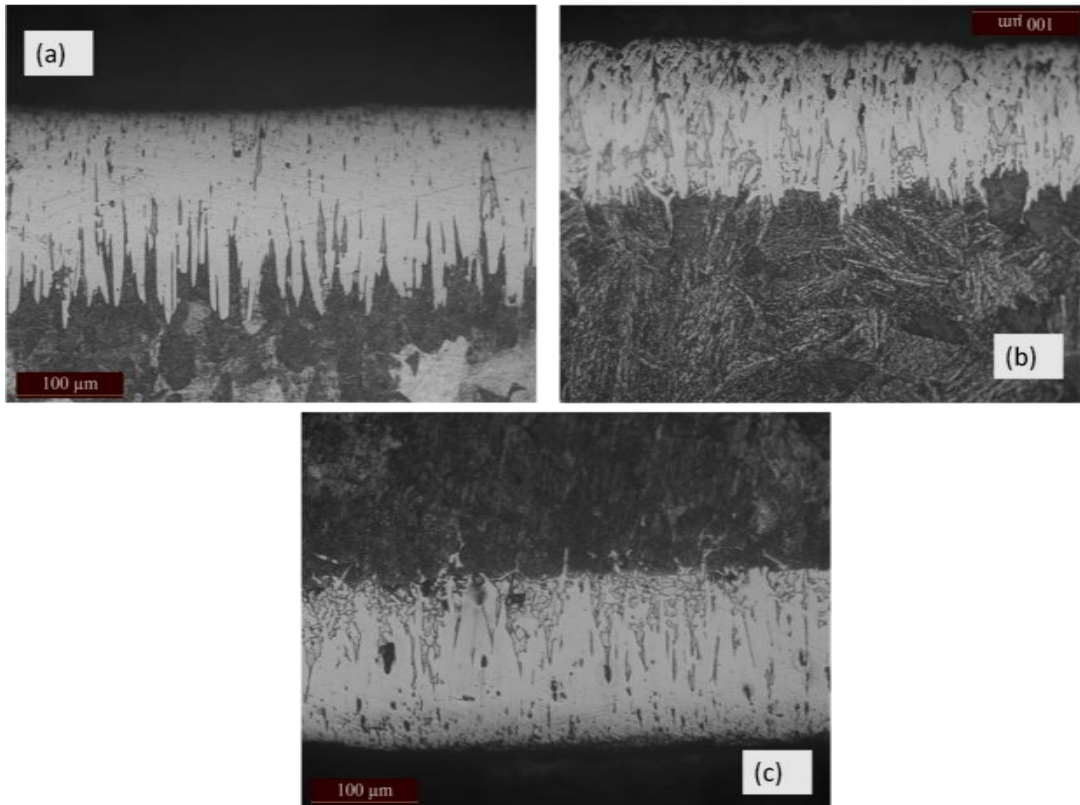


**Figure 5.8: Morphology of boride layer in specimens (a) EN19 (b) EN24 (c) EN41B carried out at 950°C for 4h.**

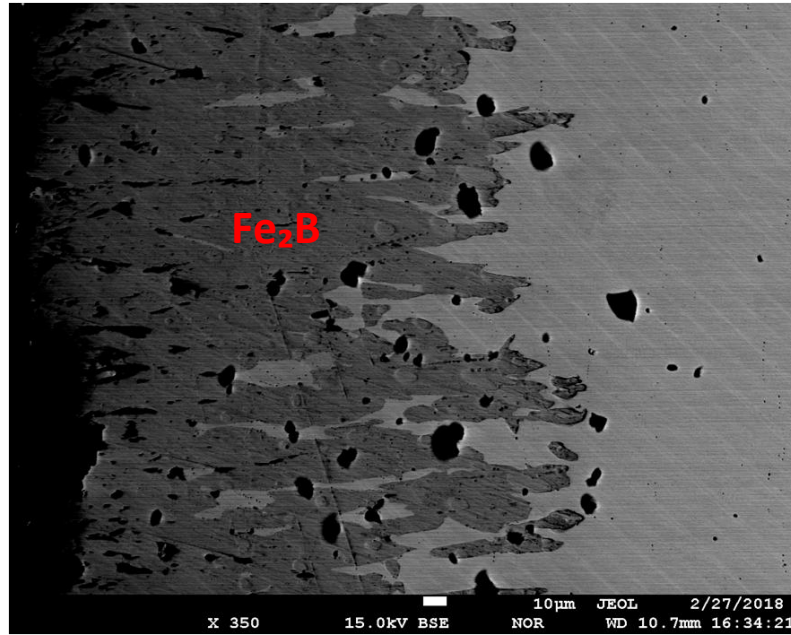


Figure 5.9: SEM image showing the morphology of boride layer EN19 carried out at 950°C for 4h

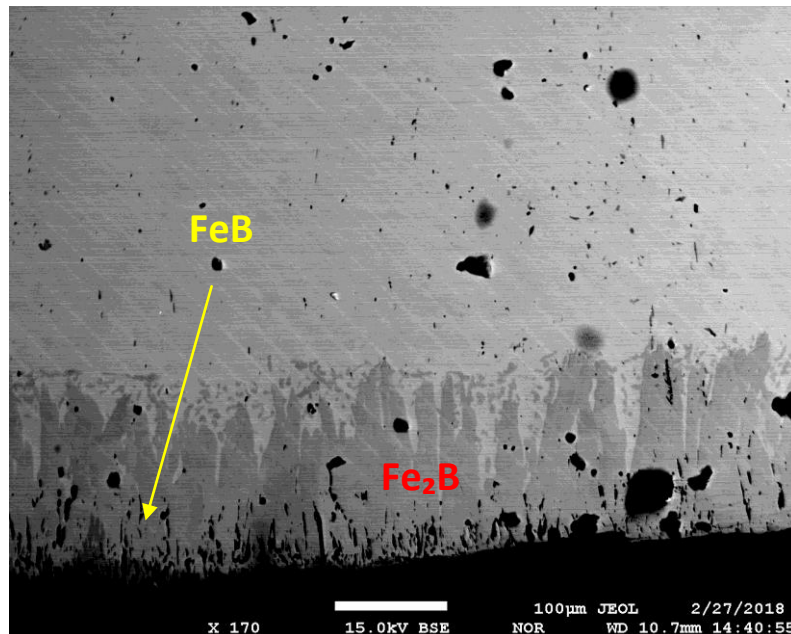
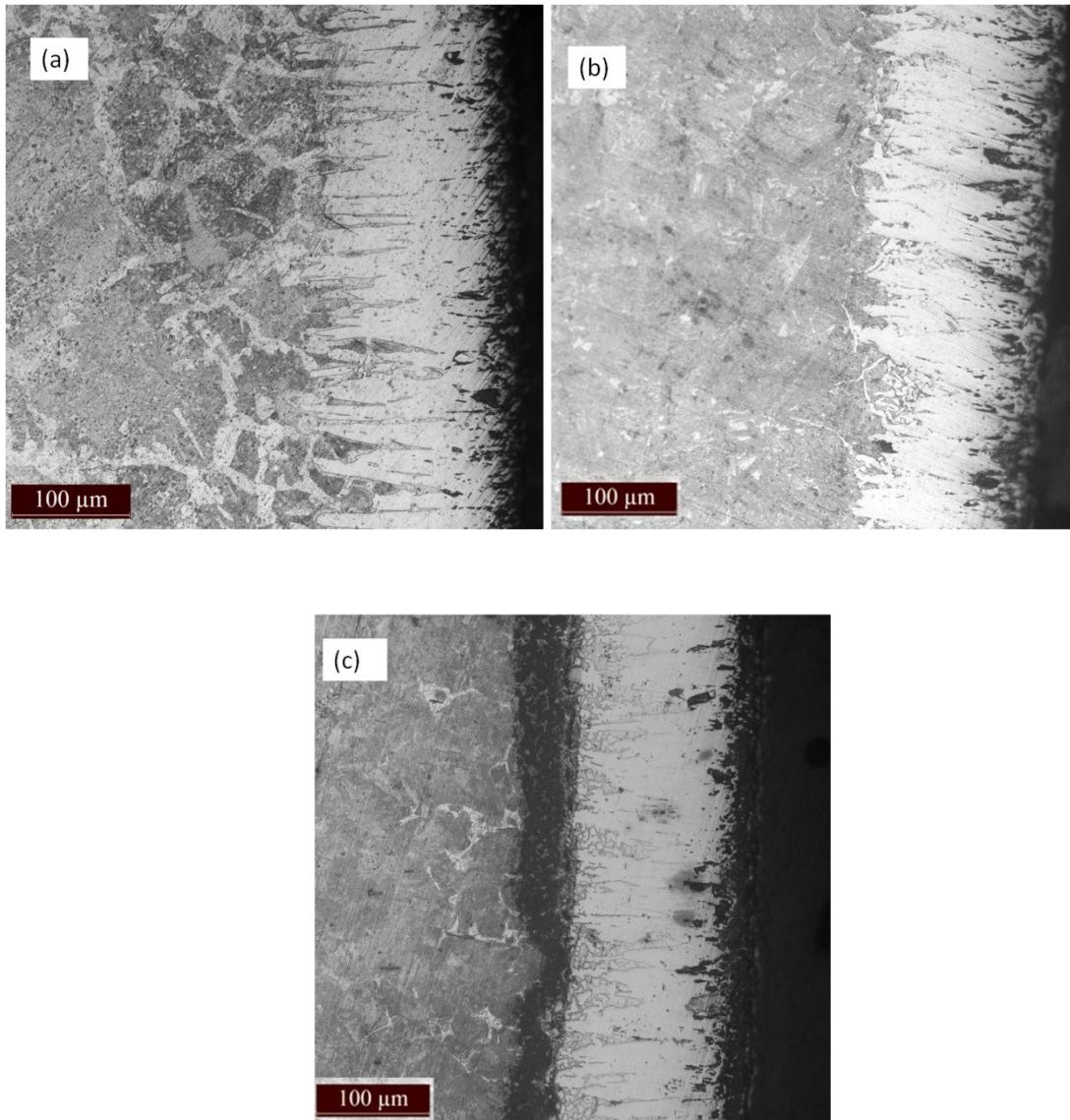


Figure 5.10: SEM image showing the morphology of boride layer EN41B carried out at 950°C for 4h.



**Figure 5.11: Morphology of boride layer in specimens (a) EN19 (b) EN24 (c) EN41B carried out at 950°C for 6h.**

Optical and SEM images of the specimens boronized at 950°C for 2h, 4h and 6h. The following observations were made,

- i. Boride layers were having the saw tooth/needle shaped morphology.
- ii. Boride layer was mainly consisting of  $\text{Fe}_2\text{B}$ . Optical micrographs revealed the absence of  $\text{FeB}$  phase, but SEM images had shown a small amount of  $\text{FeB}$  phase at some points in the specimen boronized for 4h. Homogeneous  $\text{FeB}$  layer was not observed.
- iii. Optical micrographs/SEM showed three different zones.

- a. Iron boride layer including mainly Fe<sub>2</sub>B with a very small amount of FeB.
  - b. Diffusion zone.
  - c. Steel matrix.
- iv. Higher amount of precipitation was observed at the interface between the steel and boride layer in EN41B steel boronized at 950°C as compared to the steel boronized at 850°C. This could be due to the presence of Al and Ni because these elements have lower solubility in iron borides therefore concentrated beneath the boride coating in the form of precipitates of borides of Al, Ni.
- v. Boride layer became more homogeneous and compact as the boronizing treatment time and temperature was increased which was also supported by *Uslu et al* [14][37]
- vi. It was observed that the boride layer thickness increased together with boronizing duration and temperature. S. Sahin has also reported the same [55].
- vii. As the % concentration of alloying elements was increased the saw tooth morphology was decreased and boride layer became smoother. [54]
- viii. It was observed that the layer was having porosity and lateral cracks in the top region of the layer in the specimen. It could be due to the evaporation of material at higher temperature. It was observed that the specimens boronized for 4h and 6h were having more porosity as compared to specimens boronized for 2h.
- ix. Optical images taken from the centre of the sample, boronized for 4h and 6 h at 950 °C revealed that the sample had grain growth. This could be due to the heating of steel at higher temperature followed by air cooling.

#### **5.2.2.2. Coating Thickness**

Coating thickness measured on the optical microscope for each treatment is shown in the table. Specimen boronized at 950°C were having a thicker boride layer as compared to the specimens boronized at 850°C. Boride layer thickness was increasing with boronizing time and boronizing temperature. Same effect of alloying

elements was observed. Specimens with more concentration of alloying elements were having the lower layer thickness.

**Table 5.6: Showing the layer thickness for different samples boronized at 950°c for 2h**

<u>Sr.NO.</u>	<u>Sample</u>	<u>Layer thickness(μm)</u>
1	EN19	82±10
2	EN24	70±10
3	EN41B	68±10

**Table 5.7: Showing the layer thickness for different samples boronized at 950°c for 4h**

<u>Sr.NO.</u>	<u>Sample</u>	<u>Layer thickness(μm)</u>
1	EN19	154±20
2	EN24	144±15
3	EN41B	130±20

**Table 5.8: Showing the layer thickness for different samples boronized at 950°c for 6h**

<u>Sr.NO.</u>	<u>Sample</u>	<u>Layer thickness(μm)</u>
1	EN19	175±20
2	EN24	153±10
3	EN41B	146±20

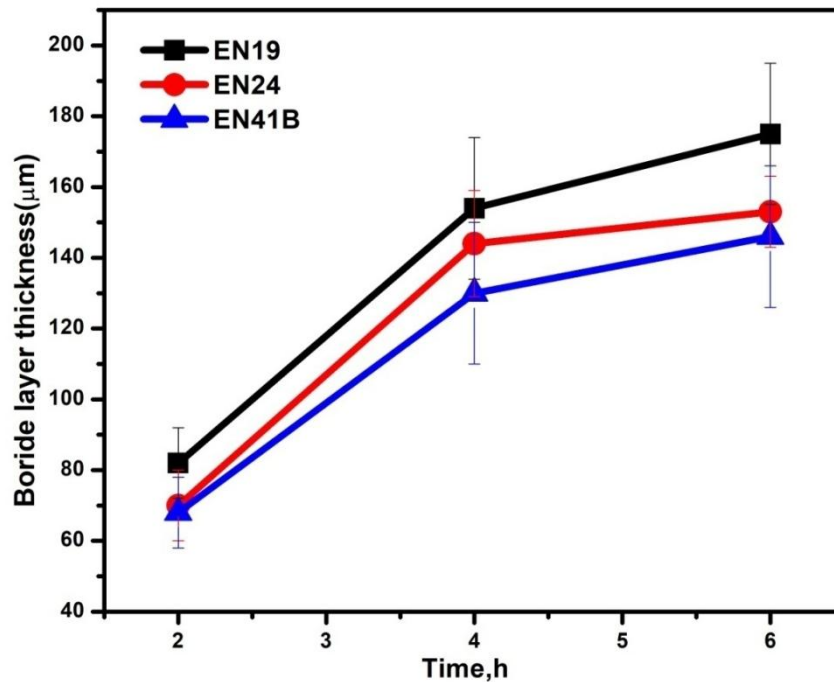


**Figure 5.12: Variation of boride layer thickness vs. Time for different specimens**

Figure 5.12 shows the variation in the layer thickness with time for different specimens boronized at 950°C.

From the plot it is observed that boride layer thickness is increasing with time for all the specimens [14] but as the concentration of alloying elements is increasing the layer thickness is decreasing[20] [54].

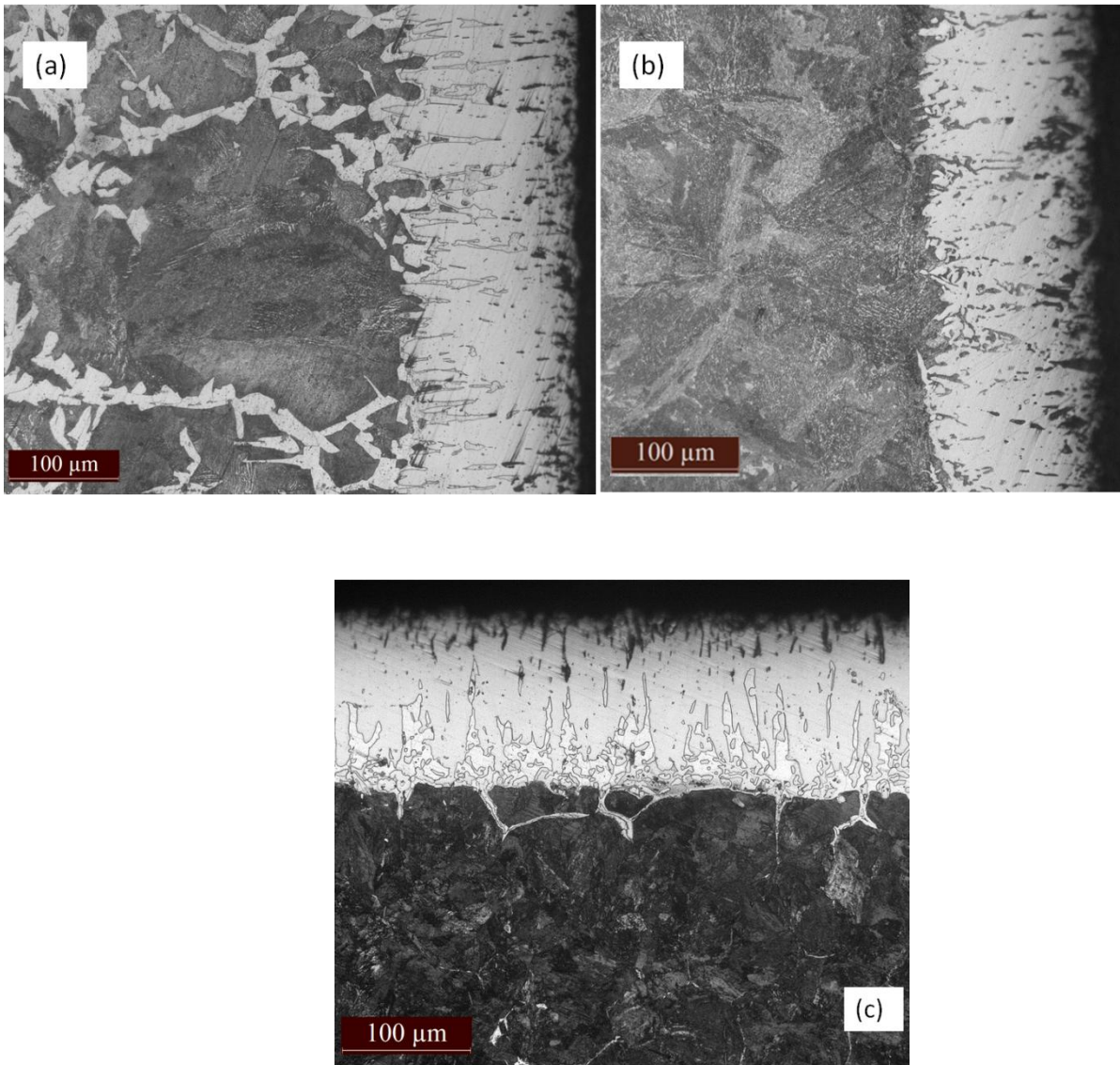
### 5.2.3. Boronizing at 1050°C

Pack boronizing was conducted at 1050°C for 2h, 4h and 6h holding time. Following observations were made:

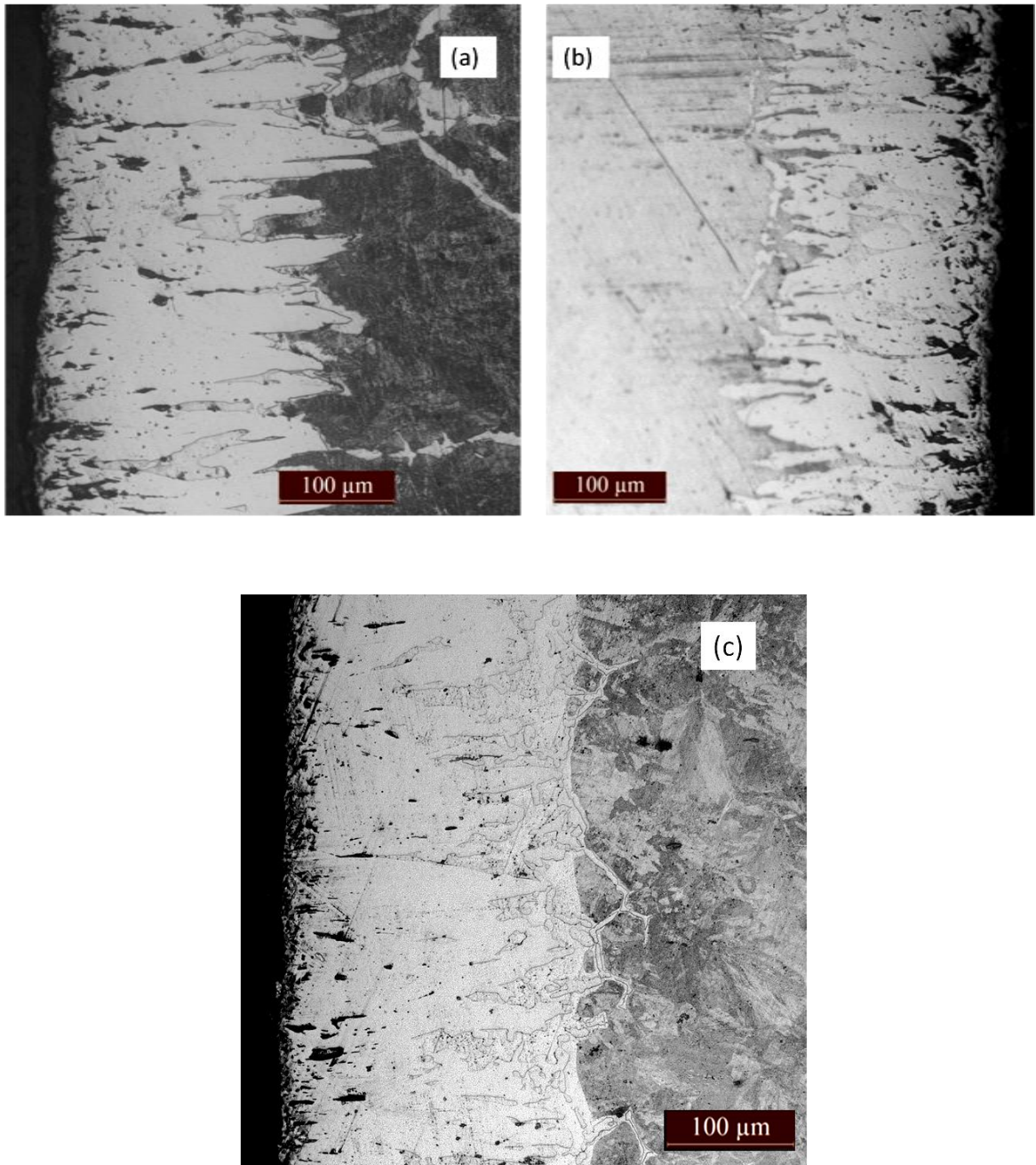
- i. A homogeneous surface was obtained with powder sticking on all the samples. The powder was a fused salt, which was stuck to the specimens due to the higher working temperature. The powder was not removed with soap water. Specimens were slightly polished to remove the fused salt. After polishing a rough surface was obtained

### 5.2.3.1. *Microstructure*

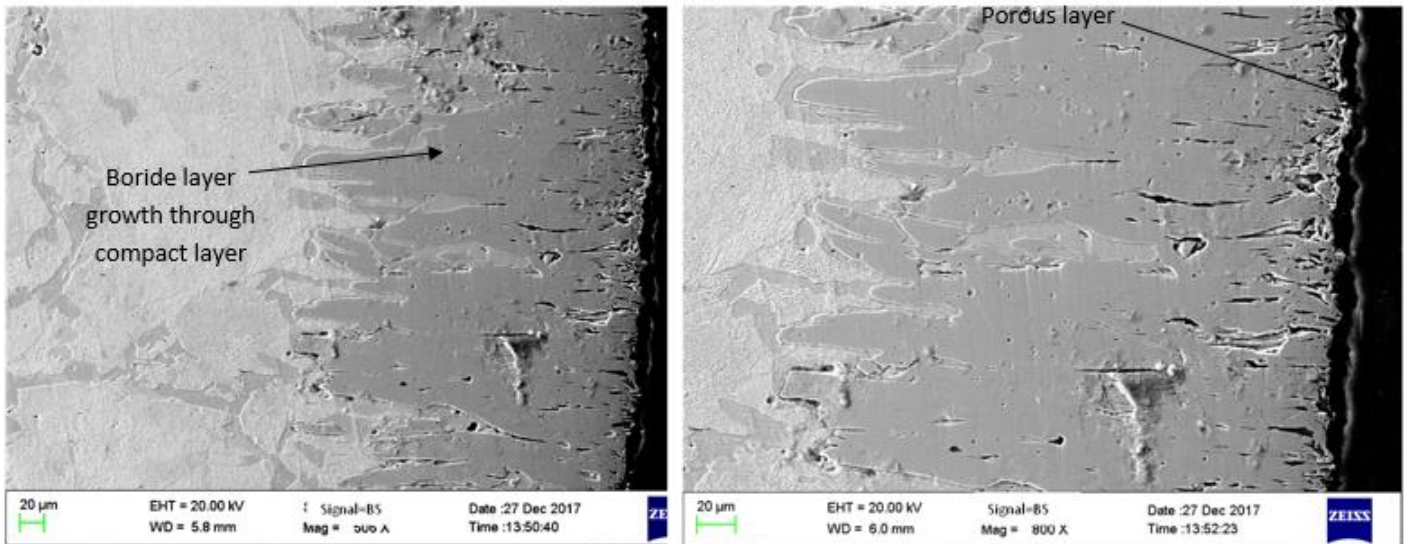
The cross section optical micrographs of the boronized EN19, EN24 and EN41B steel at temperature 1050°C for 2h, 4 h, and 6h are shown in figures below.



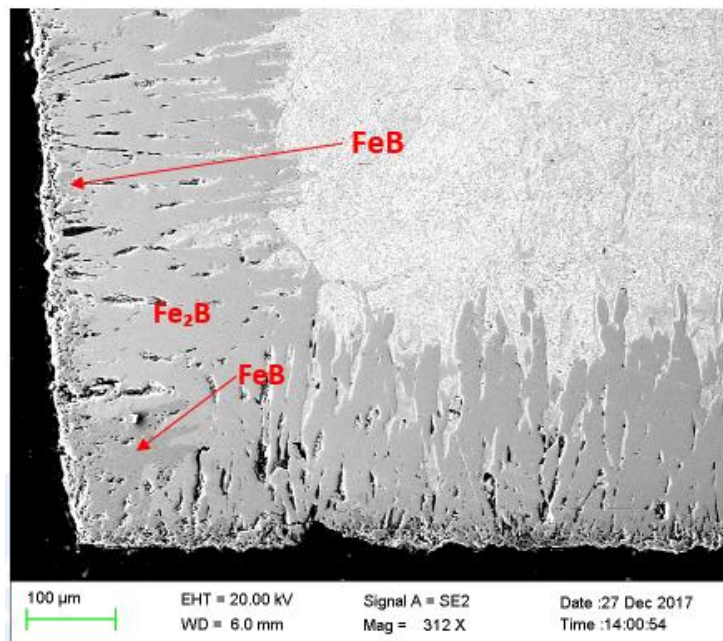
**Figure 5.13: Morphology of boride layer in specimens (a) EN19 (b) EN24 (c) EN41B carried out at 1050°C for 2h.**



**Figure 5.14: Morphology of boride layer in specimens (a) EN19 (b) EN24 (c) EN41B boronized at 1050°C for 4h**



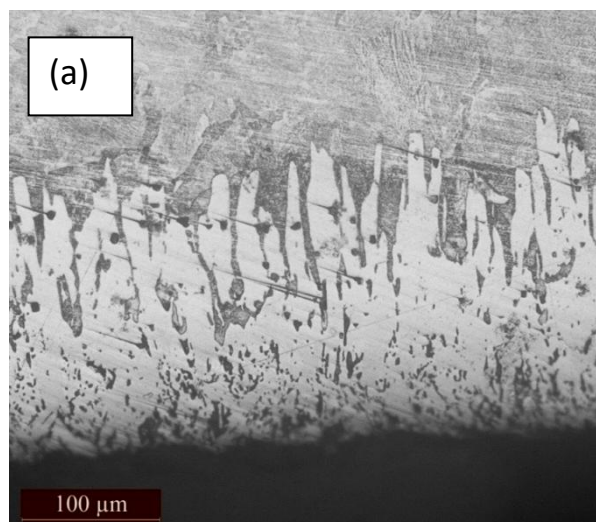
**Figure 5.15: SEM image showing the Morphology of boride layer in EN19 boronized at 1050°C for 4h.**



**Figure 5.16: SEM image showing the Morphology of boride layer in EN19 boronized at 1050°C for 4h.**



**Figure 5.17: SEM image showing the Morphology of boride layer in EN24 boronized at 1050°C for 4h.**



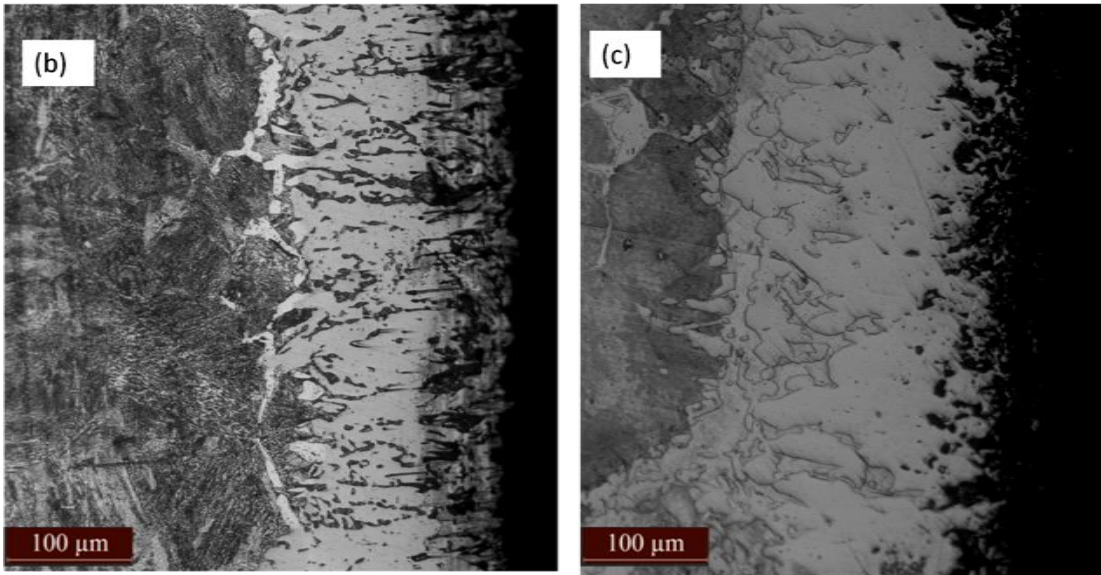


**Figure 5.18: Optical images showing the Morphology of boride layer in (a)EN19 (b)EN24 (c)EN41B boronized at 1050°C for 6h.**

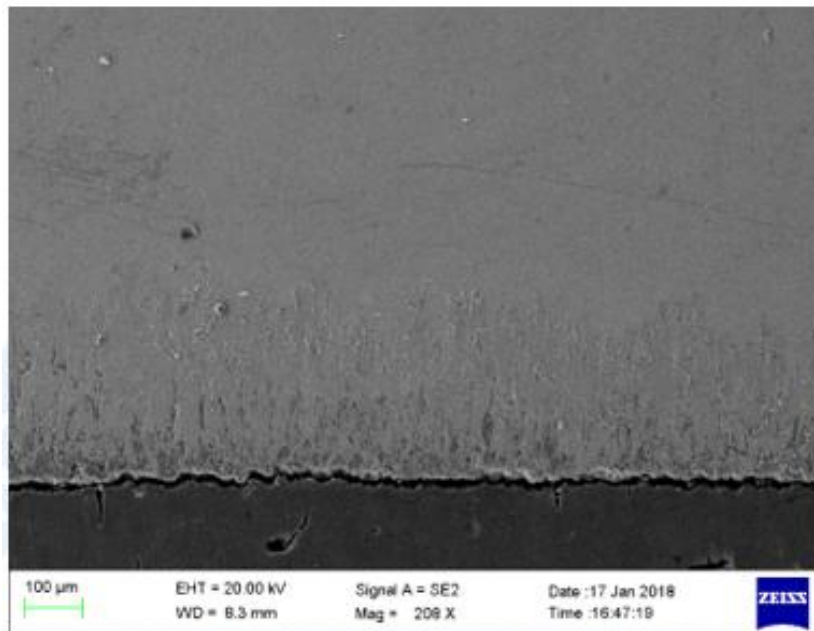


**Figure 5.19: SEM images showing the Morphology of boride layer in EN19 boronized at 1050°C for 6h**

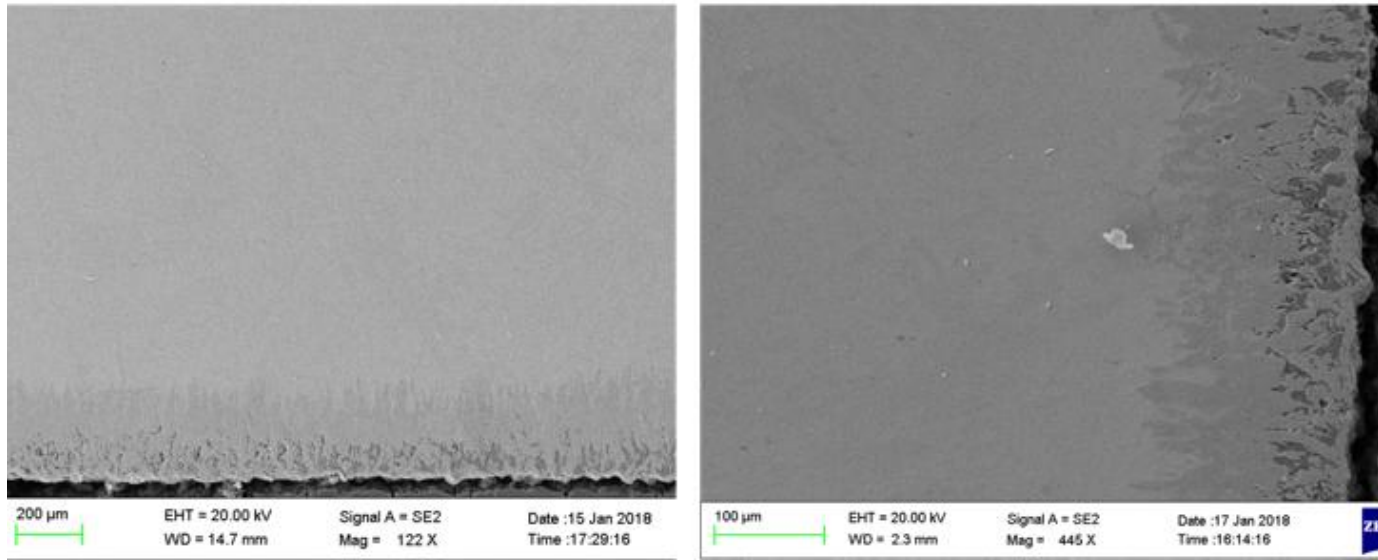


**Figure 5.20: SEM images showing the Morphology of boride layer in EN24 boronized at 1050°C for 6h**

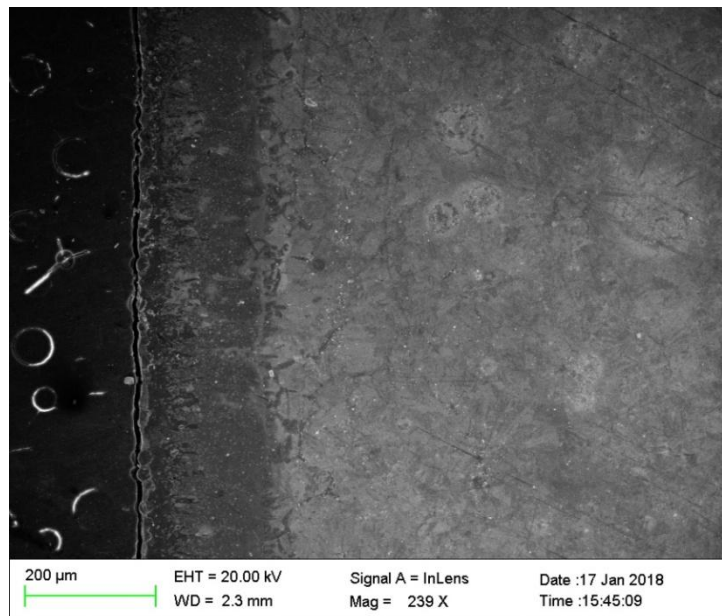


**Figure 5.21: SEM images showing the Morphology of boride layer in EN41B boronized at 1050°C for 6h**

Optical/SEM images of the steels boronized at 1050°C for 2h, 4h and 6h. Following observations were made:

- i. Boride layers were having the saw tooth/needle shaped morphology.
- ii. Optical micrographs revealed the absence of FeB phase. But steels boronized at 1050°C for 4h and 6h were having a little amount of FeB phase at some places of the boride layer, i.e. at the top and at the corners which was revealed by SEM images.
- iii. Specimens were having three different zones
  - a) Single phase boride layer consisting of Fe<sub>2</sub>B only with a small amount of FeB.
  - b) Diffusion zone
  - c) Steel matrix
- iv. Optical micrographs showed the presence of precipitation under the boride layer in EN41B due to the presence of Al and Ni because these elements had lower tendency to dissolve in iron borides therefore concentrated beneath the boride coating.
- v. Boride layer became more homogeneous and compact with boronizing treatment time and temperature. Highest layer thickness was obtained in the specimens boronized at 1050°C as compared to the specimens boronized at 850°C and 950°C. The same effect was reported by *Oslo et al.* [14] [34]
- vi. It was observed that the boride layer thickness increased with the boronizing duration. With the increased temperature, the boride layer thickness was observed to increase.
- vii. As the %concentration of alloying elements was increased the saw tooth morphology was decreased and smooth layer was observed as compared to the layer obtained in specimens having lower concentrations of alloying elements.
- viii. The saw tooth morphology was also decreasing with increasing temperature. The specimens boronized at 1050°C were having a smooth layer as compared to the specimens boronized at lower temperatures.
- ix. It was also observed that the layer was having porosity in the top region of the boride layer. It could be due to the evaporation of material at higher

temperature. It was observed that the specimens boronized for 4h and 6h were having more porous layer as compared to specimens boronized for 2h.

- x. Optical images taken from the centre of the sample boronized for 6 h at 1050°C revealed that the sample has grain growth. This is because the sample was cooled in air after boronizing at 1050°C.

### 5.2.3.2. Coating Thickness

Coating thickness measured on the optical microscope for each treatment is shown in the table. Specimens boronized at 1050°C were having a thicker boride layer as compared to the specimens boronized at 850°C and 950°C. Boride layer thickness was increasing with time. Same effect of alloying elements was observed as the specimens having more concentration of alloying elements were having the lower layer thickness.

**Table 5.9: Showing the layer thickness for different samples boronized at 1050°C**

<u>Sr.NO.</u>	<u>Sample</u>	<u>Layer thickness(µm)</u>
<b>1</b>	<b>EN19</b>	<b>141±10</b>
<b>2</b>	<b>EN24</b>	<b>130±10</b>
<b>3</b>	<b>EN41B</b>	<b>120±20</b>

**Table 5.10: Showing the layer thickness for different samples boronized at 1050°C for 4h**

<u>Sr.NO.</u>	<u>Sample</u>	<u>Layer thickness(µm)</u>
<b>1</b>	<b>EN19</b>	<b>218±20</b>
<b>2</b>	<b>EN24</b>	<b>189±20</b>
<b>3</b>	<b>EN41B</b>	<b>171±20</b>

**Table 5.11: Showing the layer thickness for different samples boronized at 1050°c for 6h**

<u>Sr.NO.</u>	<u>Sample</u>	<u>Layer thickness(um)</u>
1	EN19	227±20
2	EN24	225±20
3	EN41B	220±20

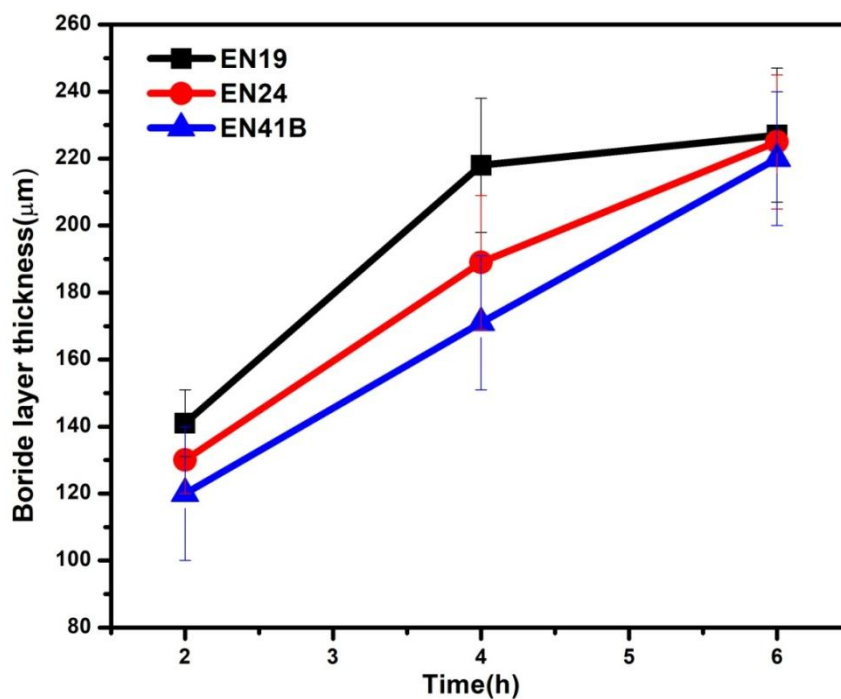


**Figure 5.22: Variation of Boride layer thickness vs. Time for different steels.**

Figure 5.22 shows the variation of boride layer thickness with time for different specimens boronized at 1050°C. From the plot, it can be observed that boride layer thickness is increasing with time for all the specimens but as the concentration of alloying elements is increasing the layer thickness is decreasing. [14] [20] [54]. It can be observed that the specimens boronized at 1050°C for 6 h are having almost the same thickness of boride layer. It could be due to some external factors like experimental setup and conditions.

### 5.3. XRD Studies

Generally Boronizing results in the formation of boride layers consisting of either  $\text{Fe}_2\text{B}$  or  $\text{FeB}$  or  $\text{Fe}_3\text{B}$ . The phases obtained by boronizing process at different temperatures and time were determined by XRD analysis. XRD peaks confirmed the presence of  $\text{Fe}_2\text{B}$  in all the specimens boronized at  $850^\circ\text{C}$ ,  $950^\circ\text{C}$ ,  $1050^\circ\text{C}$  for 2h, 4h and 6h duration. XRD results had shown that  $\text{FeB}$  phase was not present in the boronized specimens. Unidentified peaks were expected to be the peaks of complex Fe, B, Si based oxides.

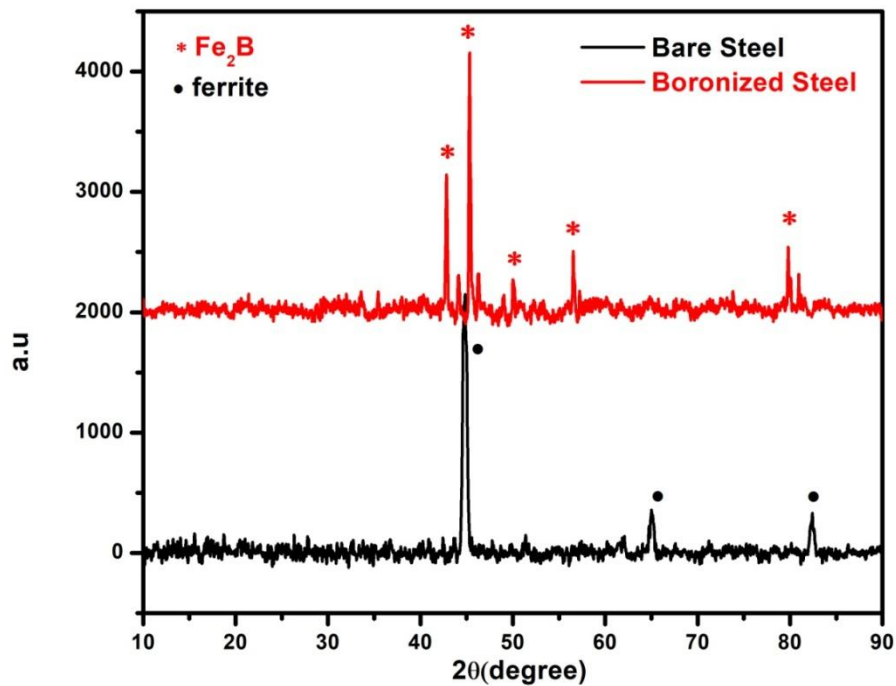


Figure 5.23: XRD patterns of boronized EN19 Steel at  $1050^\circ\text{C}$  for 6h.

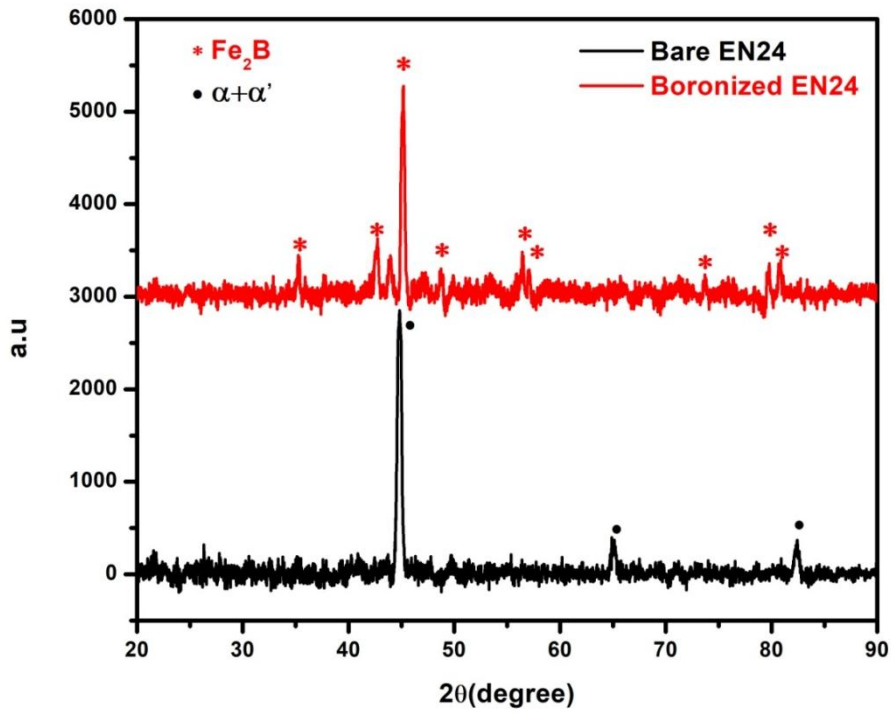


Figure 5.24: XRD patterns of boronized EN24 Steel at 1050°C for 6h

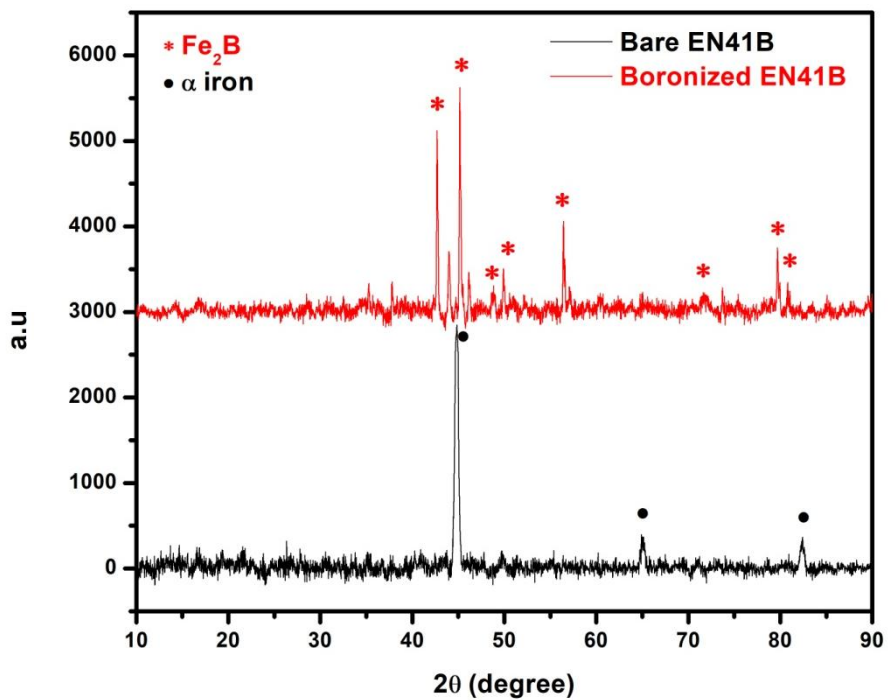
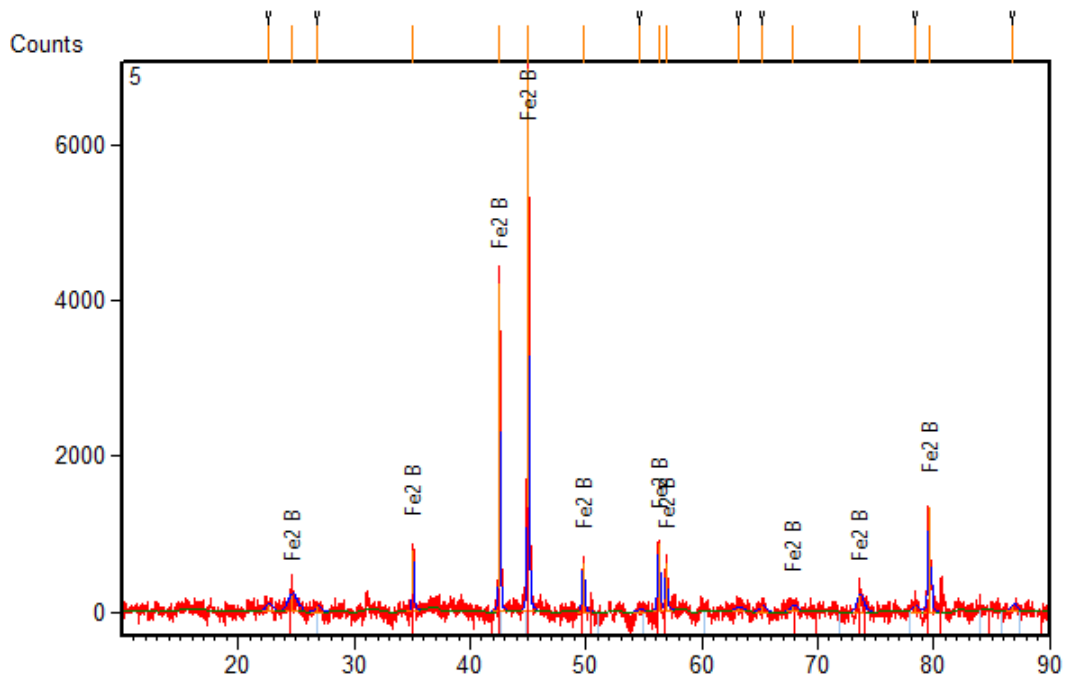


Figure 5.25: XRD patterns of boronized EN24 Steel at 1050°C for 6h



**Figure 5.26: XRD patterns of boronized EN41B Steel at 950°C for 4h.(used for EPMA)**

### **FeB Observations**

It was observed that specimens were well boronized at different parameters. Boronizing resulted in the Formation of boride layer. It was observed that all the specimens preliminarily contained single phase layer containing  $\text{Fe}_2\text{B}$ . FeB was observed in specimens boronized at 1050°C for higher time duration. It could be due to the presence of higher boron potential with time. FeB growth occurred at some points of the top layer of the specimen (Layer was not continuing). Basically, FeB growth was limited to top layer which was porous and corners of the specimens. Corner area had shown more FeB phase compared to the top side due to the higher boron concentration and less substrate area.

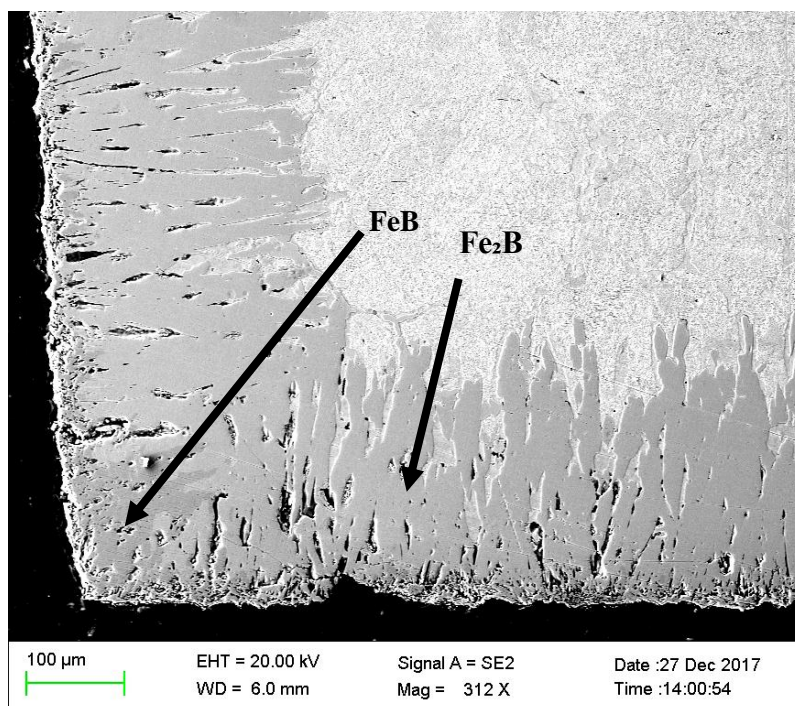


**Figure 5.27: SEM image showing the presence of FeB phase in boronized steel.**

FeB phases were not identified by XRD. The specimens were slightly polished before XRD to remove the oxides and fused salt from the surface. As the FeB was only restricted to the top surface (very thin layer), it might be removed during polishing of the specimens.

In order to minimize FeB formation, heating rate were kept high as reported by S.Timur et.al[11] and same arrangements were used for pack boronizing(Medium size container) as reported by A. A. JOSHI and S. S. HOSMANI[25].

#### **5.4. EPMA Analysis**

Elemental distribution from the boride layer to the steel matrix was studied with WDS. Elemental mapping was also done to know about the uniformity of the boride layer. WDS and elemental mapping was done on the specimens EN19 and EN41B boronized at 950°C for 4h to know about the variation in alloying element distribution from surface to the interior. WDS gives a quantitative and qualitative distribution of elements. Figure 5.28 shows the results of WDS line scan performed

on boronized EN19 steel. The data were collected on 19 spots along the scan line and listed in [table 5.12](#) showing the elemental distribution (atomic %) at four different spots.

**Table 5.12: The element contents (at. %) of the corresponding spots A, B and C**

<b>Spot</b>	<b>Displacement</b>	<b>B</b>	<b>Fe</b>
<b>A</b>	<b>30</b>	<b>27.1263</b>	<b>63.6677</b>
<b>B</b>	<b>90</b>	<b>26.3904</b>	<b>65.9328</b>
<b>C</b>	<b>135</b>	<b>12.4832</b>	<b>78.1128</b>
<b>D</b>	<b>180</b>	<b>23.1908</b>	<b>68.4911</b>

It was observed from the table 5.12 that the atomic ratio of B/Fe at spot A is approximately 1:2.3, which was close to the atomic ratio of B and Fe in Fe<sub>2</sub>B. It implies that the outer boride layer is composed of Fe<sub>2</sub>B. Elemental distribution (atomic %) also confirmed the absence of FeB phase in the boride layer. Approximately same atomic ratio of B and Fe was obtained through the boride layer. At point C the ratio was approximately 1:6. This spot might be taken at the non boronized space between two saw teeth of boride layer where boride layer did not form. The spot D corresponds to the diffusion zone/transition zone. The boride layer thickness was obtained as approximately 160µm. The ratio of B/Fe at D was obtained approximately as 1:2 but Fe<sub>2</sub>B was not observed. This could be attributed to the formation of boron rich solid solution at the interface between the boride layer and steel matrix [53].

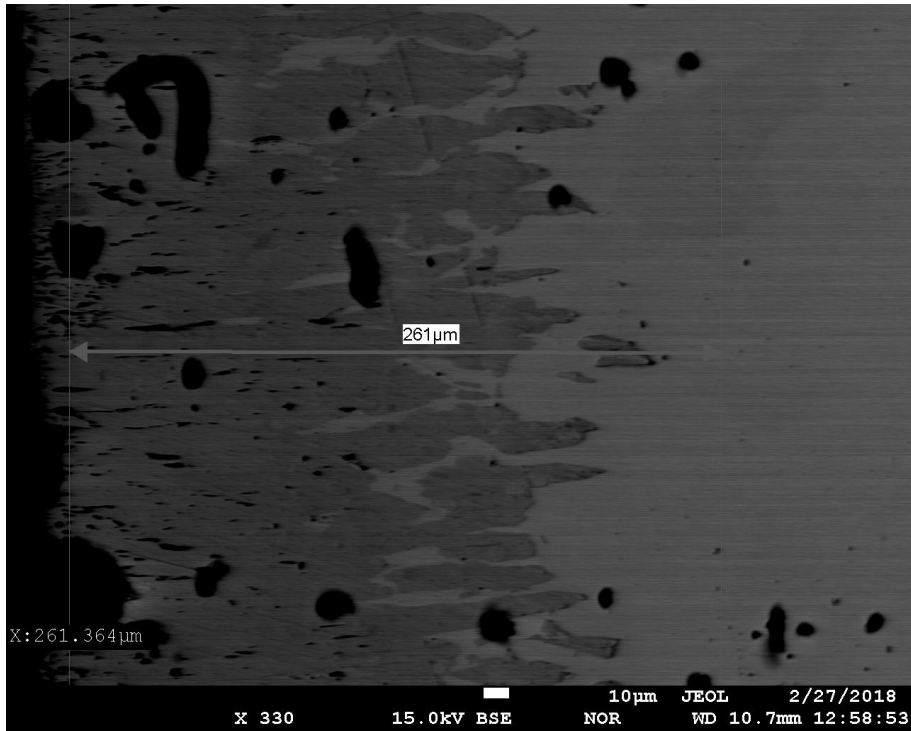


Figure 5.28: WDS line scan performed on boronized EN19 steel

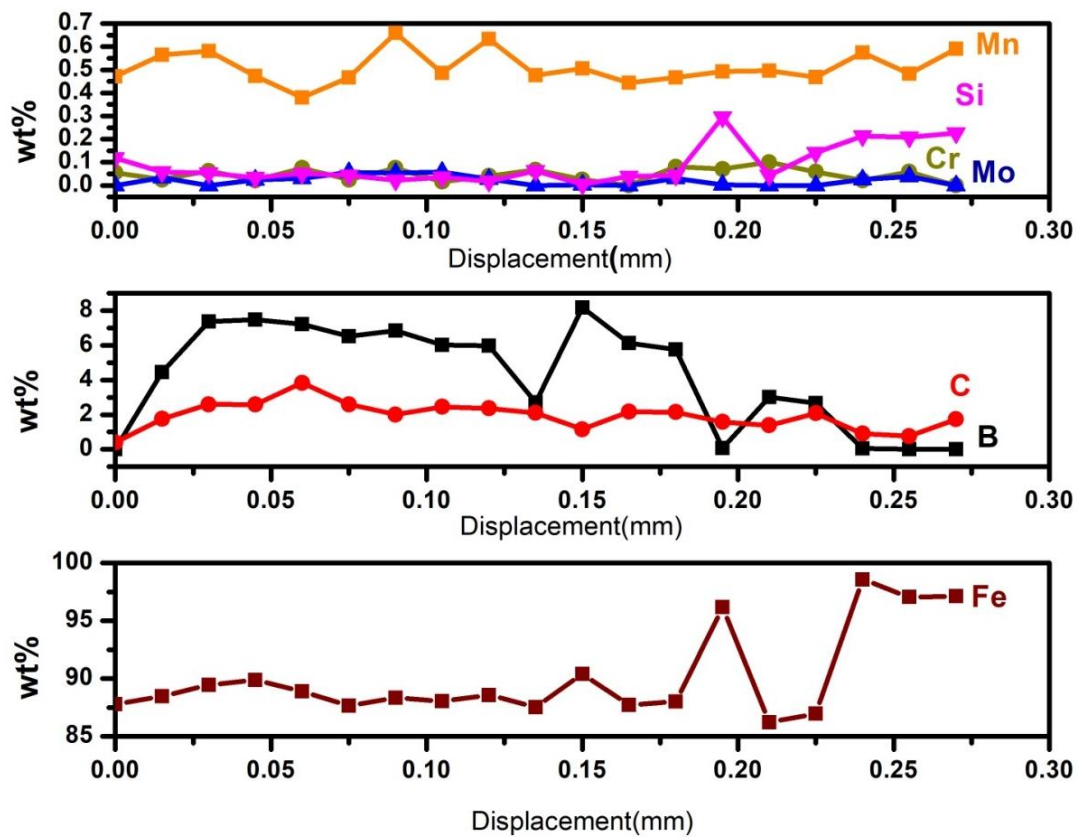
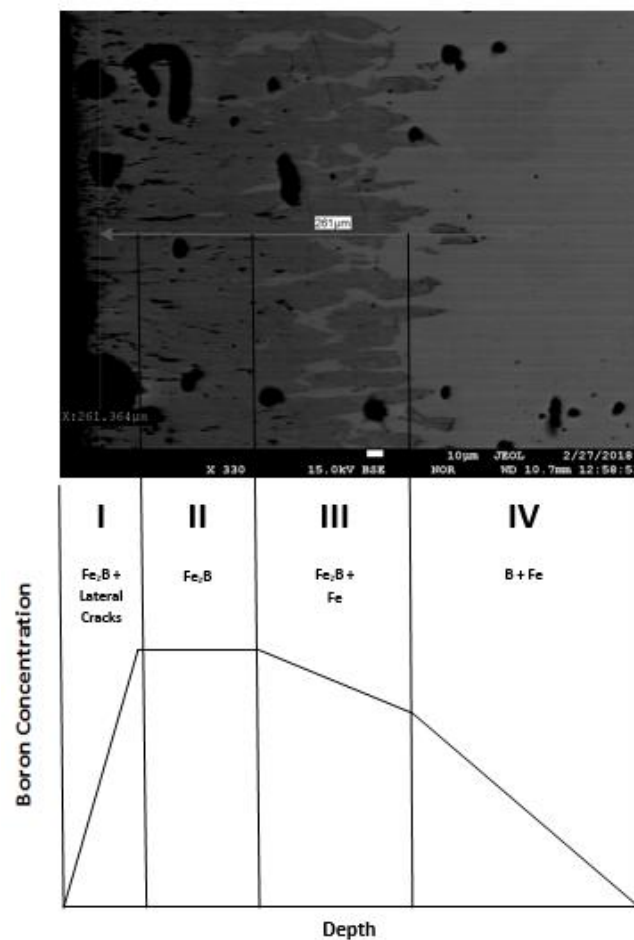


Figure 5.29: Wavelength dispersive spectra analysis showing the alloying elements distribution across the boride layers in EN19 steel.

The distribution of elements (wt %) along the WDS line scan from the boride layer to the steel matrix in EN19 boronized at 950°C for 4h is shown in Figure 5.29.

From the figure, it can be observed that the major elements in the boride layer were B and Fe. Concentration of boron in the boride layer was high at 30µm depth and it was decreasing towards the steel matrix. At 180 µm (diffusion zone), the boron concentration was about 6%. At this zone, the boron was in the form of solid solution with Fe as the concentration of boron was high. Very small amount of Si was observed in the boride layer as it would have been displaced by the boron during boronizing due to its low solubility in borides. The concentration of Si was obtained high corresponding to the depth of 180-220µm. This phenomenon is also reported by many researchers [18] [29]. Steels having more than 0.5 wt% of Si are not suitable for boronizing because of the formation of a soft ferrite region and reduced layer thickness. Similar results have been reported by *K. Genel*. [56].



**Figure 5.30: Schematic boron concentration profile from experimental data for single phase boride layers.**

Figure 5.31 shows the results of WDS line scan performed on boronized EN41B steel. The data were collected on 12 spots along the scan line. Table 5.13 shows the elemental distribution (atomic %) at four different spots.

**Table 5.13: The element contents (at. %) of the corresponding spots A, B and C**

<b>Spot</b>	<b>Displacement</b>	<b>B</b>	<b>Fe</b>
<b>A</b>	<b>20</b>	<b>23.2119</b>	<b>57.8296</b>
<b>B</b>	<b>60</b>	<b>21.4241</b>	<b>61.3289</b>
<b>C</b>	<b>120</b>	<b>25.4332</b>	<b>62.1386</b>
<b>D</b>	<b>160</b>	<b>27.3017</b>	<b>62.9957</b>

It can be observed from the table 5.13 that the atomic ratio of B/Fe at spot A is approximately 1:2.4, which was close to the atomic ratio of B and Fe in Fe<sub>2</sub>B. It implies that the outer boride layer is composed of Fe<sub>2</sub>B. Elemental distribution (atomic %) also confirmed the absence of FeB phase in the boride layer. Approximately same atomic ratio of B and Fe was obtained throughout the boride layer. This can also be attributed to the formation of the smooth layer (compact layer due to the decreased saw tooth morphology). The spot D corresponds to the diffusion zone/transition zone. The boride layer thickness was obtained as approximately 130µm. The ratio of B/Fe at D was also obtained approximately as 1:2 but Fe<sub>2</sub>B was not observed. This could be attributed to the formation of boron rich solid solution at the interface between the boride layer and steel matrix. Formation of boron rich zone was also reported by Uslu I and C.Bindal in their study [34] [53].

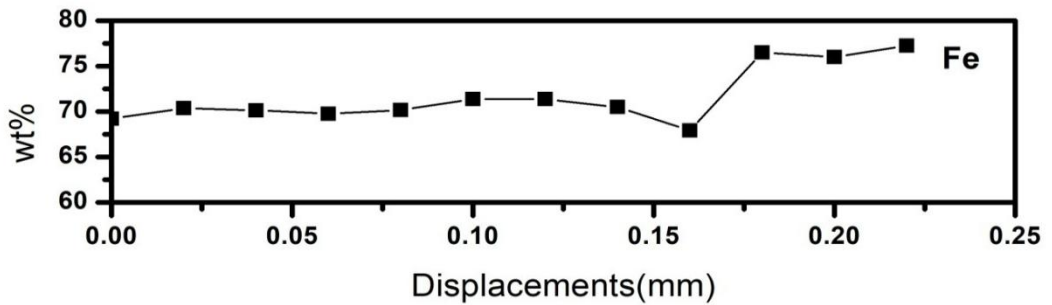
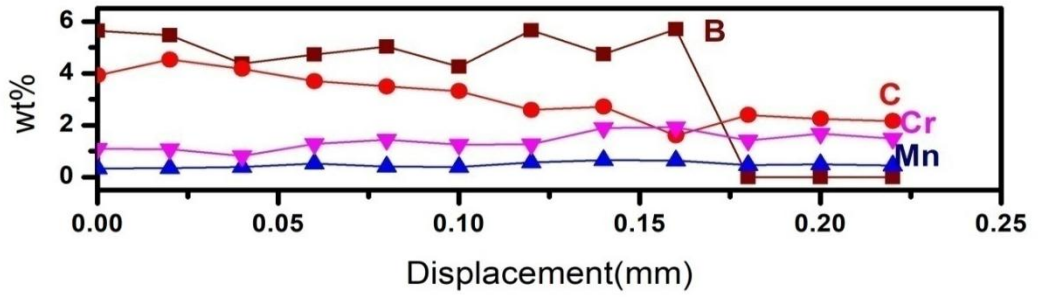
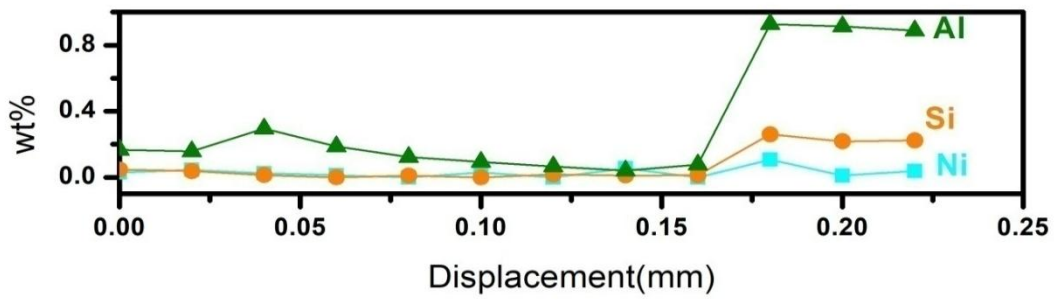
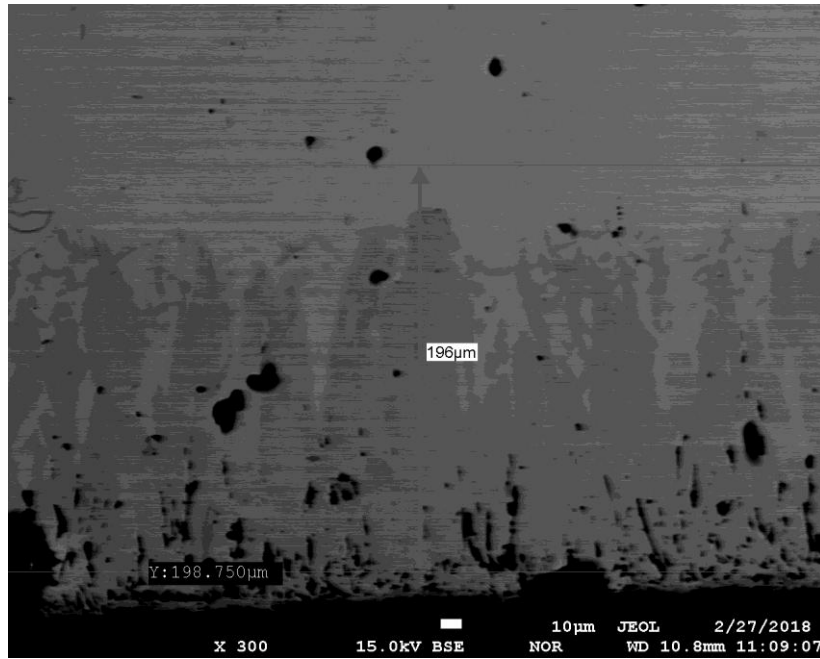


Figure 5.31: Wavelength dispersive spectra analysis showing the elemental distribution (wt %) across the boride layers

The distribution of elements (wt %) along the WDS line scan from the boride layer to the steel matrix in EN41B boronized at 950°C for 4h is shown in Figure 5.31.

From the figure, it can be observed that the major elements in the boride layer were B and Fe. Concentration of boron in the boride layer was high at 20µm depth and it was decreasing towards the steel matrix. At 160 µm (diffusion zone), the boron concentration was about 6%. At this zone, the boron was in the form of solid solution with Fe as the concentration of boron was high. From the depth of 30µm, small concentration of alloying elements Al, Si, Ni was detected due to the displacement by the boron in the boride layer. The displaced Al, Si and Ni accumulated at the interface between borides and steel matrix. The concentration of Si, Ni and Always obtained high corresponding to the depth of 180-220µm. Same effect has been also reported by many researchers [18] [20] [29]. Carbucicchio et al has reported that Ni display lower tendency to dissolve in iron borides as a result, it tends to accumulate below the boride layer towards the steel matrix forming low Nickel iron borides. He also reported that higher amount of Nickel present in the steel decreases the hardness of Fe<sub>2</sub>B layer.[20]

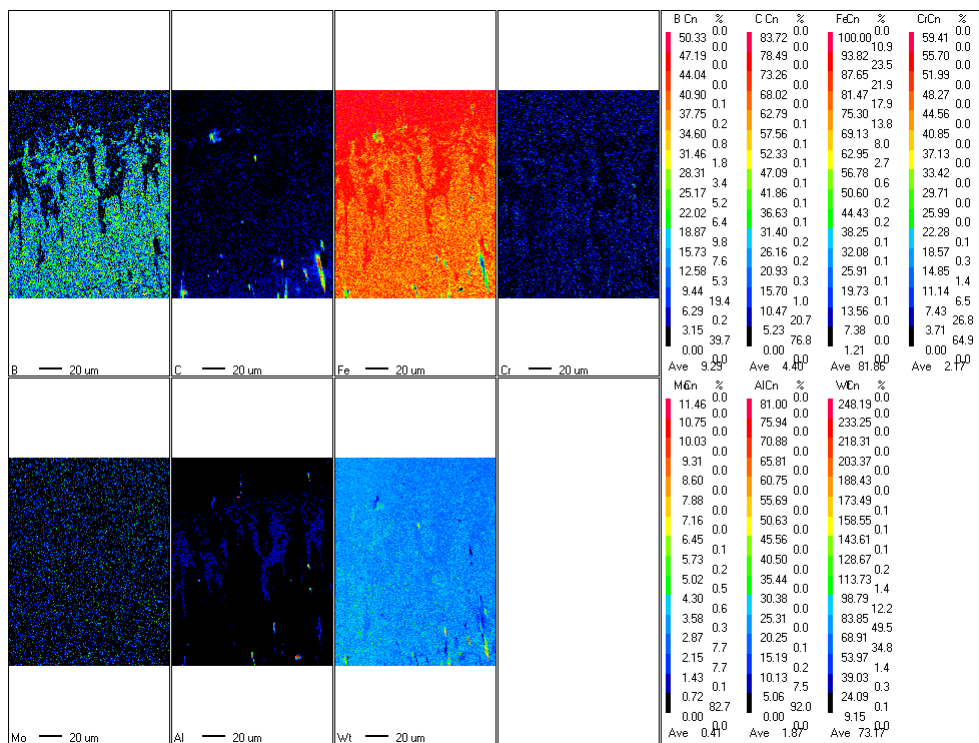
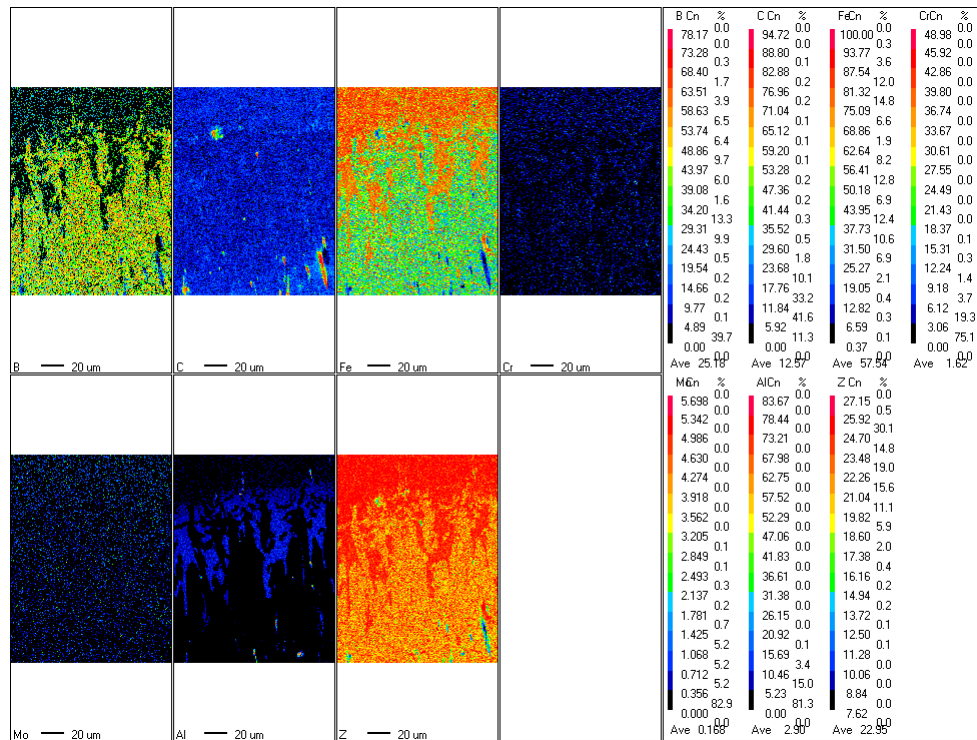


Figure 5.32: Elemental Mapping of EN19 Steel



**Figure 5.33: Elemental Mapping (atomic %) of EN41B Steel**

Elemental mapping also supported the results obtained from WDS. Elemental mapping showed a homogeneous boride layer with the average 22-24 wt% of boron. Mapping had also shown the distribution of boron particles below the boride layer (dark blue colour). It could also be observed that the Al concentration in the boride layer was almost zero, confirming the displacement of Al during boronizing. The region below the boride layer had shown a higher concentration of Al. These results supported the fact that Al had been displaced from the boride layer due their less solubility and accumulated beneath the boride layer.

## 5.5. General Review on Boronizing

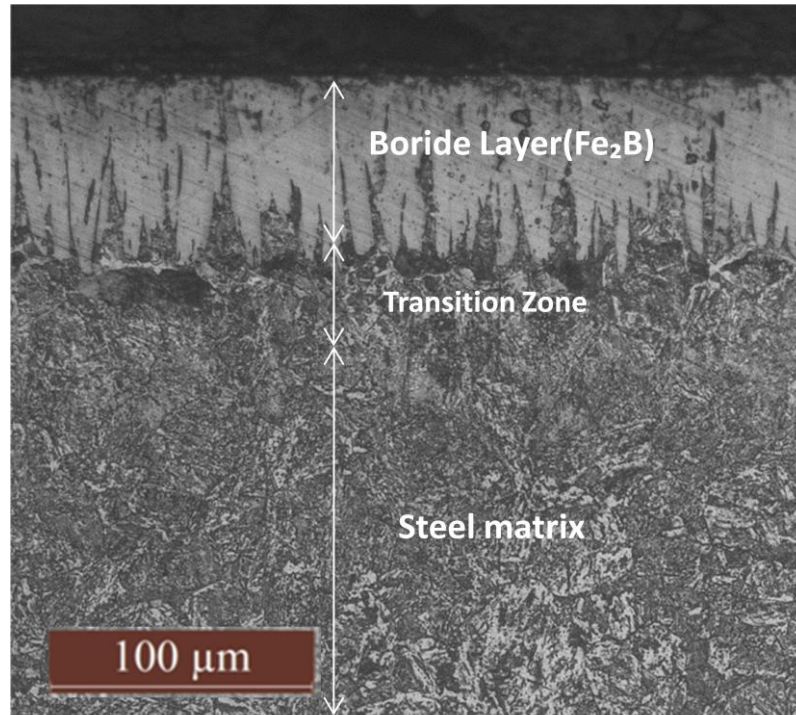
During boronizing of low alloy steel, boron atoms diffused into the steel surface. The diffusion of boron resulted in the formation of  $Fe_2B$  in the steel [7]. The formation of  $FeB$  and  $Fe_2B$  greatly depends upon the availability of boron potential.  $FeB$  formed at higher boron potential (16.23%B) whereas  $Fe_2B$  formed at lower boron potential (8.23%B).  $FeB$  phase formed adjacent to the surface, whereas  $Fe_2B$  formed near the surface also supported by I. Uslu[14]. It was reported by Palumbo et al that  $FeB$  and

Fe<sub>2</sub>B are stoichiometric inter metallic compounds with constant composition. [57]. In this study only Fe<sub>2</sub>B phase was obtained.

Boride layer was formed with saw tooth morphology. In case of low alloy steel layer thickness and morphology greatly depended upon the process parameters (time and temperature), composition of steel. Sinha and Meric et al had reported the same [17] [20] [43]. Strong toothing occurred in the steel with the lowest concentration of alloying elements and tooth became smooth with increased concentration of alloying elements. I.Uslu (2007) and M.Carbucicchio (1987) had also reported the same [20] [34]. Campos et al had reported that the formation of the boride starts with the nucleation and growth occurs in a columns perpendicular to the surface and transform into an acicular structure with increasing time and temperature. The growth occurs in a particular direction due to anisotropic diffusion of boron atoms in a preferential direction [0 0 1] [54]. Same morphology was observed in this study. The boride layer has good adhesion property due to this acicular structure.

On the basis of results obtained from micro structural study, EPMA analysis and micro hardness measurement (see section 5.6) it can be concluded that the boronized steels have three different zones

- I. Boride layer mainly consisting of Fe<sub>2</sub>B.
- II. Diffusion or transition zone where the boron concentration is high and boron is making a solid solution with steel. Hardness of this diffusion zone is lower than borides and higher than the steel matrix. The concentration of some elements like Ni, Si and Al is also high in this zone, but it is not high enough to make softer ferrite zone.
- III. Steel matrix which is free from boron.



**Optical micrograph showing the different zones in boronized steel.**

### **5.5.1. Proposed Mechanism of Boronizing**

Boronizing process consists of two main reactions. The first reaction takes place between boron medium and the surface of the component. A thin, compact layer of boron yielding powder is formed around the surface. Boronizing process starts with the formation of nuclei at the substrate surface. The preferable location for the start of nucleation is the defect points of the metal surface like macro defects (surface roughness, scratches, etc.) and micro defects (grain boundaries, dislocation, etc.). The boron atoms start to diffuse in [001] crystallographic direction and form Fe<sub>2</sub>B which has a body centered tetragonal lattice structure. In this way maximum, atomic density is achieved in [001] direction. Growth of the Fe<sub>2</sub>B layer occurs according to the diffusion law ( $x^2=Rt$ ). Fe<sub>2</sub>B growth continues with time, but as temperature increases more and more boron become available. When boron potential reaches 16.23 wt. %, FeB starts forming and FeB grow over Fe<sub>2</sub>B.

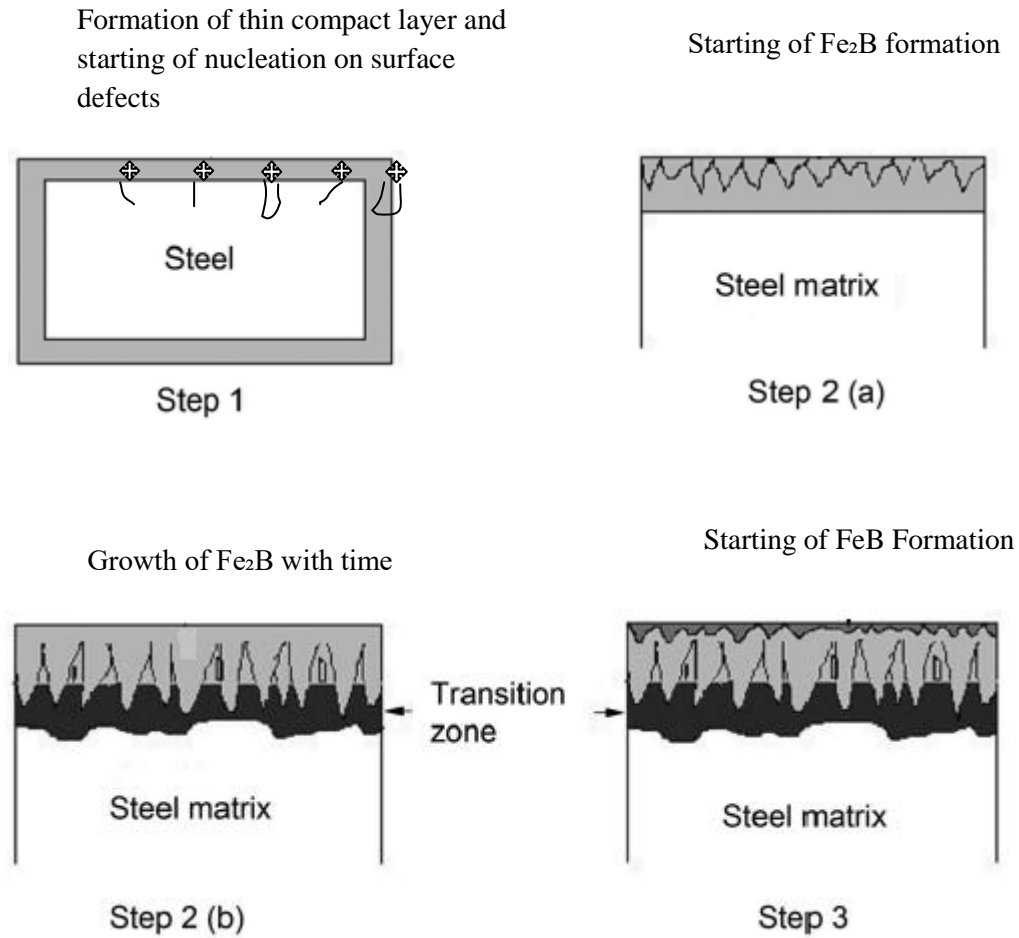


**Figure 5.34: Schematic presentation of the mechanism of boronized layer formation on the steel surface.**

## 5.6. Growth Kinetics

In this study, the effects of the processing temperature and boronizing on the diffusion growth kinetics of the boronizing layer were also investigated. Kinetic parameters such as processing temperature and time must be known for the control of the boronizing treatment.

The relationship between boride layer thickness and boronizing time is parabolic which can be seen in figure 5.35. Variation of boronizing layer thickness with time at different temperatures is shown here. The square of the thickness of the boride layer

as a function of time is described by Eq. (1) and the growth rate constants were calculated by using Eq. (1)

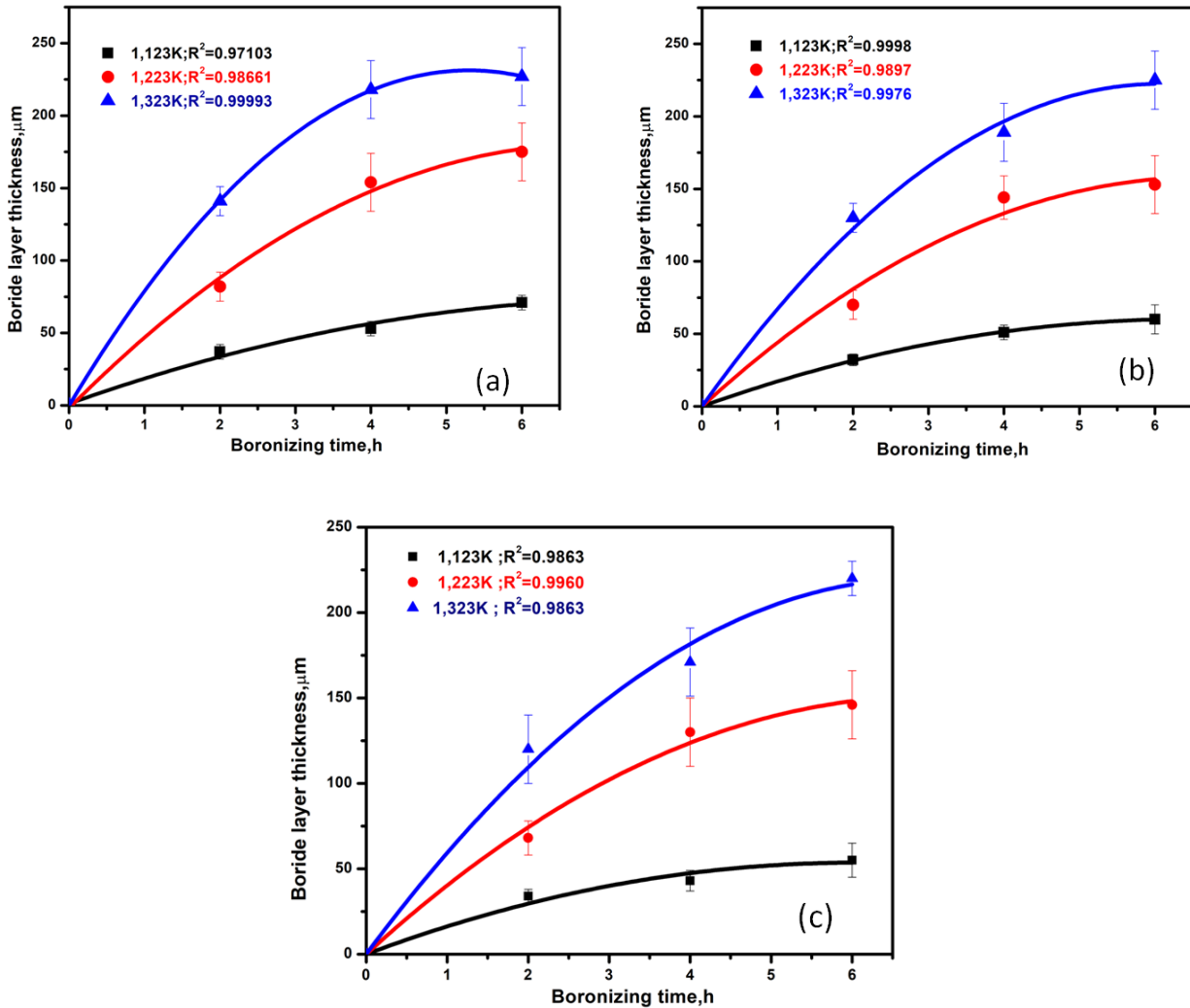


**Figure 5.35: Variation of Boriding layer thickness with time at different temperatures: (a) EN19 (b) EN24 (c) EN41B.**

The plots of square of boride layer thickness versus treatment time for different specimens were obtained as straight line. It indicates that the growth of layer had a parabolic dependence to time which is also supported by many researchers [5][9][13][32] [33] [34] [35] [36] [37] [38] [39] [40]. The values of the growth rate (R) were obtained from the slopes of the plots between squares of boride layer thickness versus boronizing time. Figure 5.36 are showing the plot between square

of boride layer thickness and boronizing time for EN19, EN24 and EN41B respectively.

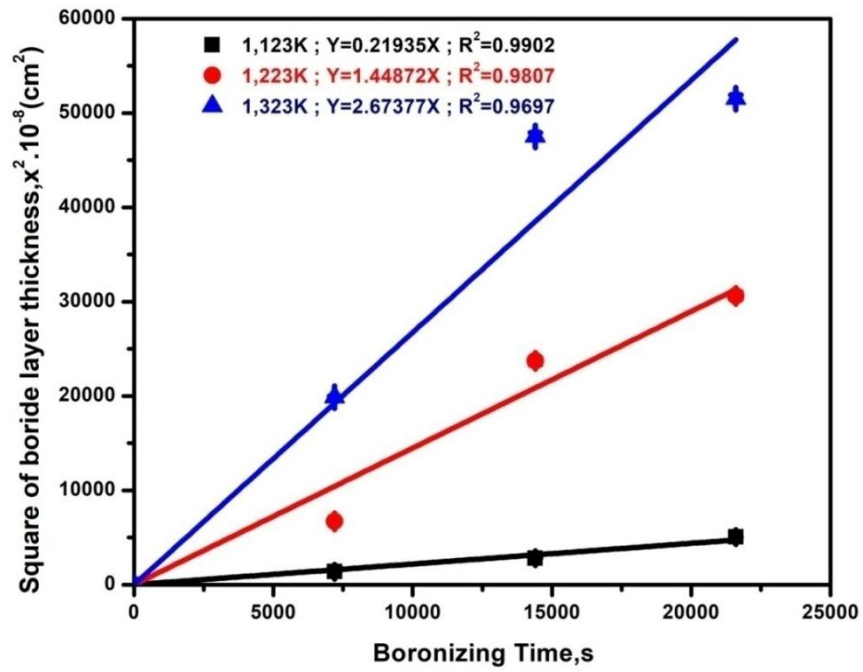


**Figure 5.36: Square of boride layer thickness versus boronizing time at various temperatures for EN19 steel.**

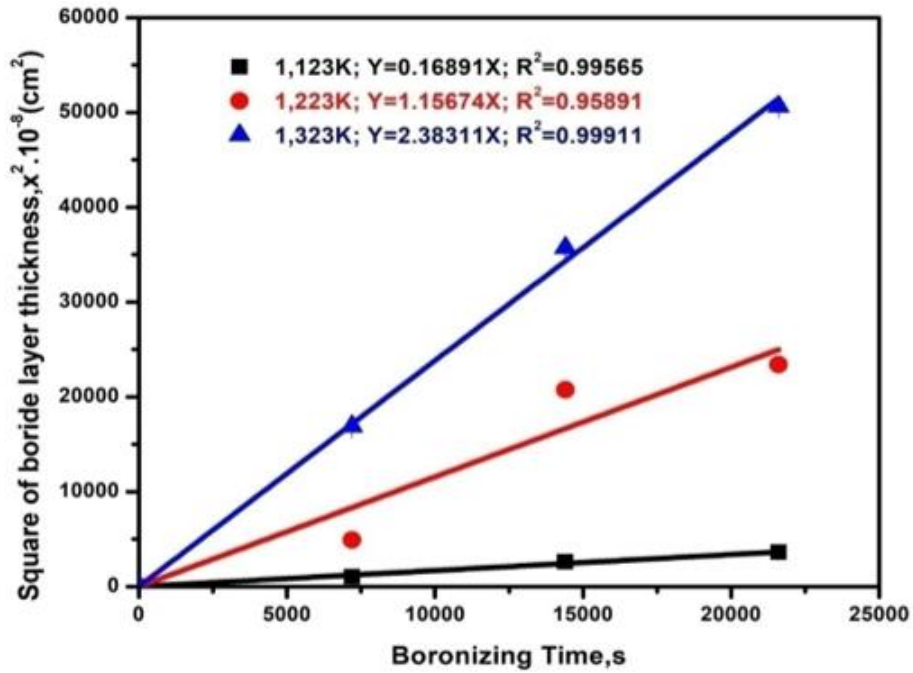


Figure 5.37: Square of boride layer thickness versus boronizing time at various temperatures for EN24 steel.

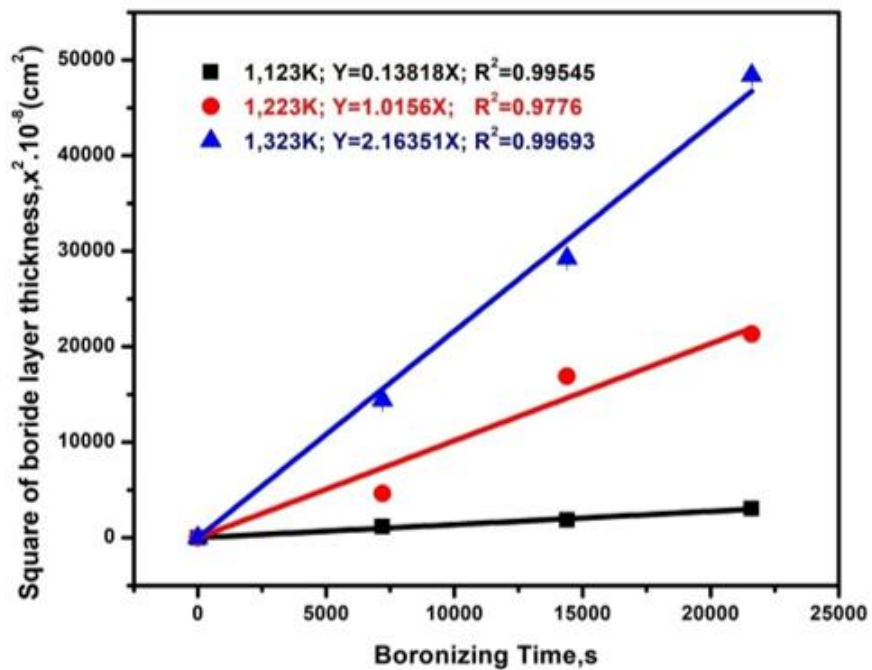


Figure 5.38: Square of boride layer thickness versus boronizing time at various temperatures for EN41B steel.

The values of the growth rate for EN19, EN24 and EN41B were calculated from the plots shown in figure 5.36, Figure 5.37 and Fig 5.38 respectively.

Table 5.14 shows the growth rate (R) with a function of boronizing temperature for different specimens. It was observed that with the increase in temperature from 1123 K to 1323 K, an increase occurred in the diffusion rate values of boron in the boride layer for EN19, EN24, and EN41B. It could be due to the reason that the diffusion process speeds up along with the increase in boronizing temperature [11][18][32][33][34][35][36][37][38][39][40].

The specimens with higher concentration of alloying elements were having a lower value of growth rate. It was found that EN19 was having a highest diffusion rate, whereas EN41B was having lowest diffusion rate. It could be attributed to the presence of additional alloying elements in EN 24 and EN41B specimens.

Ni, Al, Si present in EN24 and EN41B would have been acted as the diffusion barrier resulted in the lower diffusion growth rate. Many researchers also reported that the value of growth rate decreases with increased concentration of alloying elements. [18][34][37][38][39][46].

**Table 5.14: Growth rate (R) as a function of Boriding temperature for EN19, EN24 and EN41B specimens.**

Sr. No.	Steel	Growth Rate (cm <sup>2</sup> s <sup>-1</sup> )		
		Temperatures, K		
		<u>1,123</u>	<u>1,223</u>	<u>1,323</u>
1	EN19	2.1935*10 <sup>-9</sup>	1.44872*10 <sup>-8</sup>	2.67377*10 <sup>-8</sup>
2	EN24	1.6891*10 <sup>-9</sup>	1.15674*10 <sup>-8</sup>	2.38311*10 <sup>-8</sup>
3	EN41B	1.3818*10 <sup>-9</sup>	1.0156*10 <sup>-8</sup>	2.16351*10 <sup>-8</sup>

As discussed in section 2.3.6 that the relationship between growth rate constant( $R$ ) and temperature can be expressed by an Arrhenius type equation (2).Figure 5.39 is showing the plot between  $\ln(R)$  vs.  $1/T$  for EN19, EN24 and EN41B specimens. Consequently, the activation energies ( $Q$ ) for the boron diffusion in the boride layer determined by the slope obtained from the plot of  $\ln(R)$  vs.  $1/T$ . The plot of  $\ln(R)$  and  $1/T$  shows a linear relationship and the activation energies ( $Q$ ) were calculated by the slop of the plots.

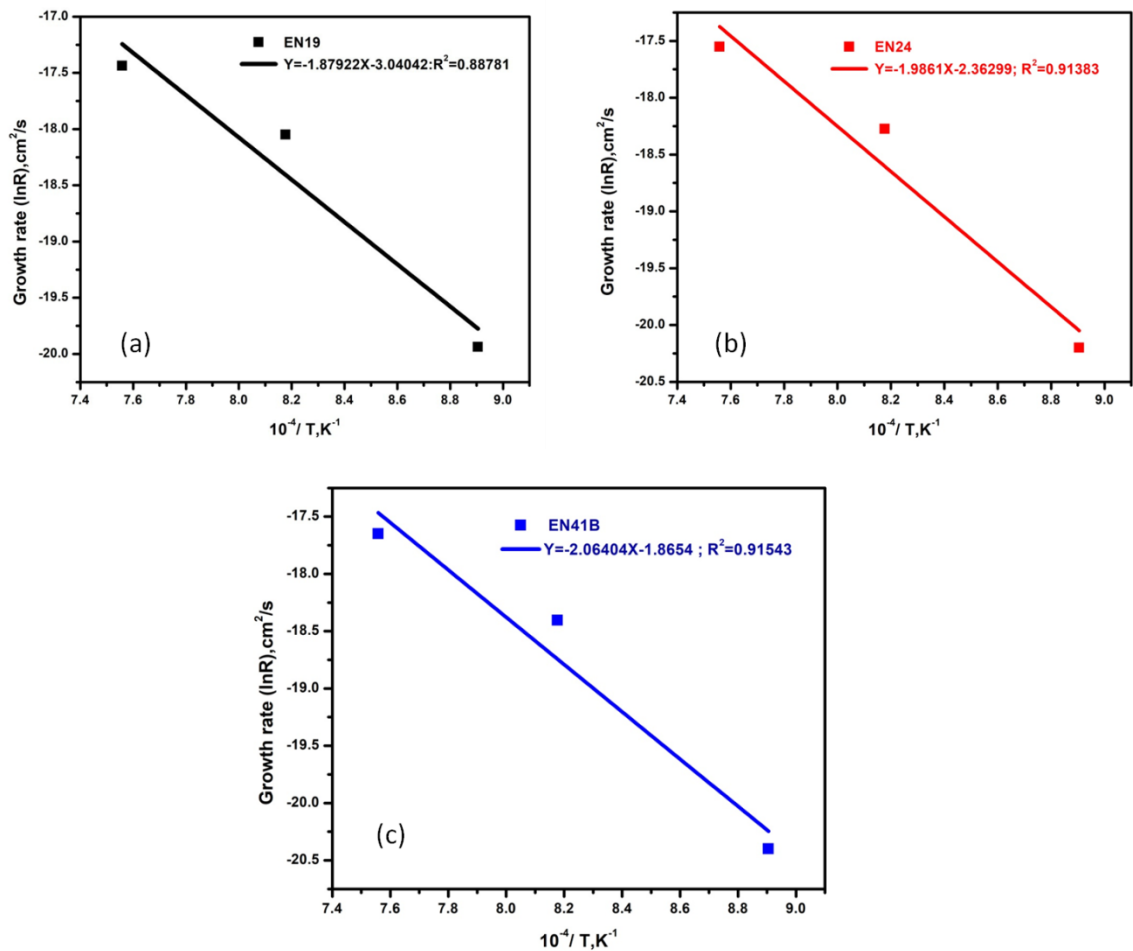


**Figure 5.38: Natural logarithm of growth rate as a function of reciprocal of boronizing temperature for (a) EN19, (b) EN24 (c) EN41B steel**

**Table 5.15: Shows the growth rate (R) and activation energies (Q) with a function of boronizing temperature for EN19, EN24 and EN41B specimens.**

Sr. No.	Steel	Growth Rate(cm <sup>2</sup> s <sup>-1</sup> )			Activation Energy (kJ/mol)
		Temperatures, K			
		<u>1,123</u>	<u>1,223</u>	<u>1,323</u>	
1	EN19	2.1935*10 <sup>-9</sup>	1.44872*10 <sup>-8</sup>	2.67377*10 <sup>-8</sup>	156.162
2	EN24	1.6891*10 <sup>-9</sup>	1.15674*10 <sup>-8</sup>	2.38311*10 <sup>-8</sup>	165.044
3	EN41B	1.3818*10 <sup>-9</sup>	1.0156*10 <sup>-8</sup>	2.16351*10 <sup>-8</sup>	171.521

The calculated values of activation energies for the boronizing process for EN19, EN24 and EN41B steels were obtained as 156.16, 165.04 and 171.52 kJ/mol respectively. The activation energies for boronized EN19 EN24 and EN41B steels were found to be different. The difference in the activation energies could be caused due to the different composition of steels. EN41B and EN24 have a higher concentration of alloying elements than EN19 which resulted in higher activation energies for the diffusion of boron atoms in the respective steel. Al and Ni present in EN24 and EN41B steel has a lower solubility in borides and act as diffusion barrier for the boron atoms. Due to which Boron atoms had to displace Al and Ni atoms for successful diffusion into the surface of steels causing the higher values of activation energy.

It is clear that the important factor for the activation energy is the composition of the steel being bronzed. Alloying elements are the prime factors in boronizing process. Alloying elements are responsible for hindering the diffusion process of boron in boride layer during boronizing. Number of elements will have a direct effect on the thickness of boride layer. The thickness is less when the number of elements is more and higher activation energy is required for the diffusion process.

[18][34][37][38][39][46]

Empirical expressions for boronizing of EN19, EN24 and EN41B steels have been derived with the help of classical kinetic equations (1,2) and the results obtained in this study.

**For EN19**

$$X^2=4.78*10^{-4}.t.exp\left(\frac{156.16}{R^0T}\right) \quad (X \text{ in } m)$$

**For EN24**

$$X^2=9.41*10^{-4}.t.exp\left(\frac{165.04}{R^0T}\right) \quad (X \text{ in } m)$$

**For EN41B**

$$X^2=1.54*10^{-3}.t.exp\left(\frac{171.52}{R^0T}\right) \quad (X \text{ in } m)$$

**Table 5.16:** Values of the Activation Energies of the Borided Steels from the Literature and current study

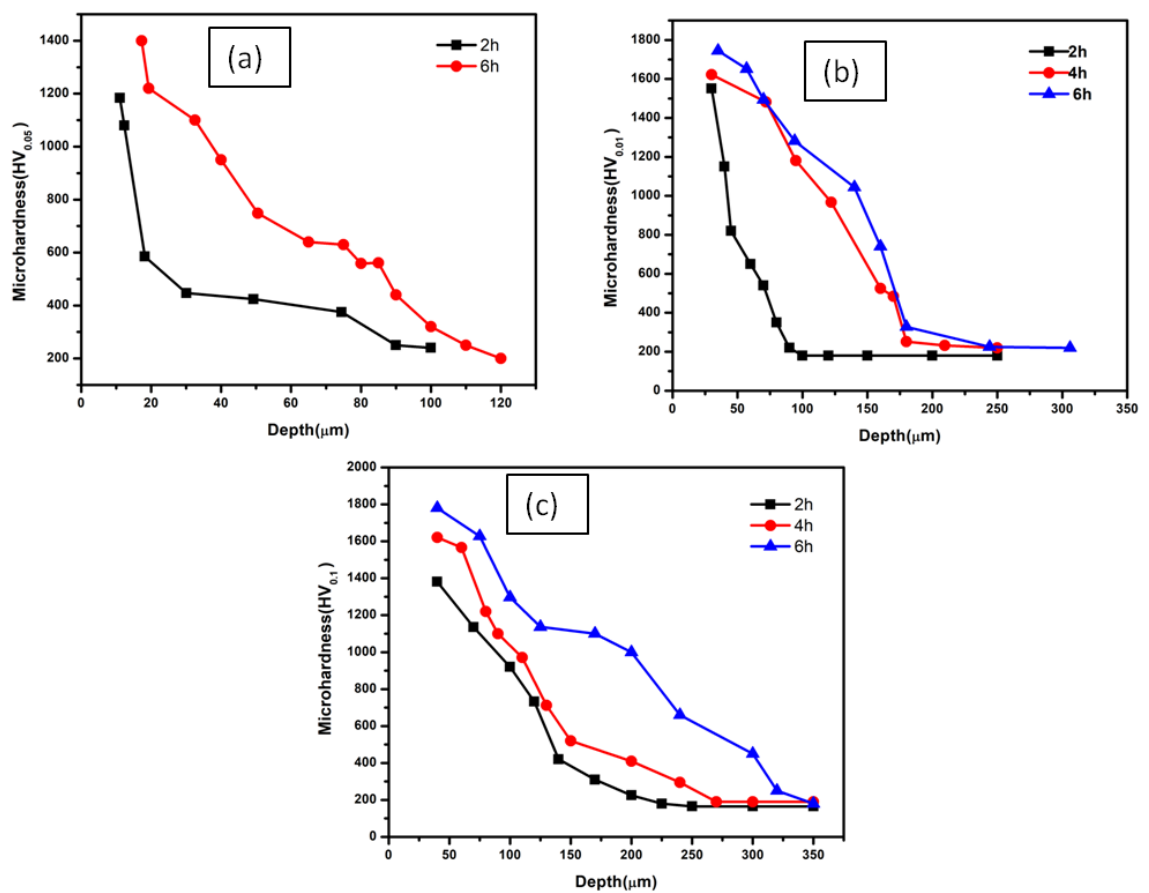
Steel	Temperature Range (K)	Boronizing Medium	Activation Energy (kJ/mol)	References
AISI316	1073-1223	Pack boronizing	199	[11]
AISI304 H13	1073-1223	Salt boronizing	244.37-253.35	[18]
AISI4140	1023-1223	Paste	168.5	[32]

AISI 316	973-1073	Plasma Paste	250.8	[33]
AISI 1040 AISI P20	1073-1223	Pack Boriding	168-200	[34]
AISI 51100	1123-1223	Plasma	106	[35]
X200CrMoV1 2 P	1173-1273	Powder	199.37	[36]
AISI420, AISI304 AISI304L	1123-1223	Pack boronizing	206.161,234.641 222.818	[37]
31CrMoV9 34CrAlNi7	1123-1223	Pack Boriding	230-270	[38]
AISI 52100, AISI 440C	1123-1223	Pack boronizing	269.638,340.426	[39]
AISI P20	1123-1223	Pack Boriding	Conventional furnace: 256.485, Micro-wave furnace: 213.935	[40]
AISI 304	1023-1223	Plasma paste Boriding	123	[42]
AISI5140 AISI4340/EN 24 AISID2	1123-1223	Salt Bath	223 234 170	[46]
EN19	1123-1323	Pack	156.16	Present study
EN24	1123-1323	Pack	165.04	Present study

EN41B	1123-1323	Pack	171.52	Present study
-------	-----------	------	--------	---------------

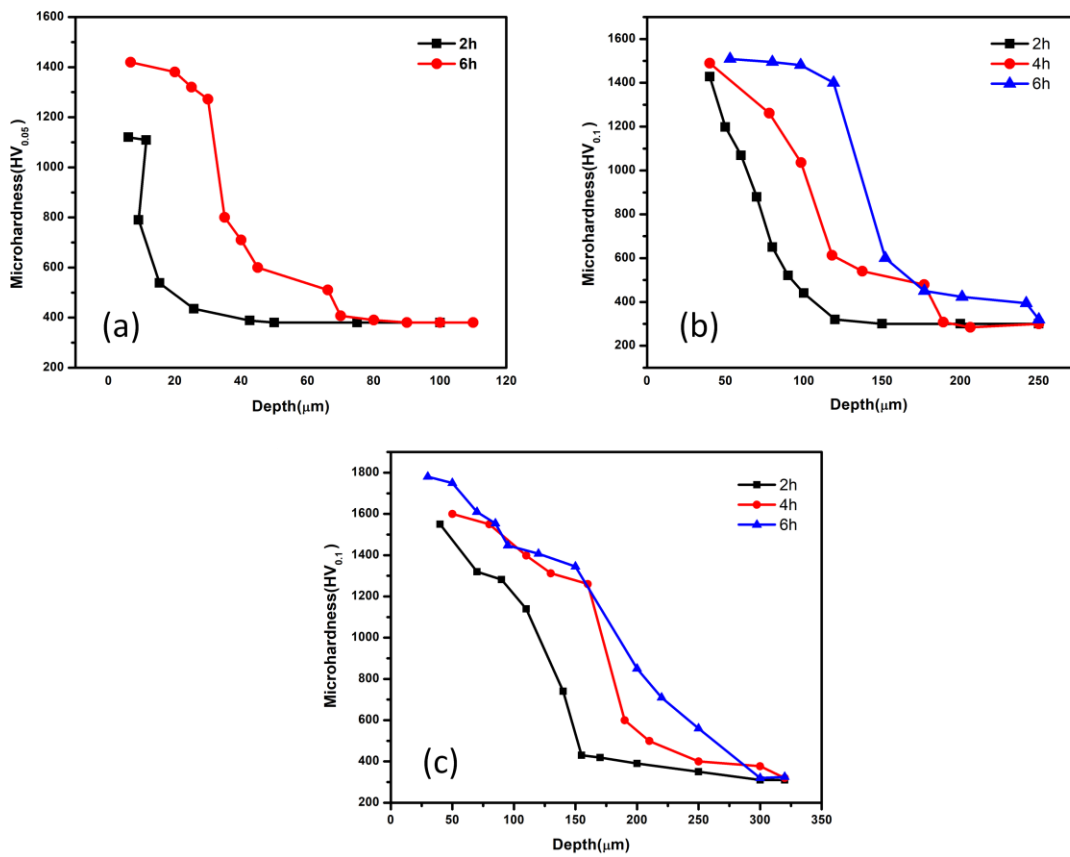
### 5.7. Effect of Boronizing on Surface Hardness

Hardness values of the boride layer formed on different specimens for different parameters were calculated. It was found that the hardness of the boride layer was much higher than that of steel matrix. The variation in the hardness with depth was observed for boronized specimens at different parameters.



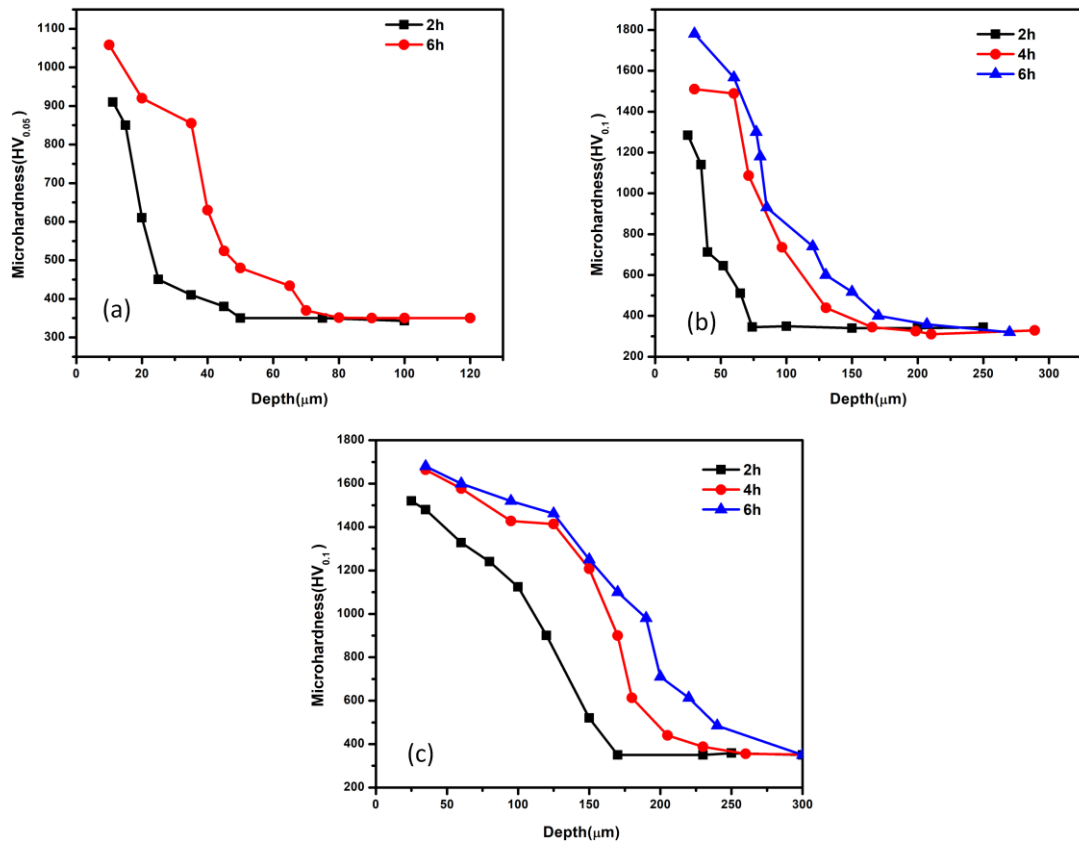
**Figure 5.39: Micro hardness depth profile of EN19 Steel boronized at (a) 850°C (b) 950°C (c) 1050°C**

Figure 5.40 shows the micro hardness depth profile for EN19. Microhardness of the boride layers was found in the range of 1400-1200 HV0.05 (850°C), 1750-1550 HV0.1 (950°C) and 1800-1400 HV0.1 (1050°C).



**Figure 5.40: Micro hardness depth profile of EN24 Steel boronized at (a) 850°C (b) 950°C (c) 1050°C**

Figure 5.41 shows the micro hardness depth profile for EN24. Microhardness of the boride layers was found in the range of 1420-1120 HV<sub>0.05</sub> (850°C), 1550-1420 HV<sub>0.1</sub> (950°C) and 1750-1550 HV<sub>0.1</sub> (1050°C).



**Figure 5.41: Micro hardness depth profile of EN41B Steel boronized at (a) 850°C (b) 950°C (c) 1050°C**

Figure 5.42 shows the micro hardness depth profile for EN41B. Microhardness of the boride layers was found in the range of 1050-950 HV<sub>0.05</sub> (850°C), 1780-1280 HV<sub>0.1</sub> (950°C) and 1750-1520 HV<sub>0.1</sub> (1050°C).

It was observed from the hardness depth profiles that the hardness values of the borides are much higher than those of the matrix. Hardness decreased with distance towards the steel matrix.

There different zones were identified on the basis of hardness depth profile and WDS analysis;

(i) Borides, (ii) Diffusion zone or Transition zone, where hardness was more than steel matrix, but less than the boride layer and (iii) matrix [53].

It was observed during EPMA that boron concentration was high in diffusion/Transition zone, due boron made a solid-state solution with the steel which

resulted in the higher hardness in diffusion zone [21][53]. It was also observed that the hardness values were increasing with process time and temperature. Meric et al had also reported that the micro hardness values of boride layer on low carbon steels increases with process temperature and process time [43].

## 5.8. Corrosion Test

The corrosion resistance of the boride layer formed on specimen EN41B was examined by acid immersion tests. The tests were performed on boronized EN41B as well as on the untreated sample.

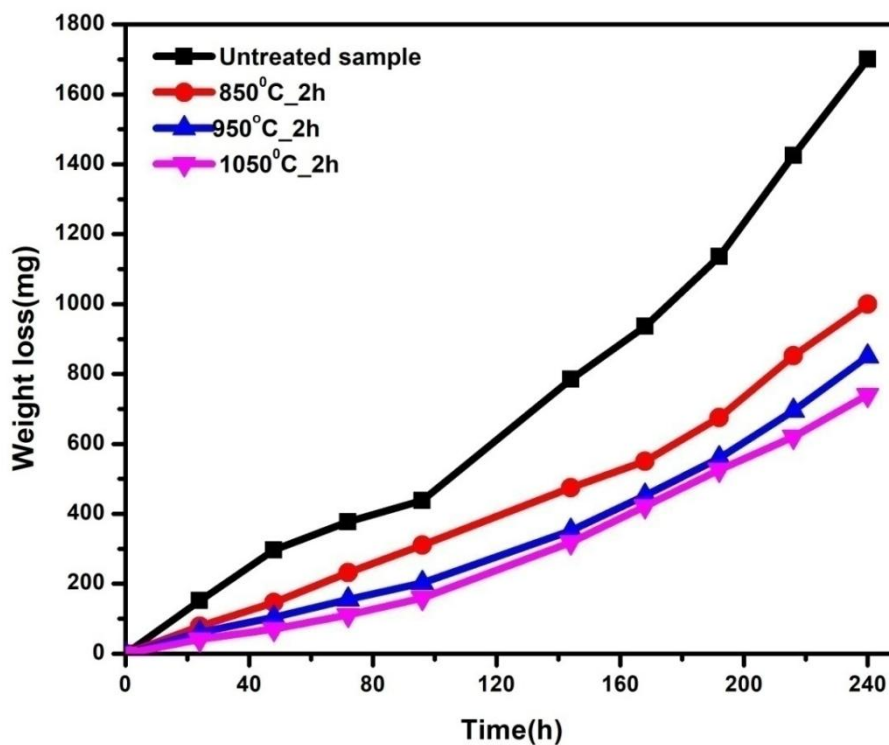


**Figure 5.42: Weight loss of immersion tests of the untreated and boronized EN41B steel in HCl 5M solutions**

The time-dependent variation of weight loss was calculated and given in a Figure 5.43 for the 4% M HCl solution.

It was observed that the weight loss in the untreated specimen increased with the increase in the processing time. It was calculated that while the weight loss in the acid solution during 96 h was 438.3 mg, the corrosion weight loss of the raw specimen increased to 1700 mg. After 240 h for untreated EN41B (Figure 5.43).

Whereas the weight loss for the boronized EN41B was lesser as compared to untreated specimen. In the boronized specimen after the corrosion test, it was observed that the weight loss for EN41B specimen boronized at, 850°C, 950°C and 1050°C for the same duration in the corrosion test solution during 96 h was 310 mg, 202.2mg and 159.3mg respectively and it was increased to 1000mg, 850mg and 740mg after 240 h. The lowest weight loss was observed in the boronized EN41B specimen (40.90mg.) at the temperature of 1050°C. Whereas the weight loss for the untreated EN41B specimen was 151.2 mg. It could be stated that the value of weight loss was dropped as a result of the boronizing process for EN41B steel.

It could be stated that the solubility of corrosion was decreased with the boronizing treatment of the steel. The process is generally called “Passivation”. It means that the surface of a metal is corroded and the corrosion products form a protective layer if the corrosion products are hardly soluble; it therefore blocks the metal beneath it from further corrosion. If the corrosion products are soluble, this protective layer can be washed away and the metal is exposed to further oxidation.

In untreated EN41B, the initially formed corrosion products were somewhat soluble in acid and the metal surface was exposed to corrosive medium all the time which resulted in the higher weight loss in untreated specimens. In addition, it was observed that the decreased solubility of corrosion in the boronized EN41B specimens led to a decrease in the amount of material loss. It was observed that the solubility of corrosion of the boronized specimens were lower than that of the untreated specimen. This significant decrease in weight loss and increase in corrosion resistance might be due to the formation of a protective surface coating treatment. As a result of which the corrosion resistances of the EN41B steel increased by the boronizing treatment. This result is similar as reported by Xi Y, Liu D and Han D [58].

## 5.9. Heat Treatment with used Boronizing Mixture

In this heat treatment Pack boronizing was conducted at 1050°C with used commercial Boropak powder inside the muffle furnace.

### 5.9.1. Heat Treatment with used Boronizing Mixture without activator

Pack boronizing was performed on EN19, EN24 and EN41B specimens at 1050°C for 4h with used commercial Boropak powder inside the muffle furnace.

The powder was used without adding any external activator. After boronizing was completed container was opened and the specimens were taken out from the container and prepared for further studies.

#### 5.9.1.1. *Microstructure*

The cross sectional optical micrographs of the specimens EN19, EN24 and EN41B steel boronized at temperature 1050°C for 4 h are shown in figure 5.44.

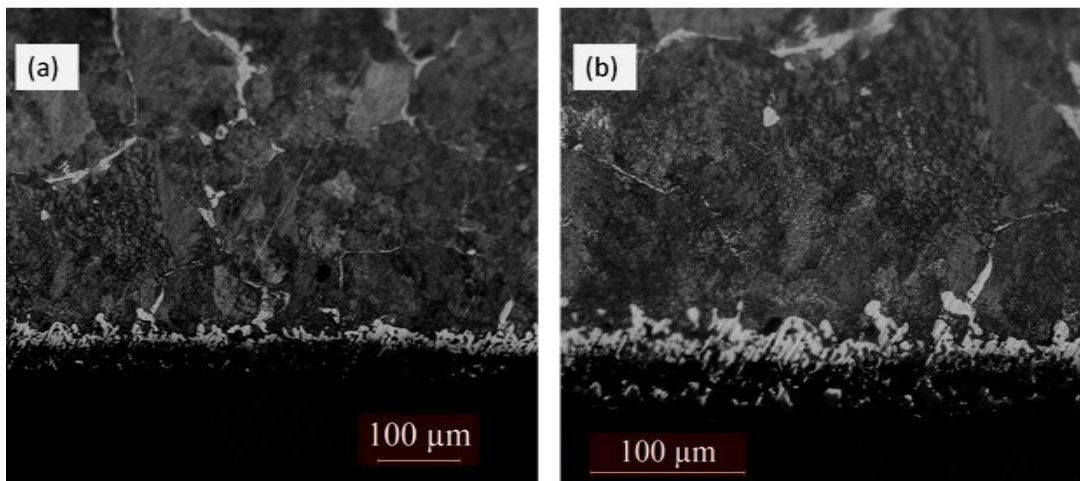


**Figure 5.43: Optical micrograph of EN19 specimen boronized at 1050°C for 4h with used Boropak powder without activator at (a) 100X (b) 200X magnifications**

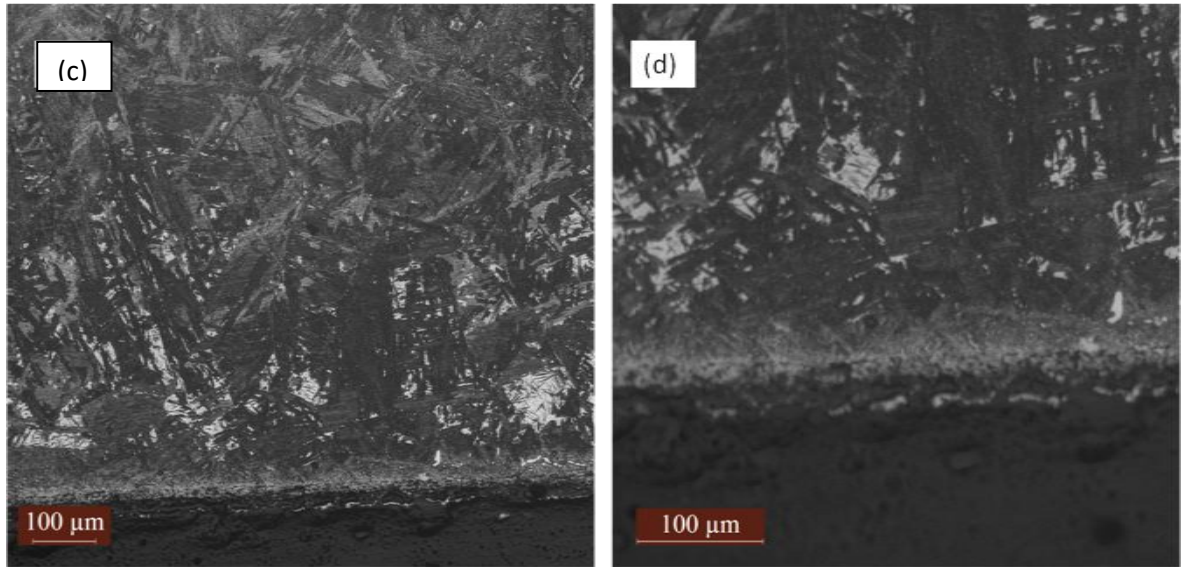


**Figure 5.44: Optical micrograph of EN24 specimen boronized at 1050°C for 4h at (c) 100X (d) 200X magnifications.**

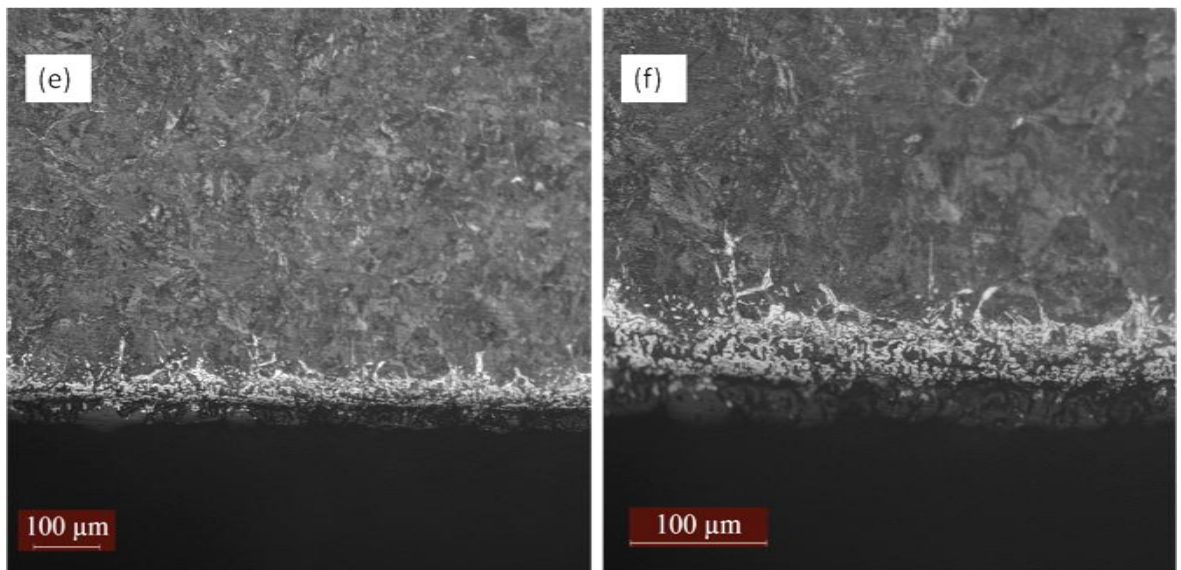


**Figure 5.45: Optical micrograph of EN41B specimen boronized at 1050°C for 4h at (e) 100X (f) 200X magnifications**

From the optical micrographs it was observed that the surfaces of the boronized specimens were composed of two distinct regions:-

- I. A thin, compact layer formed on the top of the surface.
- II. Steel matrix, which was not affected by the boronizing process.

Microstructure photographs of all specimens boronized in the used boronizing mixture without activator at 1050°C for 4h shows a thin compact layer formed around the specimen. No columnar morphology was observed, indicating that the boronizing could not occur. Boride layer could not develop in this heat treatment where activator was not used. The one or more reasons for the same are listed below;

- a) It might be due to the low boron potential. All the available boron concentration might be utilized when the boronizing mixture was used for the first time. Although thin, compact layer was formed, but due to the less available boron potential, there was no growth of borides through the thin compact layer. As it was reported that the Fe<sub>2</sub>B starts forming when boron potential reaches up to 8.83 wt.%. It might be happening that boron potential was not reached up to 8.83weight%. As a result of which Fe<sub>2</sub>B growth could not occur.
- b) It might be due to the unavailability of activator in the boronizing mixture. As an activator plays an important role in creating and accelerating the formation of boron rich atmosphere [28].

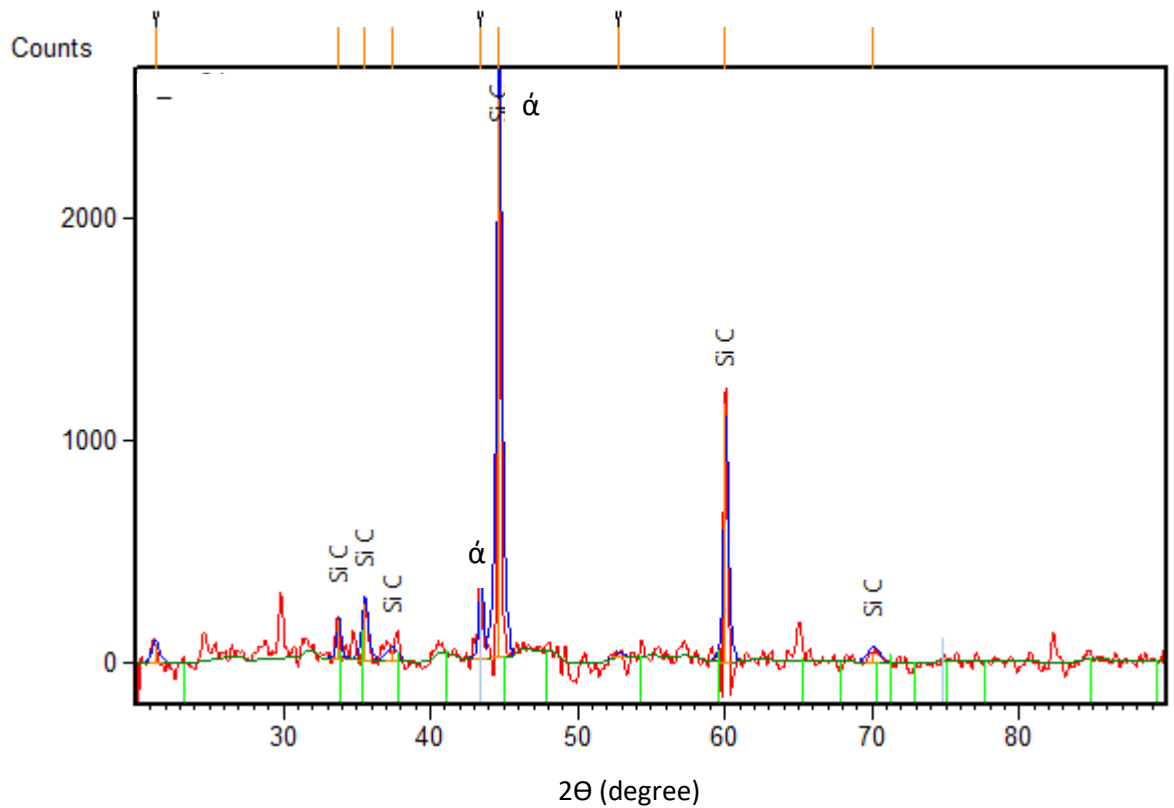
#### ***5.9.1.2. Microhardness***

Due to porous and very thin layer micro-hardness measurement was not possible. But the micro hardness was measured below the compact layer. The value was obtained as 400HV0.05. The hardness value was more for the region below the layer. This suggested that the diffusion of boron occurred to some extent, but it was not enough to make a solid state solution of B and Fe. Therefore, formation of Fe<sub>2</sub>B could not occur.

#### ***5.9.1.3. XRD Study***

XRD was done to confirm the presence of boride phase in the specimens. XRD pattern showed that borides were not present in all the specimens. No peaks belonging to Fe<sub>2</sub>B were observed in the XRD pattern. In all three specimens, the

predominant phase was SiC and Fe ( $\alpha$ ). Unidentified peaks were expected to peak of complex Fe, Si based oxides.



### 5.9.2. Heat Treatment with used Boronizing Mixture with activator

Pack boronizing was performed on EN19, EN24 and EN41B specimens at 1050°C for 4h with used commercial Boropak powder inside the muffle furnace.

The powder was used with external activator. 2 wt%  $\text{NH}_4\text{Cl}$  was mixed with used boronizing mixture. After boronizing was completed container was opened and the specimens were taken out from the container and prepared for further studies.

#### 5.9.2.1. *Microstructure*

The cross sectional optical micrographs of the specimens EN19, EN24 and EN41B steel boronized with the used boronizing mixture with activator at temperature of 1050°C for 4 h are shown in figure 5.47.

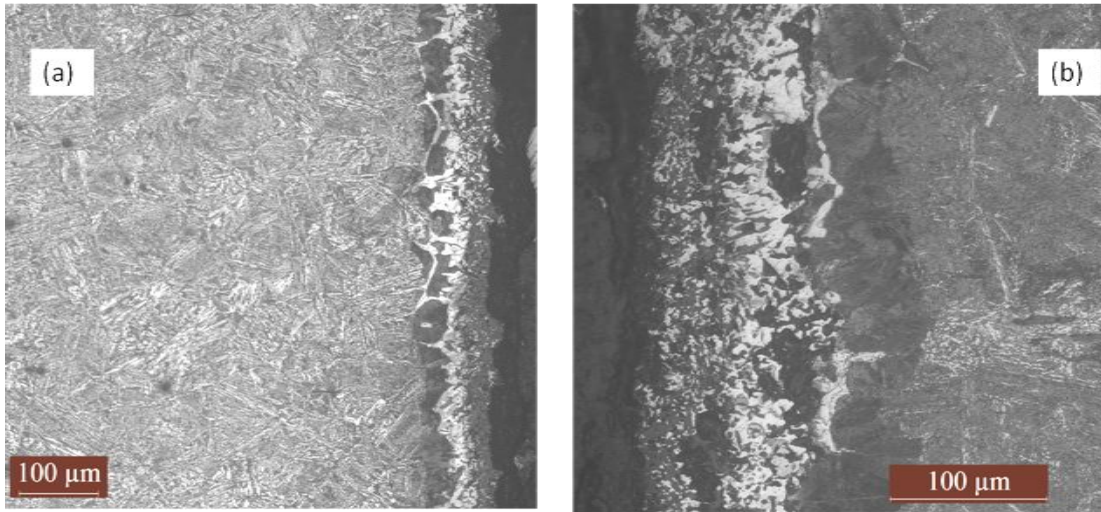


**Figure 5.46: Optical micrograph of EN19 specimen boronized at 1050°C for 4h with used Boropak powder and activator at (a) 100X (b) 200X magnifications.**

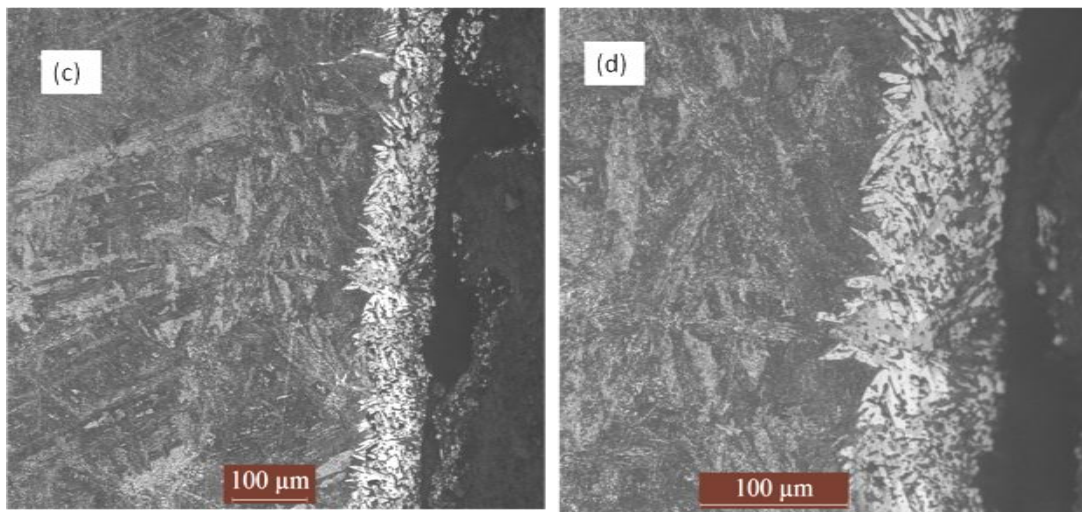


**Figure 5.47: Optical micrograph of EN24 specimen boronized at 1050°C for 4h with used Boropak powder and activator at (c) 100X (d) 200X magnifications**

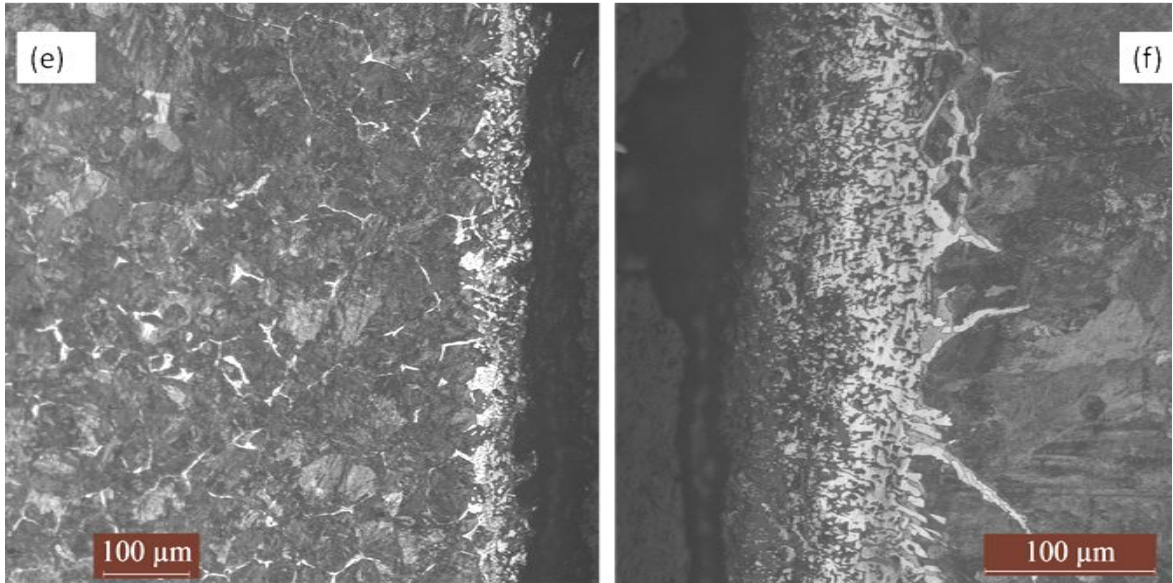


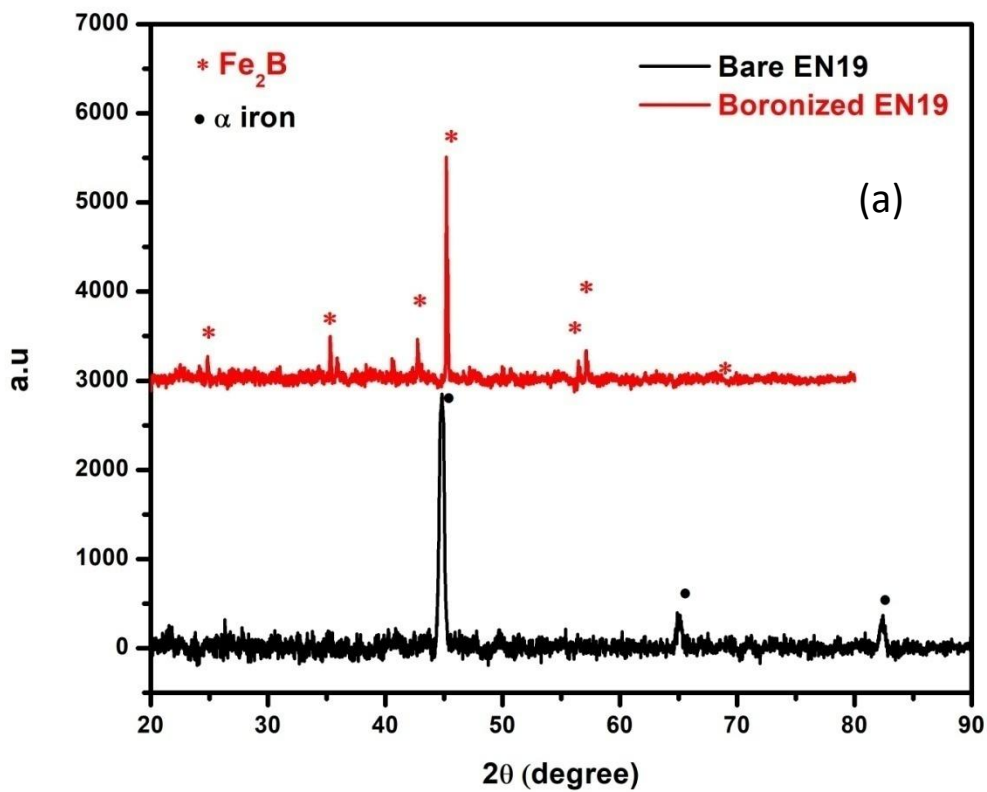
**Figure 5.48: Optical micrograph of EN41B specimen boronized at 1050°C for 4h with used Boropak powder and activator at (e) 100X (f) 200X magnifications**

Form the optical micrographs it was observed that the surfaces of specimens were composed of two distinct regions;

- I. A thin, compact layer at the one surface and a thick layer on the other side of the surface which was looking like something had diffused into the surface of the specimen and a layer were formed. We were not sure about the layer being a boride layer because the morphology was different as that of the boride layer. As we know that generally boride layer has a columnar morphology along the diffusion axis [28] but in the specimens boronized with used boronizing mixture and activator it was observed that the layer was not having columnar morphology which had grown along the diffusion axis. The columns were observed to be grown in all the directions. Further characterization like EDS or GDOES needs to be done to confirm the composition of layers.
- II. Steel Matrix.

### 5.9.2.2. XRD Studies

The X-ray diffraction patterns of the heat treated EN19; EN24 and EN41B steels boronized with the used boronizing mixture are given in Figure 5.50. XRD was done to confirm the presence of boride phase in the specimens. Figure 5.50 shows X-ray diffraction spectra of EN19, EN24 and EN41B specimens boronized with used boronizing mixture. It could be noted that the boronizing treatment as resulted in formation of boride based phases. In all three specimens, the predominant phase was  $Fe_2B$ . Unidentified peaks were expected to the peaks of complex Fe, B, Si based oxides.



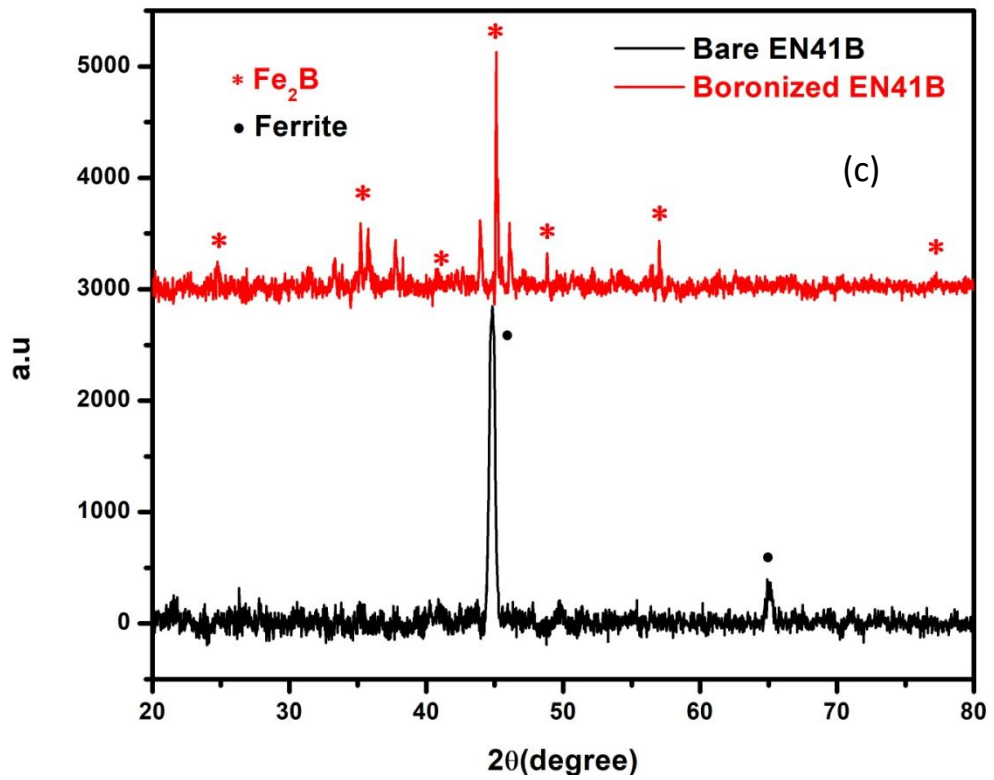
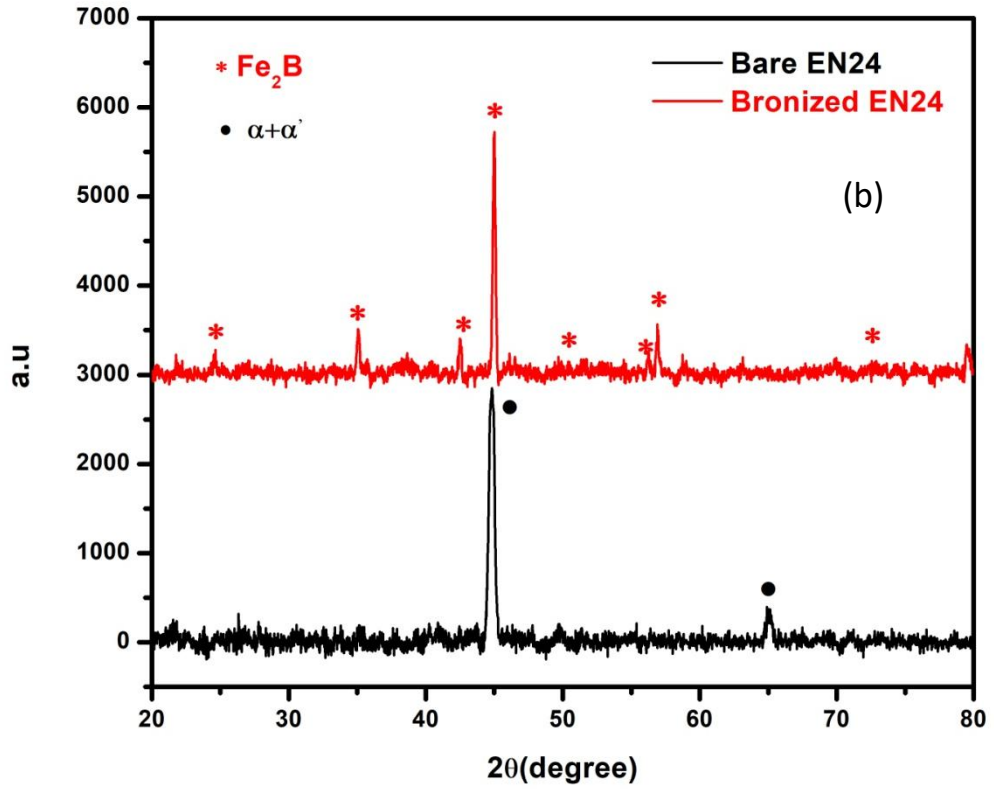


Figure 5.49: XRD patterns of boronized with used boronizing mixture specimens (a)EN19, (b)EN24, (c)EN41B

### **5.9.2.3. *Microhardness***

Micro hardness of the diffused layer was measured at different locations. The micro hardness in the outer part of the bronzed layer was not measured due to porous layer and crystallographic disorder. The micro hardness value was found as 890-570 HV0.05 for EN19 steel, 1100-920 HV0.05 for EN24 steel and 1150-900 HV0.05 in EN41B steel. The values corresponding to the layer were more than the hardness of the steel matrix.

## 6. Conclusion

In this study, the *pack* boronizing of low alloy steels (EN19, EN24, and EN41B) was done successfully using different process parameters. Boronized layer was analysed using optical microscopy, scanning electron microscopy (SEM), electron probe microanalyser (EPMA), Vickers micro-hardness tester, and X-ray diffraction (XRD). Following are the conclusions of the study:

1. Sawtooth (columnar) morphology of boride layer was observed. The extent of sawtooth morphology was reduced with increase in the concentration of alloying elements. Therefore, the extent of zig-zag appearance of the interface between the boronized layer and core was more for the EN19 than the EN24 and EN41B steels.
2. The XRD analysis confirmed the presence of  $\text{Fe}_2\text{B}$  phase in the bronzed steels. XRD analysis didnot reveal the presence of  $\text{FeB}$  phase.
3. EPMA analysis supported the formation of  $\text{Fe}_2\text{B}$  phase. EPMA analysis confirmed the displacement of Si, Al, and Ni by the growing front of the boride layer during boronizing process.
4. Unlike the EN19 steel, EN24 and EN41B steels showed the presence of small islands of borides between the columnar morphology of  $\text{Fe}_2\text{B}$ .
5. Surface hardness of the boronized steels was in the range of about 1400-1800 HV.
6. Based on EPMA analysis and microhardness depth profile, cross-section of the boronized steels showed the three different zones: (i) boride layer consisting of  $\text{Fe}_2\text{B}$  (ii) transition-zone containing  $\text{Fe}_2\text{B}$  and the surrounding non-boronized region (but enriched with the displaced elements like Si, Al, and Ni), and (iii) core (free from boron and the displaced elements).
7. Morphology and thickness of the boride layer were affected by the process parameters like temperature, time, and the composition of steels.
8. The thickness of the boride layer was increased parabolically with time for all steel. However, it was reduced by increasing the amount of alloying elements. Kinetics of boronizing was fastest for the EN19 steel and the lowest for the EN41B steel.

9. A kinetic study was done to estimate the activation energy for the diffusion of boron in low alloy steels. The activation energies were calculated from the slope of the plot obtained between  $\ln(R)$  and  $1/T$ , where  $R$  is the growth rate (calculated from the slope of the plot between (boride layer thickness)<sup>2</sup> and time), and  $T$  is the temperature. The activation energies were affected by the composition of steels. The calculated values of the activation energies for EN19, EN24, and EN41B steels were 156, 165 and 172 kJ/mol respectively.
10. A corrosion test was performed to know about the corrosion behavior of the boronized steel. The boronizing treatment improved the corrosion resistance of the steel.
11. The boronizing-capability of the *used* pack-mixture was determined *with* and *without* the addition of activators. The appreciable thickness of the boronized layer was observed in the optical microscope due to the addition of activators in the used pack-mixture. XRD analysis confirmed the presence of  $\text{Fe}_2\text{B}$  phase in the boronized specimens.

## **7. Future Scope of the Study**

As discussed earlier Boronizing is a very popular method to improve the mechanical properties of the surfaces. Multi component boronizing (B-Al, B-C r, B-Ti etc.) is having a large area for research. These techniques may provide the solution for wear and corrosion problems while improving the mechanical properties of steels. Non-ferrous alloys specially the alloys of Mg,Ni,Ti have a large scope for future work when combined with boronizing. Recovery of boron from the used boronizing mixture must be investigated for cost effectiveness and technical feasibility.



## 8. References

- [1] Tadeusz Burakowski, Tadeusz Wierzchon, "Surface Engineering of Metals, principles, Equipment, Technologies ", CRC press 1998
- [2] S. Bagheri, M. Guagliano, "Review of shot peening processes to obtain nanocrystalline surfaces in metal alloys", Surface Engineering 2009 ,VOL 25, NO 1.
- [3] C. Donnet ,A. Erdemir, "Tribology of diamond-like carbon films: recent progress and future prospects," J. Phys. D: Appl. Phys., vol. 39, pp. R311–R327, 2006.
- [4] O. Culha, M. Toparli, S. Sahin, T. Aksoy, " Characterization and determination of Fe<sub>2</sub>B layer, mechanical properties" J. Mater. Process. Tech., 206, 231, 2008.
- [5] O. Ozdemir, M.A. Omar, M. Usta, S. Zeytin, C. Bindal, A.H. Ucisik, "Kinetics of the formation of Fe<sub>2</sub>B layers in gray cast iron: Effects of boron concentration and boride incubation time", Vacuum 83, 175, 2009.
- [6] M. A. Bejar, E. Moreno "Abrasive wear resistance of boronized carbon and low-alloy steels", J. Mater. Process. Tech. 173, 352, 2006.
- [7] O. Allaoui, N. Bouaouadja, G. Sainderran, "Characterization of boronized layers on a XC38 steel", Surface Coating Technology 201, 3475, 2006.
- [8] V. Jain, G. Sundararajan, "Influence of the pack thickness of the boronizing mixture on the boriding of steel", Surface Coating Technology 149, 21, 2002.
- [9] M. Keddou, S.M. Chentouf, "A diffusion model for describing the bilayer growth (FeB/Fe<sub>2</sub>B) during the iron powder-pack boriding", Applied Surf. Science 252, 393, 2005.
- [10] C. Bindal ,S. Sen, U. Sen, "Tribological properties of oxidised boride coatings grown on AISI 4140 Steel", Materials Letters, vol. 60, pp. 3481-3486, 200.
- [11] ASM Handbook: Heat Treating. ASM International, 1991, vol. 04.
- [12] V. Sista, O.L. Eryilmaz, A. Erdemir G. Kartal S. Timur, "The growth of single Fe<sub>2</sub>B phase on low carbon steel via phase homogenization in electrochemical boriding (PHEB)," Surface & Coatings Technology, vol. 206, pp. 2005-2011, 2011.
- [13] IBRAHIM GUNES, " Kinetics of borided gear steels" Sa<sup>-</sup>dhana<sup>-</sup> Vol. 38, Part 3, June 2013, pp. 527–541, Indian Academy of Sciences
- [14] M. Ipek, F. Celebi, O. Ozdemir, C. Bindal, I. Uslu, H. Comert, "A comparison of borides formed on AISI 1040 and AISI P20 steels," Materials and Design, vol. 28, pp. 1819-1826, 2007.
- [15] ASM Handbook of Alloy Phase Diagrams. ASM International, 1992, vol. 3.
- [16] V.I. Dybkov, W. Lengauer , K. Barmak, " Formation of boride layers at the Fe–10% Cr alloy–boron interface" Journal of Alloys and Compounds, 398 (2005), 113–122
- [17] ASM Handbook: Heat Treating. ASM International, 1991, vol. 04.
- [18] Sukru Taktak, " A study on the diffusion kinetics of borides on boronized Cr-based steels" J Mater Sci (2006) 41:7590–7596

- [19] Y. Azakli, K.O. Gunduz, M. Tarakci, Y. Gencer, "A Comparative Study on Boride Layer Morphology of Fe-4Co, Fe-4V and Fe-4W Binary Alloys", *ACTA PHYSICA POLONICA A*, Vol. 127 (2015)
- [20] M.CARBUCICCHIO, G.PALOMBARINI, "Effect of alloying elements on the growth of iron boride coatings", *Journal of materials science letters* 6 (1987) ,1147-1149.
- [21] P.GOEURIOT, R.FILLIT, F. THEVENOT, J.H. DRIVER, H.BRUYAS, *Mater. Sci. Engng* 55 (1982) 9.
- [22] O. Ozdemir, M. Usta, C. Bindal, A.H. Ucisik, "Hard iron boride (Fe<sub>2</sub>B) on 99.97wt% pure iron", *Vacuum* 80 (2006) 1391–1395.
- [23] I.Ozbek, C. Bindal, "Mechanical properties of boronized AISI W4 steel", *Surf. Coat. Technol.* 154 (2002) 14–20.
- [24] M. Tabur, M. Izciler, F. Gulb, I. Karacanc, "Abrasive wear behaviour of boronized AISI 8620 steel", *Wear* 266 (2009), 1106–1112
- [25] O. Kayacan, S. Sahin and F. Tastan, "A STUDY FOR BORONIZING PROCESS WITHIN NONEXTENSIVE THERMOSTATISTICS", *Mathematical and Computational Applications*, Vol. 15, No. 1, pp. 14-24, 2010.
- [26] Palombarini, G., and Carbuicchio, "On the morphology of Thermo chemically produced Fe<sub>2</sub>B/Fe interface", *Journal of Materials Science Letters*, 3, 1984, p 792-794.
- [27] Goeuriot, P., et al., "Surface treatment of steels: Borudif, A new Boriding Process", *Wear*, Vol. 78, 1981, p67-76.
- [28] A. JOSHI AND S. S. HOSMANI, "Pack-Boronizing of AISI 4140 Steel: Boronizing Mechanism and the Role of Container Design", *Materials and Manufacturing Processes*, 29: 1062–1072, 2014
- [29] Edgar E Vera Ca´rdenas, Roger Lewis, "Characterization and wear performance of boride phases over tool steel substrates", *Advances in Mechanical Engineering* 2016, Vol. 8(2) 1–10
- [30] Tispas, D.N., and J.Rus., "Boronizing of alloy steels", *Journal of Materials Science Letters* 6, 1987, p118-120.
- [31] Campos Silva, I. Domínguez, M. Lopez-Perrusquia, N. Meneses-Amador, A. Escobar-Galindo, R. Martínez-Trinidad, J. "Characterization of AISI 4140 borided steel". *Applied Surface Science* 2010, 256, 2372–2379.
- [32] Z. Nait Abdellah, M. Keddám, A. Elias, "Evaluation of the effective diffusion coefficient of boron in the Fe<sub>2</sub>B phase in the presence of chemical stresses", *International Journal of Materials Research*, 104(2013) 3, 260–265, doi:10.3139/146.110862
- [33] Redouane Chegroune, Mourad Keddám, Zahra Nait Abdellah, Sukru Ulker, Sukru Taktak, Ibrahim Gunes "CHARACTERIZATION AND KINETICS OF PLASMA-PASTE-BORIDED AISI 316 STEEL", *MTAEC9*, 50(2)263(2016)

- [34] Uslu I, Comert H, Ipek M, Ozdemir O, Bindal C, “ Evaluation of borides formed on AISI P20 steel”, *Mater Des* 2007;28:55–61.
- [35] M. Ipek, G. Celebi Efe, I. Ozbek, S. Zeytin, and C. Bindal, “Investigation of Boronizing Kinetics of AISI 51100 Steel”, *JMEPEG* (2012) 21:733–738
- [36] O. Azouani a, M. Keddab b,\* , A. Brahimi c, A. Sehisseh “DIFFUSION KINETICS OF BORON IN THE X200CrMoV12 HIGH-ALLOY STEEL” *J. Min. Metall. Sect. B-Metall.* 51 (1) B (2015) 49 - 54
- [37] Y. Kayali, “Investigation of the diffusion kinetics of borided stainless steels” ,*Phys. Metals Metallogr.* 114 (12) (2013) 1061e1068.
- [38] G.C. Efe, M. Ipek, I. Ozbek, C. Bindal, “Kinetics of borided 31CrMoV9 and 34CrAlNi7 steels”, *Mater. Charact.* 59 (2008) 23e31.
- [39] Y. Kayali, I. Güneş , S. Ulu, “Diffusion kinetics of borided AISI 52100 and AISI440C steels”, *Vacuum* 86 (10) (2012) 1428e1434.
- [40] Yusuf kayali, “Investigation of diffusion kinetics of borided AISI P20 steel in microwave furnace” *Vacuum* 121 (2015) 129e134
- [41] Ibrahim Gunes , Sukru Ulker ,Sukru Taktak, “Plasma paste boronizing of AISI 8620, 52100 and 440C steels” ,*Materials and Design* 32 (2011) 2380–2386
- [42] Yoon JH, Jee YK, Lee SY, “ Plasma paste boronizing treatment of the stainless steel AISI 304”. *Surf Coat Technol* 1999; 112:71–5.
- [43] Meric C, Sahin S and Yilmaz S S, “ Investigation of the effect on boride layer of powder particle size used in boronizing with solid boron-yielding substances” , *Mater. Res. Bull.* 35: 2165–2172
- [44] M.KulaK, O.Oskaya,A.Temizkana, B.Karacab,L.C.Kumruoğlua,B.Topçua, “Effect of boronizing composition on boride layer of boronized GGG-60 ductile cast iron”, *Vacuum*, Volume 126, April 2016, Pages 80-83
- [45] C.Bindal, S.Sen, U.Sen, "Tribological properties of oxidised boride coatings grown on AISI 4140 Steel”, “*Materials Letters*”, vol. 60, pp. 3481-3486, 2006.
- [46] Saduman Sen, Ugur Sen, Cuma Bindal , “An approach to kinetic study of borided steels” *Surface & Coatings Technology* 191 (2005) 274–285.
- [47] Selcuk, B., Ipek R., Karamis, M.B., “An investigation on surface properties of treated low carbon and alloyed steels (boriding and carburizing)”, *Journal of Materials Processing Technology*, Vol. 103, No. 2, pp. 310-317, 2000
- [48] Ibrahim Gunes, Muzaffer Erdogan, Atila Gürhan Çeli, “Corrosion Behaviour and Characterization of Plasma Nitrided and Borided AISI M2 Steel” *Materials research*.2014; 17(3):612-618
- [49] Selcuk, B., Ipek, R. and Karamis, M.B. “A study on friction and wear behaviour of carburized, carbo nitrided and borided AISI 1020 and 5115 steels”, *Journal of Materials Processing Technology*, Vol. 141, No. 2, pp. 189-196, 2003

- [50] El-Amoush, A.S., Abu-Rob, A., Edwan, H., Atrash, K. and Igab, M. "Tribological properties of hard chromium coated 1010 mild steel under different sliding distances", *Solid State Sciences*, Vol. 13, No. 3, pp. 529-533, 2011.
- [51] Márquez-Herrera , J.L. Fernandez-Muñoz , M. Zapata-Torres , M.Melendez-Lira , P. Cruz-Alcantar "Fe<sub>2</sub>B coating on ASTM A-36 steel surfaces and its evaluation of hardness and corrosion resistance" *Surface & Coatings Technology* 254 (2014) 433–439
- [52] Campos-Silva, M. Ortiz-Domínguez, O. Bravo-Bárceñas, M.A. Doñu-Ruiz, D. Bravo Bárceñas,C. Tapia-Quintero, M.Y. Jiménez-Reyes, "Formation and kinetics of FeB/Fe<sub>2</sub>B layers and diffusion zone at the surface of AISI316 borided steels", *surface & Coatings Technology* 205 (2010) 403–412
- [53] G. Celebi,M. Ipek, C. Bindal, A.H. Ucisik, "Some mechanical properties of borides formed on AISI 8620 steel", *Mater. Forum* 29 (2005) 456–460.
- [54] Campos, J. Oseguera, U. Figueroa, J.A. Garcí'a, O. Bautista, G. Kelemenis, "Kinetic study of boron diffusion in the paste boriding process", *Mater. Sci. Eng. A* 352 (2003) 261–265.
- [55] S. Sahin, "Effects of boronizing process on the surface roughness and dimensions of AISI 1020, AISI 1040 and AISI 2714", *J. Mater. Process. Technol.* 209 (4) (2009) 1736–1741.
- [56] K. Genel, " Boriding kinetics of H13 steel", *Vacuum* 80 (2006) 451–457
- [57] Palumbo, M., Cacciamani, G. Bosco, E. and Baricco, M. "Driving forces for crystal nucleation in Fe-B liquid and amorphous alloys", *Intermetallics*, Vol. 11, No. 11-12, pp. 1293-1299, 2003.
- [58] Z. G. SU, X. TIAN, J. AN, Y. LU, Y. L. YANG,S. J. SUN , "Investigation on Boronizing of N80 Tube Steel" *ISIJ International*, Vol. 49 (2009), No. 11